1964

Theoretical and experimental investigation of the auxiliary discharge type converter

Edward Mary Walsh
Iowa State University

THEORETICAL AND EXPERIMENTAL INVESTIGATION OF THE AUXILIARY DISCHARGE TYPE CONVERTER

by

Edward Mary Walsh

A Dissertation Submitted to the
Graduate Faculty in Partial Fulfillment of
The Requirements for the Degree of
DOCTOR OF PHILOSOPHY

Major Subject: Electrical Engineering

Approved:

Signature was redacted for privacy.

In Charge of Major Work

Signature was redacted for privacy.

Head of Major Department

Signature was redacted for privacy.

Dean of Graduate College

Iowa State University
Of Science and Technology
Ames, Iowa

1964

TABLE OF CONTENTS

INTRODUCTION

The auxiliary discharge converter depends fundamentally on the thermionic effect for the direct conversion of heat into electrical energy. The basic electrical circuit is shown in Figure 1. The emitter electrode, when heated to 1400-2200° K, emits electrons with a current density of about 5 amps/cm^2. If these electrons are collected by another electrode, the collector, whose work function (ϕ_C) is lower than the emitter work function (ϕ_E) a current (I_L) will flow in an external circuit connecting the two electrodes. If the resistance of this external circuit is R_L, then an electrical power of $I_L^2 R_L$ is obtained. Thus direct energy conversion from heat to electricity is achieved.

As is evident, the basic principle of the conversion process can be traced back to 1880 when Thomas Edison discovered thermionic emission. However, although the theoretical possibility of thermionic energy conversion was recognized for most of this century, no serious consideration was given to the idea until about 1958. The main reason was the lack of a suitable heat source and practical application for such a converter until that date. Since the converter depends on thermionically emitted electrons, high temperatures in the range of 2000° K are required in most cases to provide emission at acceptable current densities. Prior to the development of the nuclear reactor such temperatures were not readily available and prior also to this period the demand for portable compact electrical power units for military and space applications did not exist.

In addition to these "external" difficulties, a fundamental electrical problem existed within the thermionic converter. This is the so called "space charge neutralization problem" which still remains at the

focus of attention in all the various systems under study and development today. The space charge effect is associated with all electron emitters, in that a stream of electrons leaving an emitter tend to repel other electrons from doing so, and hence limits the maximum current which can be drawn. This current is determined from the well known Child-Langmuir three-halves power equation (9) for plane electrodes

$$J_o = \frac{2.335 \times 10^{-6} \, V^{3/2}}{d^2} \text{ Amperes/Unit area} \qquad (1)$$

where V is the potential difference between the electrodes and d is the interelectrode spacing.

The Vacuum Converter

The first approach to overcoming the current limitation imposed by the presence of space charge was based directly on Equation 1. It is seen that the space charge limited current varies as the reciprocal of the interelectrode spacing squared. In order to achieve acceptably high current densities, d must be made as small as possible. The potential difference between the electrodes is governed in effect by the difference in emitter and collector work functions and by the load current. A typical potential profile (30) for space charge limited conditions is shown in Figure 2. It should be noted that, although this is the accepted profile representation, the direction of increasing potential is downwards and so an electron under the influence of this profile would tend to move towards one or the other of the electrodes. V_L is the potential difference between the two Fermi levels and is equal to the output voltage across the load. V_m is the potential with respect to the emitter surface of the

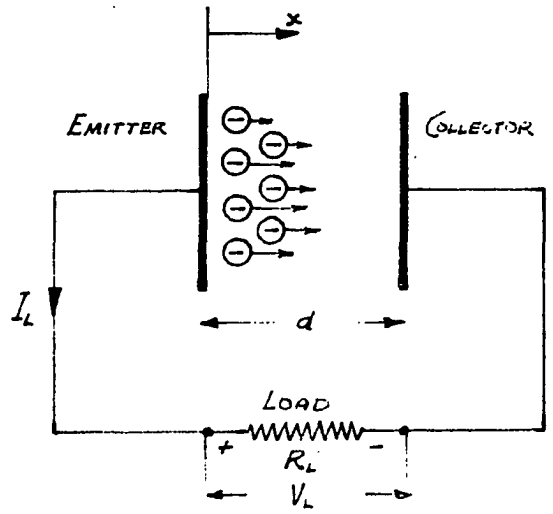

Figure 1. Basic thermionic converter circuit

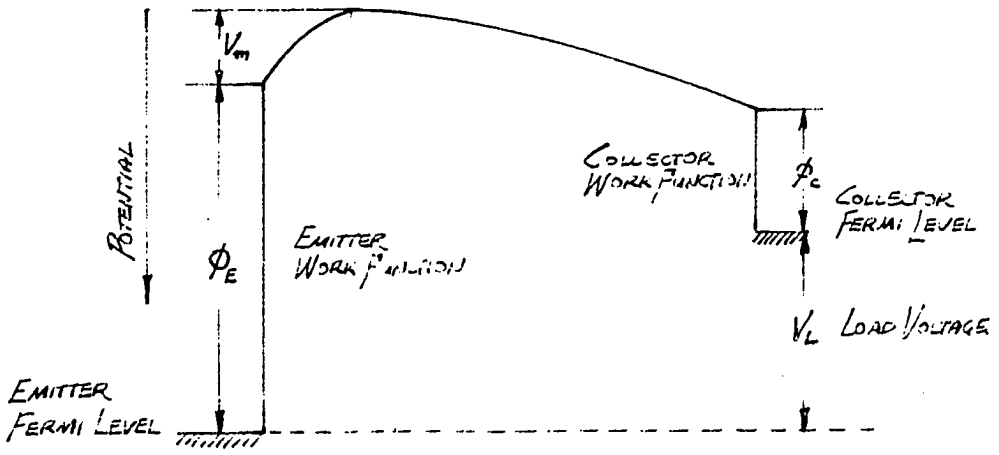

Figure 2. Potential profile for space charge limited conditions

interelectrode potential minimum created by the space charge. The emitter and collector work functions, being governed by properties of the electrode materials, are restricted within relatively small limits. Since the power output of the converter is of main interest the product of V_L and I_L is of concern. V_L may be made large by choosing the emitter and collector materials so that ϕ_E is large and ϕ_c is small. However, if ϕ_c is too large, the emitter must be heated to excessively high temperatures in order to achieve acceptable current densities. Therefore, a compromise must be made when selecting the work function of the emitter. In practice an emitter work function of about 2.3 electron volts is found to be best. No compromise is in general required when selecting the collector material; a material with the lowest possible work function is used. In practice a work function of 1 electron-volt (eV) is as small as can be expected. Therefore, under short circuited conditions, when the Fermi levels of emitter and collector are at the same potential, the interelectrode potential is 1.3 volts. In a practical converter a current density of at least 5 amps/cm^2 would be required. Under these conditions, Equation 1 gives

$$5 = \frac{2.335 \times 10^{-6} \, (1.3)^{3/2}}{d^2} \text{ Amperes/cm}^2$$

and

$$d = 0.0083 \text{ mm.}$$

Such an interelectrode space is impracticable, being less than one hundreth of a millimeter. The problem of course is not in achieving such a

small spacing initially but in achieving the necessary flatness and smoothness of the emitter during the operating life of the converter. Relatively large areas would be required in order to achieve the required power output, and it is irrevelant to make a comparison with the closely spaced systems developed successfully in the vacuum tube field for such requirements as high figure of merit or minimum electron transit time. In these cases the total emitter area is in the 1 cm^2 range and even then their cost is high.

Since the problem of space charge current limitation could not be satisfactorily overcome by using a suitable geometric configuration, another approach was required. This took the form of space charge neutralization employing positive ions. All practical thermionic converters under development today employ neutralization as the means of increasing the current density to an acceptable level. The various converters are classified by the means adapted for the production of these positive ions.

The Cesium Converter

The neutralization of electron space charge by cesium ions was discussed by Hernquist (21) in a paper published in 1958. The principle is based on the phenomenon of contact ionization investigated by Langmuir (31) and his associates about 1930. It is found that if cesium vapor, at near room temperature, contacts tungsten at about 600° K, a layer of cesium forms on the tungsten. This is due to the fact that cesium has a first ionization potential of 3.87 volts and when it contacts a material with a work function greater than 3.87 eV, such as tung-

sten at 4.57 eV, the material captures a valence electron. The cesium ions so formed are restrained from leaving the material by their image force. This is verified by using a material with a work function less than 3.87 eV when it is found that no surface layer of cesium appears. It was recognized that the cesium ions formed, but held, at the emitter surface would be useful for space charge neutralization if they could be ejected from the emitter surface. Ejection is achieved thermionically by increasing the tungsten temperature and hence the ion temperature. When the tungsten is above a critical temperature all the cesium atoms which contact the hot tungsten are immediately evaporated as positive ions and so are available for space charge neutralization in the emitter region. Below the critical temperature, the emitter is partially covered by cesium and the effective surface work function is less than that of tungsten. This is fortunate since a work function of about 2.3 eV is required for the emitter. Thus, the fractional coverage may be adjusted so that the rate of formation of positive ions and the work function adjustment are optimized. The compromise between work function of the emitter and ion production results in other side effects. The increased emitter current density, caused by the decrease in effective emitter work function, requires more ions for space charge neutralization. The rate of arrival of cesium atoms at the emitter is governed by the cesium gas pressure and temperature. Therefore for high current densities it is found necessary to increase the cesium gas pressure. This increase in pressure, while serving the fundamental purpose, introduces side effects. The mean free path of the cesium atoms decreases to the order of interelectrode spacing

dimensions and so the electrons tend to be randomized by neutral gas atom collisions and a plasma is formed in the ..de. Since cesium has a large electron-neutral cross section ($3.1.10^{-14}$ m^2) at the operating temperatures, a high plasma resistivity results. In order to overcome such plasma resistance loss, small interelectrode spacing is called for. Also Rasor (38) has shown that experimental results give efficiencies considerably less than expected and he indicates that this is due to "transport" effects in the converter which are dependent on the interelectrode spacing as shown in Figure 3. For acceptable power densities small interelectrode spacing is required. Since operation at an emitter temperature in the range of 2000° K is required material and fabrication difficulties are considerable. Added to these problems is the fact that cesium itself is a very active element. Containment poses many problems and at the high temperatures and pressures required internal corrosion can be expected to play an important part of life limits of the system. From the design view-point the emitter materials are limited to those whose thermionic work function is greater than 3.87 eV, corresponding to the first ionization potential of cesium. Another criterion which indicates the effectiveness of the means for space charge neutralization is the power used in generating the ions for the neutralization of 1 ampere of emission current. In theory the relatively large value of 0.2 watts/amp is required and experimental values are considerably larger (16). It is felt that although the cesium converter has received much attention in the field of thermionic energy conversion the inherent characteristics of the system prohibit the development of a converter to a status exhibiting an acceptable combination of reliability, efficiency, and simplicity.

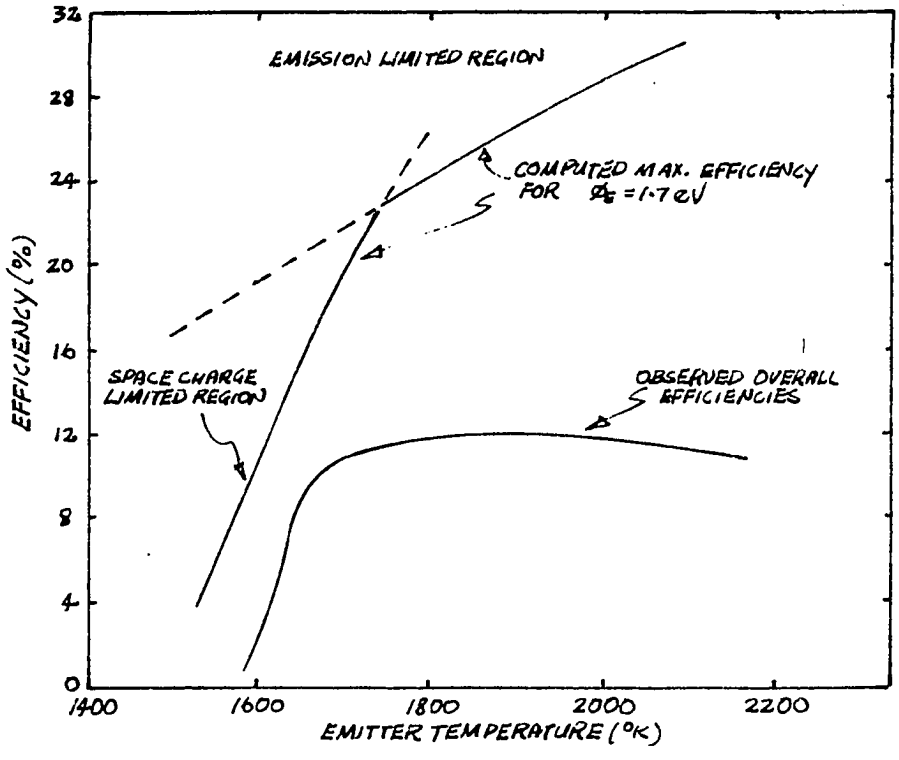

Figure 3. Comparison of computed and observed efficiencies

With the limitations associated with the cesium converter in mind, the follo..ing analysis of the other main converter types was made in the hope of detecting a system whose ultimate potential appeared unhindered by any inherent detrimental characteristics.

The Magnetic Triode Converter

The magnetic triode (7) appears on an initial theoretical analysis to present a solution to many of the problems inherent in the cesium type converter. A schematic representation is shown in Figure 4. In addition to the emitter and collector, a third accelerating electrode at a high potential is placed as shown. A transverse magnetic field is adjusted so that emitted electrons are deflected and collected by the collector electrode. The principle of operation is that the space charge electrons are swept away from the emitter by the applied electric field and so the problems of space charge are solved. Since the emitted electrons which reach the collector return to almost the same potential with respect to the accelerating plate no work is being done on them by the high potential circuit. This theory neglects any electron collisions during the transit between emitter and collector. If collisions do occur, as they do, then there is a considerable probability of the scattered electrons being collected by the accelerating plate. If only a small percentage, say one percent, of the electrons are so collected, converter action is not possible. Consider the following typical example:

E_a = 500 volts [Auxiliary potential]

ϕ_E = 2.3 eV

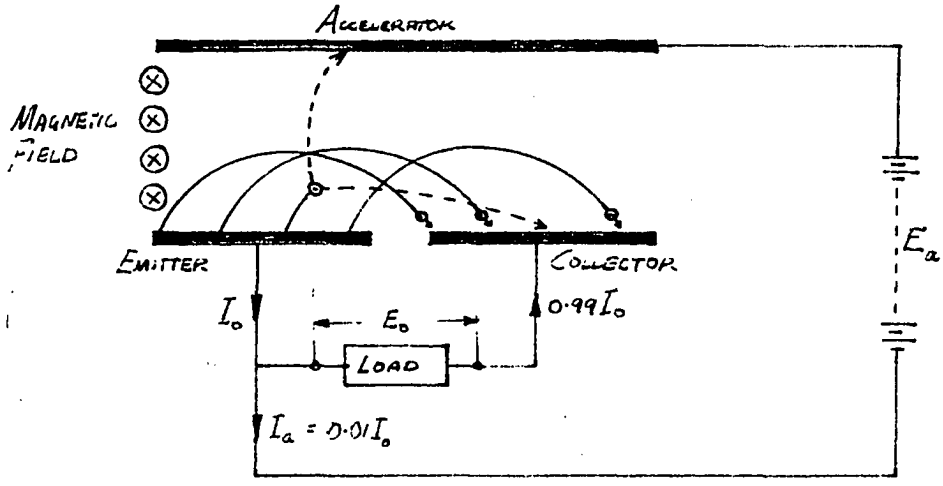

Figure 4. Schematic representation of the magnetic triode

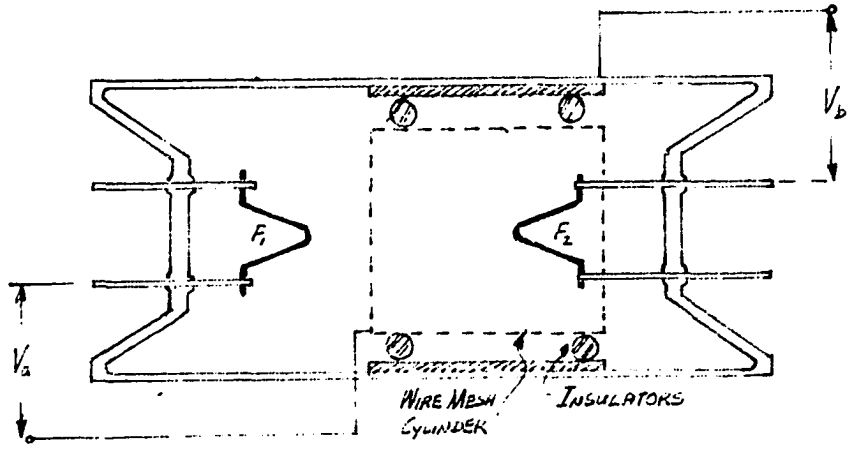

Figure 5. Cross-section of a tube used for measuring ionization potentials

$\phi_c = 1.0$ eV

$I_a = 0.01\ I_o$ [Auxiliary current]

Neglecting the plasma resistive drop, the maximum load voltage may be assumed equal to $\phi_E - \phi_c = 2.3 - 1.0 = 1.3$ volts. Then the power delivered to the load is $V_L I_L = 1.3 \times 0.99\ I_o = 1.282\ I_o$. The power supplied by the accelerating system is $E_a I_a = 500 \times 0.01\ I_o = 5\ I_o$. Thus the power supplied by the auxiliary system is almost four times the output power. The previous analysis neglected all other losses and therefore this system has been ruled from further consideration.

The Nuclear Ion Converter

This type of converter depends on a supply of fission fragments for ionization of the diode gas. Jamerson and Abrams (25) reported on a converter filled with a Penning mixture and having a fission fragment source of uranium foil. Ion densities of the order of 10^{11} cm^{-3} were achieved in the interelectrode space. This type of converter requires an external source of thermal neutrons such as would be provided by in-pile reactor operation. While such a requirement certainly in general limits the applications of the converter, it must be emphasized that there are very few heat sources other than nuclear which provide the necessary high emitter temperatures required. In this respect, the argument of limited applicability should not be made. Such a converter has many attractions. The diode gas being a Penning mixture, which may consist of the noble gasses Ne: 0.1%A, avoids the containment and corrosive problems of the cesium converter. No restriction is placed on the minimum work function of the emitter and so one can be selected as close to the optimum of 2.3 eV as

possible. Further, it is then possible to achieve the desired current densities at relatively low emitter temperatures in the 1500° K range. Such a temperature reduction eliminates the many problems encountered above 2000° K and permits the use of standard materials and fabrication techniques. However a point peculiar to the nuclear ion converter is the build-up of fission products. The system should be such that the fission products have a tolerable effect on the operation of the converter during a reasonable life time, which could be estimated by a period at least as great as the burn-up time of a typical fuel element. Forman and Ghormley (15) go one step further and use the fission product krypton as the diode filling gas. It must be recognized that since the fission product content of the diode is time dependent many restrictions and design problems should be expected. Although certain limitations and many complex problems are associated with the nuclear ion converter the fundamental principle of operation is sound and will certainly receive more attention as the thermionic technology develops. Since the field of thermionic conversion has received attention of significance only during the last five years, the basic concepts are as yet under review and not until the fundamental research and development has been completed will the problems of secondary importance such as those of the nuclear ion converter, receive attention.

The Auxiliary Discharge Converter

In this converter system ions for space charge neutralization are formed by impact ionization of an inert gas. The ions are produced in, or injected into, the main discharge region where they neutralize the

emitter space charge. This mode of space charge neutralization has many attractive features. The principal ones being:

1. The converter is filled with an inert gas, or a Penning mixture, such as Ne: 0.1%A, and so material and containment problems are at a minimum.

2. Since the formation of ions is by impact in an auxiliary region, there is no restriction on the minimum work function of the emitter material. Thus a suitable emitter material with a work function in the optimum range may be selected.

3. The converter may operate at lower emitter temperatures. With a work function of 2.3 eV a saturation current density of 5 amps/cm^2 is produced at a temperature of 1450^{o} K. This is a reduction in temperature of about 500^{o} K from that of the cesium converter. This temperature reduction is very important because it brings the required design and fabrication technique within the scope of recognized and standard procedures. It also permits versatility since, at a temperature of 2000^{o} K, few materials are available for use and many fabrication problems arise.

4. Since the emitter temperature required is relatively low it comes within the range of heat sources other than nuclear such as regular flame heat. Another important consequence of temperature reduction is the considerable decrease in energy radiated from the emitter. In general, radiation loss is the most important internal loss factor and since the radiation rate varies as the fourth power of the emitter temperature even a small temperature decrease results in considerable savings. For typical cesium and auxiliary emitter temperatures of 2050^{o} K and 1450^{o} K respectively the ratio between the radiation losses is given by

$$\frac{\text{Cesium converter radiation loss}}{\text{A. D. converter radiation loss}} = \left(\frac{2050}{1450}\right)^4 = 4.01$$

So the radiation loss in a typical auxiliary discharge converter is significantly less than that in the cesium converter.

5. Very small interelectrode spacings are not required as in the cesium converter. It is found that a spacing of about 4mm is acceptable. This eliminates the close tolerances and other side effects such as high conductive heat loss encountered with interelectrode spacings of the order of 0.5 mm in the cesium converter.

6. Due to a unique reflection phenomenon discovered by Gabor (16) and his associates the number of ions usually required for space charge neutralization is reduced by a factor in the order of 100. This has been found to reduce the cost of ions from over 0.2 watts/amp in the cesium converter to 0.05 - 0.1 watts/amp in the auxiliary discharge converter (16).

Having analyzed the principal methods available for space charge neutralization, and considered many of the associated disadvantages and advantages, the auxiliary discharge converter appears to present a system which possesses many attractive and unique features. The most objectionable limitation to be found on first analysis is the apparent requirement of a third electrode. But even this is not inherent since the elimination of this electrode may be possible, as is discussed later. As a consequence of the general survey made in the field of thermionic conversion it was decided that an investigation of the auxiliary discharge converter would certainly prove of most benefit.

REVIEW OF LITERATURE

In 1923 G. Hertz published a paper (19) in which a method and apparatus for measuring ionization potentials was discussed. Although no mention was made of energy conversion, the principle of operation depends on the neutralization of space charge by ions produced by an auxiliary electron beam. The tube, as shown in Figure 5, contains two filaments F_1 and F_2, the latter being enclosed in an insulated wire mesh cylinder. The tube filling is neon. Under operation a high accelerating potential, between F_1 and the mesh, accelerates the emitted electrons into the cylinder. Impact ionization takes place inside the mesh when the accelerating potential is great enough. These ions migrate to F_1 under the applied potential V_b and there they serve to neutralize the space charge at the filament F_2 and so permit more electron emission.

Considerably later, in 1952, the principle of auxiliary space charge neutralization was utilized by Johnson and Webster (26) in a continuously controllable gas tube called a Plasmatron. As shown in Figure 6, a plasma acts as conductor between the hot cathode and anode. This plasma depends on the auxiliary system. The electrons emitted from the cathode are focussed into a beam and injected into the main discharge region, where they form ions by impact. The electron supply thus controls the conductivity of the plasma between the emitter and collector. Unlike the thyratron, continuous control of the main current is maintained. Figure 7 shows typical curves for the variation of load current with the collector potential for different auxiliary currents. During the steeply rising part of the characteristics the collector is negative with respect to the plasma and the collected electron current is given by

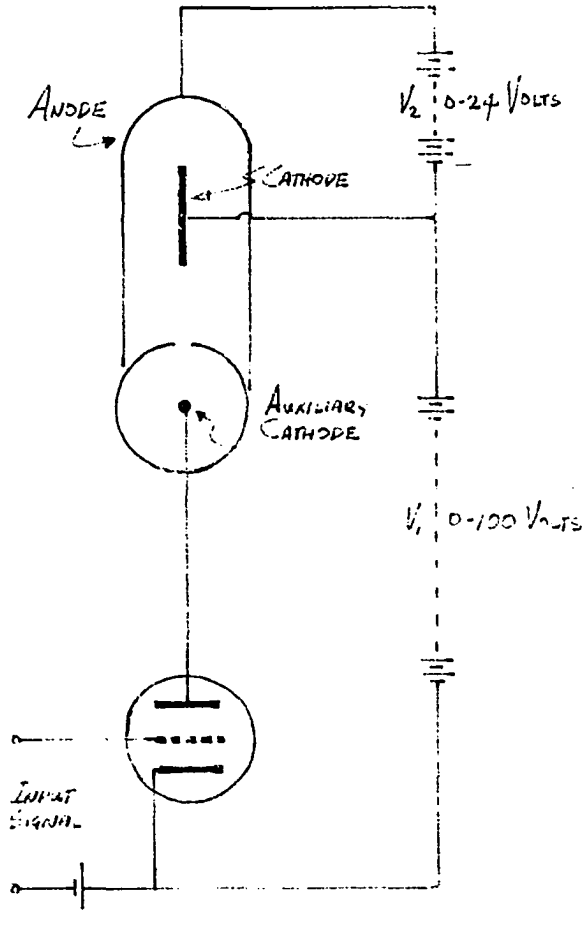

Figure 6. Schematic representation of a Plasmatron tube

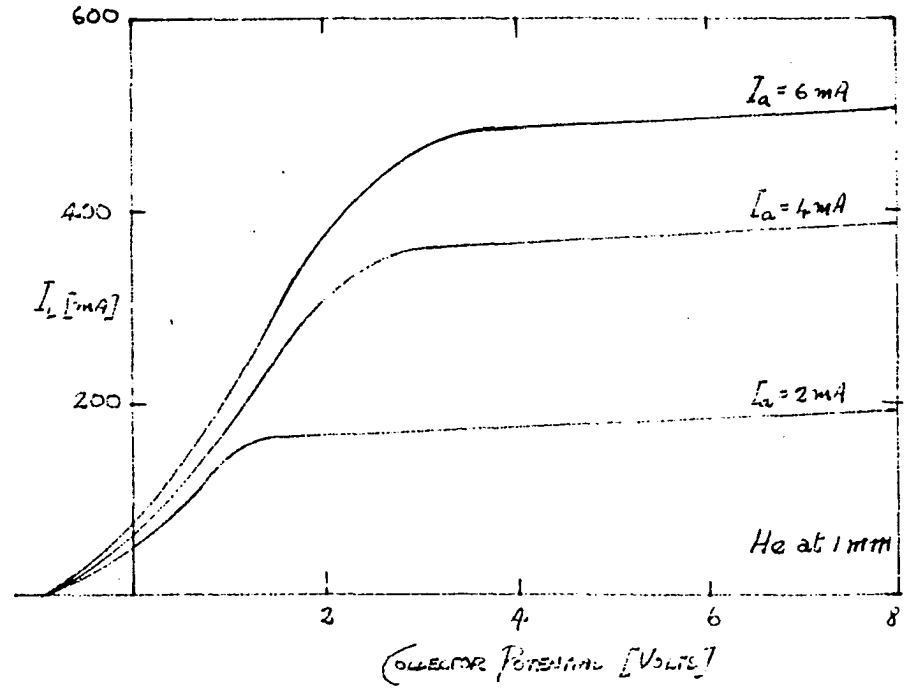

Figure 7. Plasmatron load curves

$$J_c = J_{ec}\, \varepsilon^{-\frac{eV_{cf}}{k\,T_{ec}}}$$

from Langmuir probe theory (9), where J_{ec} is the random electron current in the plasma at the collector sheath, V_{cf} is the collector fall potential, or the potential difference between the plasma and the collector. T_{ec} is the electron temperature at the collector sheath, k is the Boltzmann constant, and e is the electron charge. The knee of the curve corresponds to the point at which the collector is at the plasma potential and receiving all the random electron current. The random electron current is given by

$$J_{ec} = \frac{n_{ec}\, e\, v_{ec}}{4}$$

where n_{ec} and v_{ec} are the density and average velocity respectively of electrons in the plasma at the collector. Since a plasma is considered to have equal electron and ion densities, the value of n_{ec} increases as the auxiliary current is increased and hence the variation of maximum load current with auxiliary current.

Again, as with the Hertz tube, no mention was made in the paper of possible applications to energy conversion. However, the important point is that a source of auxiliary electrons is used to generate ions and these ions serve to neutralize the space charge. The characteristic curves of the Plasmatron indicate that an auxiliary power in the order of 0.3 watts/amp is required for space charge neutralization. This is close to the theoretical cost of 0.2 watts/amp in the cesium converter. How-

ever, the Plasmatron, being simply a control device, is not designed solely with electron and ion conservation in mind and the possibility of the adaption of the method for efficient space charge neutralization in a thermionic converter arises.

Two types of auxiliary discharge converters have since evolved. They are the single electron emitter introduced by Gabor of the Imperial College, London (16) in March, 1961 and the double electron emitter, of Plasmatron mode type, introduced by Bernstein and Knechtli of Hughes Research Laboratories, California (1) in December, 1961. Since then Bloss of the Institut fuer Gasentladungstechnik and Photoelectronik, Stuttgart Germany (4) and Cook and Fraser (11) of the General Electric Co. Ltd., Wambley, England have presented papers dealing with their work on the Plasmatron mode converter. To date, no one other than members of the Direct Conversion group at the Imperial College, London have published work in the Gabor type single emitter converter (13) and no comprehensive theoretical analysis of the auxiliary discharge conversion principle has appeared.

The Plasmatron Mode Auxiliary Discharge Converter

In his paper of 1957 concerning vacuum diode converters, Moss concluded that the required interelectrode spacing of 0.01 mm was impracticable (37). He drew attention to the Plasmatron mode, already described, as a possible means of space charge neutralization. In 1958 Hernquist and Kanefsky (21) considered several methods of space charge neutralization, and, based on the relatively irrelevant figures for ion cost from Johnson and Websters paper (26) on the Plasmatron, they concluded that other methods would be more efficient.

Schultz in 1961 (39) presented an analysis of the Plasmatron mode and using conservative values of 1300° K for the emitter temperature and a current density of 0.9 amps/cm^2 found that the cost of ions could be expected to be as low as 0.1 watts/amp. The reflection of slow ions at the emitter and collector was not considered. This in itself would considerably decrease the already low cost of 0.1 watts/amp. The configuration, Figure 8, suggested is simple and supposedly suitable for operation as a solar energy converter. The principle of operation is the same as that of the Plasmatron. The auxiliary cathode generates ions which are accelerated into the central main discharge region where they form ions by impact with the Ne: 0.1% Argon gas. These ions drift under the plasma drop gradient to the emitter where they neutralize the space charge. A conversion efficiency of 14% is predicted after account is taken of radiation, conduction and auxiliary power losses. Bernstein and Knechtli (1) of Hughes Research Laboratories, California were the first to report, in 1961, on an experimental thermionic converter employing the Plasmatron auxiliary mode. The converter consists of two Phillips-B dispenser cathodes for emitter and collector and three heated tungsten wires, as in Figure 9, which supply the auxiliary electrons for impact ion formation. Operation at an emitter temperature of 1500° K, with a filling of Argon at 1 mm Hg, provides a current of 5 amps/cm^2 with auxiliary currents of $\frac{1}{100}$ to $\frac{1}{120}$ times the emitter current. Under these conditions, the auxiliary power reported is 1 watt, representing an ion cost of only 0.2 watts/amp. This value is very low when the losses associated with such a small experimental device are considered. The fact that the electron to ion current ratio is as large as 120 is of interest in itself. Langmuir's

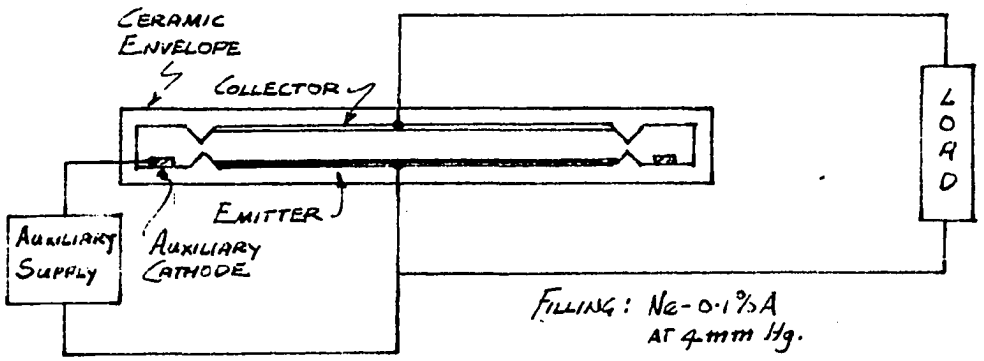

Figure 8. Auxiliary discharge solar energy converter

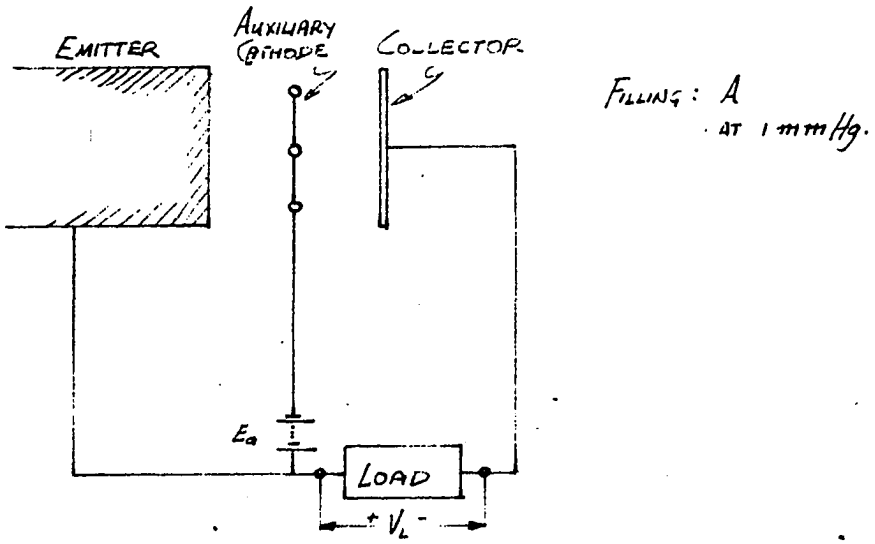

Figure 9. Auxiliary discharge Plasmatron mode thermionic energy converter

accepted sheath theory assumes that one ion neutralizes $\sqrt{\frac{M}{m}}$ electrons in passing through the emitter sheath, where $\frac{M}{m}$ is the ratio of ion to electron mass. In this case $\sqrt{\frac{M}{m}} = 270$. So the very highest ratio of electron to ion current possible should be 270. This assumes that

1. Each auxiliary electron has an ionizing collision
2. No ions are lost from the plasma
3. All ions pass through the emitter sheath only once.

Such assumptions are unjustified in the converter under consideration. Certainly considerable loss due to drift and ambipolar diffussion of ions will take place. Collection of ions by the collector can also be expected. Therefore, the unexpectedly high measured electron to ion current ratio leads to questions about the validity of directly applying the Langmuir sheath theory in this case. Considerable attention will subsequently be given to this problem.

In 1962, Bloss (4) presented a more sophisticated design in which a BaO emitter is used. In order to obtain a low collector work function, a Cs-AgO layer was formed on the glass walls of the containment vessel. This was achieved by first depositing a silver coating and then oxidizing this. A resevoir attached to the side of the containment vessel holds the cesium. The vessel may be heated as required to deposit a new layer of cesium on the silver oxide. However, although the desired low work function collector of 1.0 eV was achieved the converter utilizes cesium and so is subject to the inherent disadvantages of the cesium system. While such an arrangement is unlikely to be adopted in practical converter design, the results, using the low work function collector served to verify the previous theoretical work. Bloss claims mean efficiencies of

8-10% and a maximum value of 20%. While this latter figure should receive further investigation, the mean efficiencies of 8-10% appear realistic and indicate the feasibility of mean efficiencies of 14-16% in larger and more effectively designed converters.

Another interesting point mentioned is the fact that an interface resistance of 5 ohms exists between the base and oxide coating of the emitter and that this may be reduced to 0.5Ω by using an oxide-nickel sintercathode. From this it appears imperative that the sintercathode be used in preference to the usual oxide coated emitter proposed previously by others.

The last paper of interest on the Plasmatron mode is by Cook and Fraser (11). A unique feature of the work is the use of a symmetrical diode in order to permit investigation of different injection systems. Both main electrodes of the tube in Figure 10 are of the same material and heated to the same temperatures. The direction of current flow is governed by the polarity of V_L. The maximum current is limited by the random current in the plasma. Using Xenon as the filling gas in a modification of the tube in Figure 10, ratios of main to beam current of up to 250 are reported. A directly heated thoriated tungsten emitter is used with an oxide collector. Such an arrangement of course requires emitter temperatures above 2000° K and the advantages of low temperature operation permitted by the auxiliary discharge system are not present. A uniform production density is not possible with the configuration as shown in Figure 10. The injected electrons tend to form ions at their mean free path in the filling gas, and, although there is considerable randomization of the positive ions before they pass through the emitter sheath, a

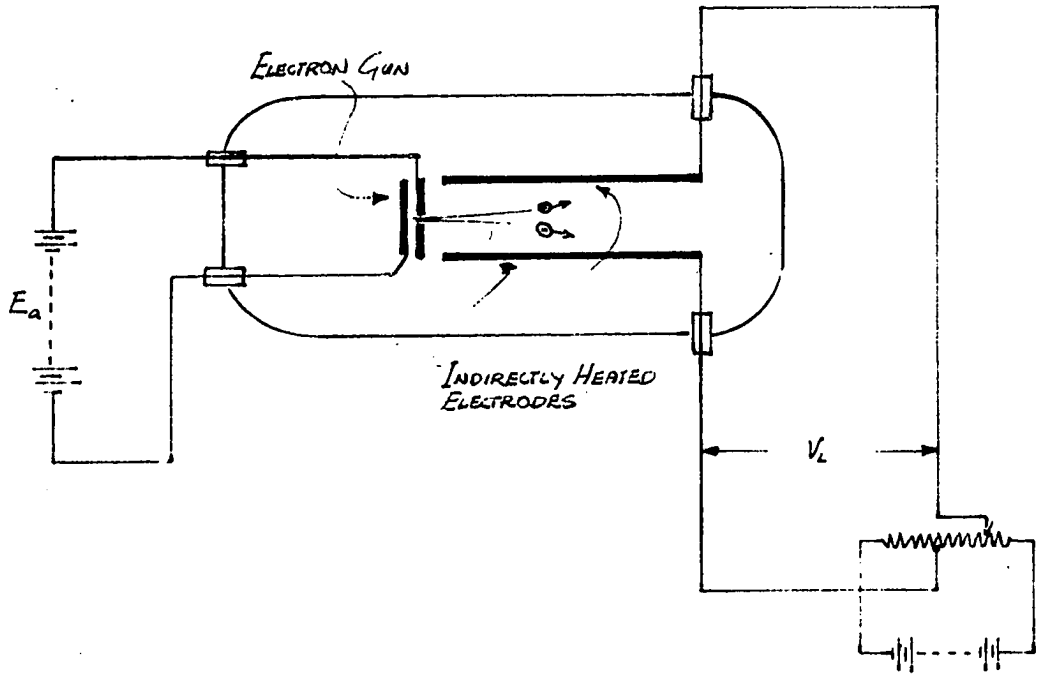

Figure 10. Symmetrical diode for investigation of different injection systems

uniform space charge neutralization cannot be realistically hoped for. This was recognized by Cook and his associates and in a recent visit to the General Electric Research Labs in London, England, they demonstrated a converter with a different configuration. In this more advanced design, electrons are injected from the complete circumference, rather than from one point, and so a more uniform space charge neutralization is hoped for. Tests are underway on this converter. A problem encountered was the requirement of a very small spacing between the auxiliary electron source and the accelerating electrode. It is essential that this be less than the electron mean free path if efficient ion production is to be achieved in the main discharge region, and sputtering of the auxiliary electron source is to be avoided. Although small experimental converters may be successful, it appears difficult to go to large scale units due to the size limitations associated with the electron mean free path.

This completes the analysis of available papers published on the Plasmatron auxiliary discharge converter to date. As is apparent, the system is at an early stage in development, and, apart from the general principle of operation, the configurations proposed vary considerably. Also, in many cases one or more of the attractive features of the auxiliary discharge system were sacrificed on behalf of the others. For example, Bloss introduced cesium in order to achieve a low collector work function. Cook and Fraser (11) resorted to high temperatures and a directly heated emitter in order to obtain a large difference in emitter and collector work functions.

The Gabor Type Auxiliary Discharge Converter

The Gabor type auxiliary discharge converter (16) is unique in its method of generating ions. No auxiliary electron source is required; a small fraction of main discharge electrons being drawn off and accelerated in order to generate the ions. The mode of operation was discovered more or less by accident when Fatmi (13), one of Gabor's associates at the Imperical College, London, was investigating the possibility of slow ion reflection. Since then work has progressed with attention being concentrated on direct energy conversion and investigation of slow ion reflection.

Other than the papers based on research conducted at the Imperial College, no publications on this mode of neutralization have been found. The Gabor mode possesses all of the advantages associated with the Plasmatron mode and in addition does not require an auxiliary source of electrons. For this reason, and the fact that no research, other than that at the Imperial College, has been undertaken in the field it is decided to concentrate the subsequent analysis on the Gabor mode.

No mathematical model of an auxiliary converter operating in the Gabor mode has been published. This in itself certainly deserves attention. Due to the relative geometric complexity, the formulation of such a model poses certain problems and the recognized approaches may not in general be successfully adopted. In the following sections a new approach, which has been based on calculations analogous to those for criticality in the nuclear fission neutron cycle, will be presented.

ANALYSIS OF THE GABOR AUXILIARY DISCHARGE MODE

Basic Configuration

Three electrodes and two separate regions constitute the basic converter configuration. The emitter is the electrode which is heated externally and thermionically generates the electron current which flows into what is termed the main discharge region. The collector is such that most of the electrons approaching within capture range are collected. However a small proportion are permitted to pass through from the main discharge region into an auxiliary discharge region as in Figure 11. Here they are under the influence of the auxiliary anode, an electrode at a relatively high accelerating potential. The load is connected between emitter and collector and an auxiliary supply provides the auxiliary anode accelerating potential. The electrodes are enclosed in a gas filled container.

Principle of Operation

A basic objective of the design is to provide an adequate supply of positive ions at the emitter for space charge neutralization. This is accomplished as follows. When the emitter is heated, some of the eletrons given off cross the main discharge region and a small fraction of these pass through the collector and come under the influence of the auxiliary anode accelerating potential. Since a gas fills the region, these electrons ionize the gas by impact provided the auxiliary anode potential is in excess of the first ionization potential of the gas. The positive ions formed drift towards the collector under the influence of the auxiliary anode potential and the electrons continue towards the auxiliary

anode. A luminous plasma exists in part of the auxiliary discharge region.

Since the positive ions are accelerated towards the collector, many of them pass through into the main discharge region. In this region there now exist electrons, neutral gas atoms and positive ions and so a plasma is formed. This is a dark plasma because in this region no potentials are applied and none are induced to cause internal ionization. Therefore, the plasma of the main discharge region depends on the emitter for its electron supply and on the auxiliary discharge for its positive ion supply.

Assuming the converter is under load there will be a small potential gradient due to plasma resistivity in the main discharge region. Under this potential gradient the positive ions drift towards the emitter where they neutralize the space charge. A typical potential profile for the complete interelectrode system is shown in Figure 12. V_p is the plasma resistivity drop in the main discharge region. V_{Ef} and V_{cf} are respectively the emitter and collector sheath fall potentials. These are typically associated with a plasma where the electron mobility is greater than the ion mobility. Potentials build up at the enclosing surfaces so that compensation is made for the difference in mobility by retarding the electrons and accelerating the positive ions to such an extend that the rates of arrival are equal. Charge equilibrium at the walls is thus maintained.

Variation of Main Plasma Profile with Load

A well known fact in plasma physics is that the variation of the load current drawn from the main discharge region has little effect on the magnitude of the emitter fall potential V_{Ef}. It is the collector fall

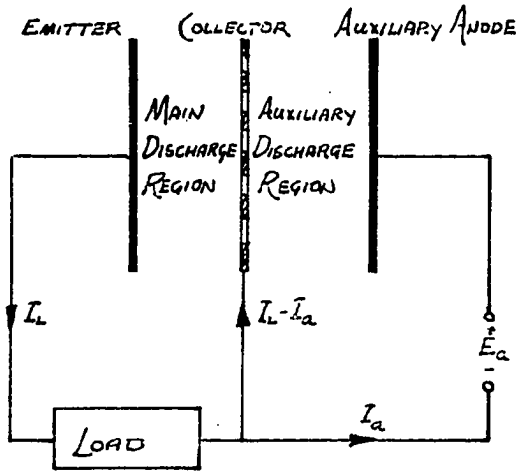

Figure 11. Auxiliary discharge Gabor mode thermionic energy converter

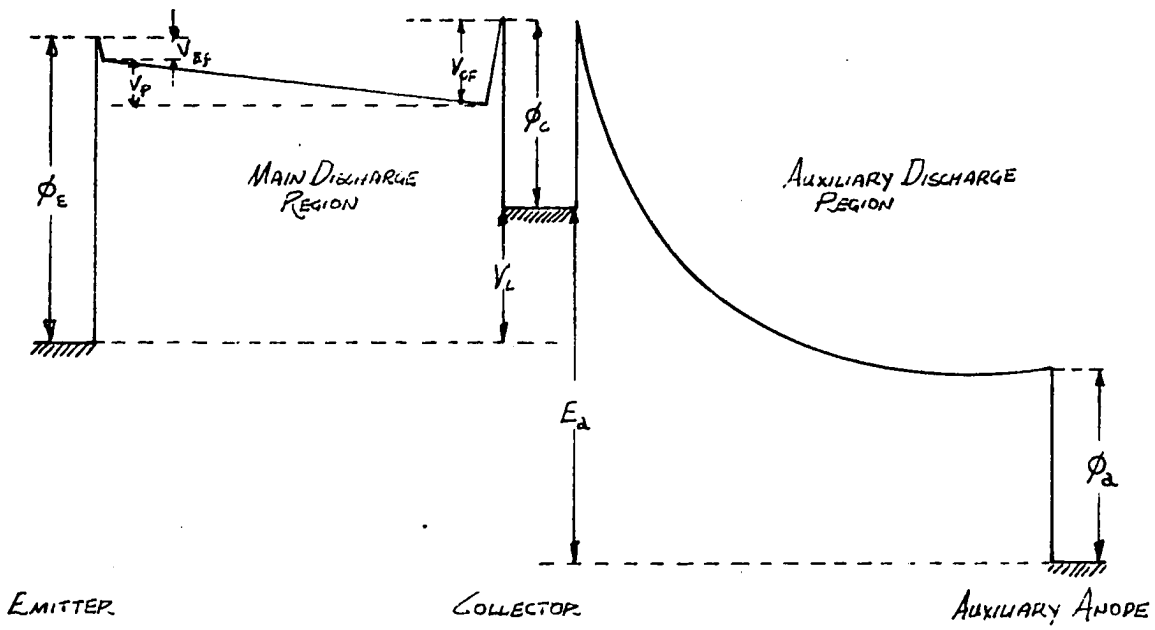

Figure 12. Interelectrode potential profile for operation in the Gabor mode

potential V_{cf}, which is influenced by this load current. In fact, V_{cf} may be imagined as a wall of an electron filled resevoir. When the load is light, V_{cf} is large and few electron "overflow" to the load circuit. As more current is required, V_{cf} decreases, permitting an increased flow of electrons. When V_{cf} is zero, the flow is a maximum, and is in fact equal to the random plasma electron current $J_{ec} = \frac{n_{ec} e v_{ec}}{4}$ at the collector.

The plasma resistivity potential drop varies with load current. Under open circuited conditions the plasma is equipotential and under loaded conditions V_p may be thought of as the potential that causes preferential drift of electrons from the emitter to the collector, and consequently a preferential drift of positive ions from collector to emitter.

The emitter fall potential is not greatly influenced by the variation of load current but rather by the conditions in the plasma at the emitter sheath. It is a plasma characteristic that the potential profile of the plasma locks onto the most positive electrode. Typical profiles are shown in Figure 13 for different collector potentials. For profiles corresponding to collector voltages V_1 and V_2, the emitter is positive relative to the collector and no change in the emitter fall potential takes place as the collector potential is varied. However, for the profiles with collector potentials, V_4 and V_5, greater than the emitter potential the profile locks to the collector and in these cases the emitter fall potential is not independent of load.

In subsequent work it will be assumed that the emitter fall potential is independent of load. The collector drop potential, as well as the plasma resistive drop potential, varies with the load current drawn from

the plasma, whereas the emitter fall potential is considered virtually independent of load variations but subject to plasma characteristics. Another specification regarding the profile is that operation is not under emitter temperature limited conditions. In other words, the electron source is emitting a number of electrons which is equal to or greater than the number capable of being neutralized by the positive ion source. In the latter case a double sheath will exist at the emitter in order to return excess electrons to the emitter. The form of the profile under such a condition is as in Figure 14. There V_{min} is the potential minimum at the emitter. Its value is governed by the rate of electron emission from the emitter and the arrival rate of positive ions for space charge neutralization. All electrons emitted with kinetic energies less than e V_{min} fail to penetrate the potential barrier and enter into the plasma. In general, optimum operating conditions are achieved just at the commencement of space charge limitation, when V_{min} is approximately zero with respect to the other potential magnitudes of the profile and may be neglected. However the finite magnitude of V_{min} will be shown to be of importance in a different aspect of the converter operation. At light loads there is therefore no double sheath, while under operating conditions V_{min} is finite but negligible.

Potential Profile in Auxiliary Discharge Region

The electrons which penetrate the collector are accelerated by the potential E_a applied to the auxiliary anode. Under operating conditions, E_a is set slightly above the first ionizing potential of the filling gas so that there is a good probability (in the range of 0.5) of an inelastic

electron-gas atom collision. Initially, a linear potential profile between collector and auxiliary anode may be assumed. However, when ionization takes place, the presence of positive ions produces a depression in the potential profile which in turn results in a high potential gradient at the collector. Thus, most of the ionizing electron-atom collisions take place close to the collector. This causes a glow to be seen above the collector. Almost all of the applied potential E_a is dropped across the narrow collector sheath and the thickness of this sheath varies with the electron mean free path. The profile is of the general form shown in Figure 15. Most of the region is at a low potential gradient. This corresponds to the so called "positive column" of the classical low-pressure glow discharge and it merely serves to maintain a conducting path between the two electrodes. With this in mind, it should be noted that as far as the ion production process is concerned it can be considered independent of the positive column. Thus in the design of the auxiliary region the positive column dimensions may be selected to minimize ion loss due to amkipolar diffusion and recombination.

Slow Ion Reflection

A most important factor in the operation of the auxiliary discharge converter is the phenomenon of slow ion reflection. This was first observed by Gabor (17) when he investigated the characteristics of the auxiliary discharge converter and found a surprisingly small ratio (1:100) between the auxiliary and main currents. He investigated further by conducting an analysis of the plasma and found a ratio of electron to ion current density of 24,000. From Langmuir's theory (31) of 1929 a ratio

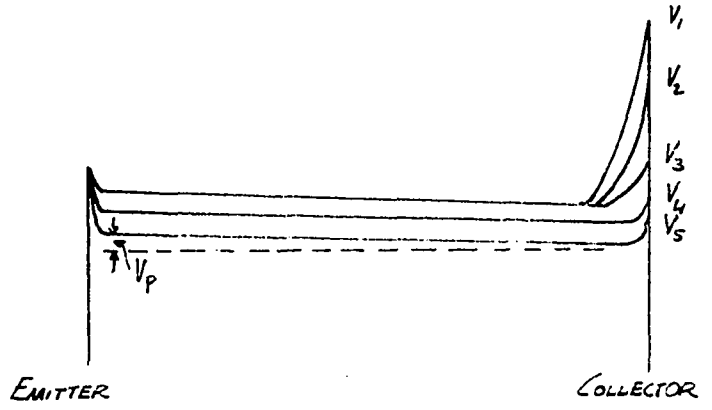

Figure 13. Potential profiles for operation with different collector potentials

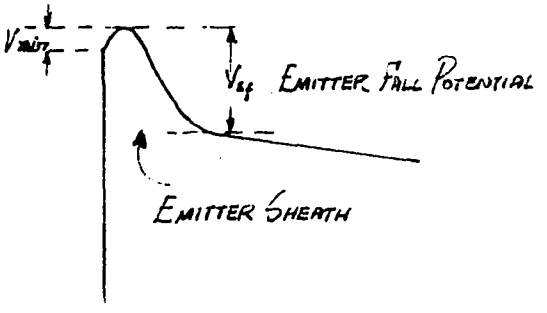

Figure 14. Double sheath potential profile at the emitter

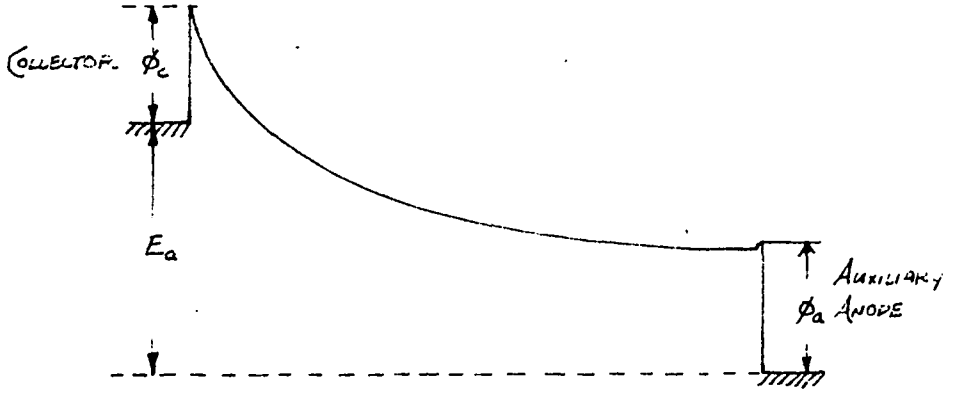

Figure 15. Potential profile in the auxiliary discharge region

of only $\sqrt{\frac{M}{m}} = 270$ would be expected. However, in this theory it is assumed that all ions are absorbed when they reach the emitter surface. The discrepancy between theory and practice of a factor of 90 is explained by the reflection of slow ions at the emitter surface. In this way ions oscillate in the emitter sheath and so are much more effective for space charge neutralization than if they passed through the sheath only once.

A high reflection coefficient for slow ions is certainly theoretically possible. The potential drop ϕ_E associated with the work function at the emitter surface is a repellent barrier for ions. Ions with a kinetic energy less than $\phi_E e$ penetrate one, or at most two, atomic layers and spend only about 10^{-13} sec in the emitter. It is therefore not unlikely that they will emerge without being neutralized. If the probability of such a reflection is R, then ions on the average make $1 + 2R + 2R^2 + 2R^3 + \ldots = \frac{1 + R}{1 - R}$ passages through the emitter sheath before being neutralized. In this way a reflected ion is $\frac{1 + R}{1 - R}$ times more effective in neutralizing the space charge than one which is immediately neutralized. Therefore the results of Gabor's experiment are explained by an effective reflection coefficient such that $\frac{1 + R}{1 - R} = 90$, which corresponds to $R = 0.98$.

A more detailed examination of the conditions existing in the emitter sheath and already described, is certainly called for.

In the reflection phenomenon it is assumed that ions which are reflected at the emitter traverse the whole emitter sheath and return to the plasma, from where they return after several collisions to the emitter sheath. Such ions are termed "pendulating ions". Although the thickness of the emitter sheath under operating conditions is less than the ion

mean free path, there is a probability of a pendulating ion colliding with a neutral atom within the sheath. The mean energy of the ions in the emitter sheath is greater than that of the neutrals there and so it is likely that the pendulating ions lose some kinetic energy on colliding. If the loss is sufficient, the ions become trapped in the sheath. Gabor estimates that 58% of the space charge neutralization is due to trapped ions. As these ions have even less energy than the pendulating ions it is likely that they are reflected at the emitter with a higher probability. So actually the reflection coefficient R is only an effective value and incorporates the contribution made by both the pendulating and the lower energy trapped ions. This effective value will be used as the reflection coefficient in the subsequent presentation.

The phenomenon of a high I_o/I_a ratio is not peculiar to Gabor's work. Just after he made the observation, Bernstein and Knechtli (1) of Hughes Research Laboratory, California reported a similar high ratio of $I_o/I_a = 120$. They were not sure of the cause but did suggest that reflection might be the factor involved. It is all the more significant that their results were obtained with a single gas, argon, where recombination could be expected to cause a reduction in the current ratios.

Characteristics of Filling Gas

All auxiliary discharge converters contain some form of filling gas. This gas is required so that it may be ionized for space charge neutralization purposes. The choice of a suitable gas or mixture of gases is governed chiefly by the requirements of a high ionization coefficient, and a low recombination coefficient under operating conditions.

Several single gases are acceptable. For example argon has readiative and dissociative recombination coefficients of $\alpha_1 = 2 \times 10^{-10}$ cm^3/sec and $\alpha_2 = 3 \times 10^{-7}$ cm^3/sec respectively and an ionization coefficient of 1.8×10^{-3} ion pairs/volt at 15 volts/cm mm Hg. Neon has similar recombination coefficients and an ionization coefficient of 8×10^{-3} ion pairs/volt. However both argon and neon have relatively large excitation probabilities. This is a disadvantage since power is wasted in exciting these atoms without causing ionization. A considerable saving may be acheived by using a suitable mixture of different gases called a Penning mixture (20). With an optimum mixture of argon and neon, the ionization coefficient may be increased to as much as 38×10^{-3} ion pairs/volt.

Explanation for the increase is as follows. Certain atoms such as Hg, He, and Ne, have excited energy levels from which the quantum theory selection rules prohibit transition to lower levels. When such is the case, the atom is said to be in a metastable state (12). It must remain in this condition until it has an accidental encounter, for example, (a) with an electron or a photon which may raise it above the metastable state to one from which it can decay, or (b) with another atom. The latter case is called a "collision of the second kind". Kinetic energy may be interchanged in such a collision so that the electron is raised to a higher level, or drops to a lower level. Only relatively small amounts of kinetic energy may be interchanged in this way so that the normally excited levels must be very near the metastable level. When atoms of other elements are present the excess energy of the metastable atom may be given up in exciting or ionizing one of these other atoms. Since all of the encounters by which a metastable atom can gain or lose energy are

special and therefore relatively unlikely to occur, the life of a metastable state is very long. The average life of a metastable state is of the order of 10^{-3} sec compared with the average life of a normal excited state of the order of 10^{-8} sec.

The energy level diagrams for neon and argon are shown in Figure 16. A neon atom, when bombarded by an electron, may be ionized if excited above 21.56 volts, or excited to lower energy levels. Two of the three energy levels are metastable, from which the excited atom cannot return to the ground state by radiation. The first ionization energy of argon is 15.76 volts so that if a metastable neon atom at 16.62 or 16.53 volts collides with it there is a good probability, particularly in the latter case, that there will be a kinetic energy transfer and ionization of the argon. In this way, the energy which normally would be lost in exciting the neon atom is available for ionization of the argon atom. An optimum neon-argon mixture exists which is seen from Figure 17, to be a ratio of 1000 parts neon to one part argon. Several other Penning mixtures are available, such as He-A, A-Hg, and Ne-Br_2. However, the Ne-A mixture seems to be the most commonly used one and there is considerable data available for it. The A-Hg mixture has been used by Gabor in some of his converters

A Cyclic Theoretical System Model

Lossless cycle

Due to the relatively complex triode configuration of the auxiliary discharge converter it is very difficult to formulate a theoretical model using recognized techniques. For this reason, none has been presented in

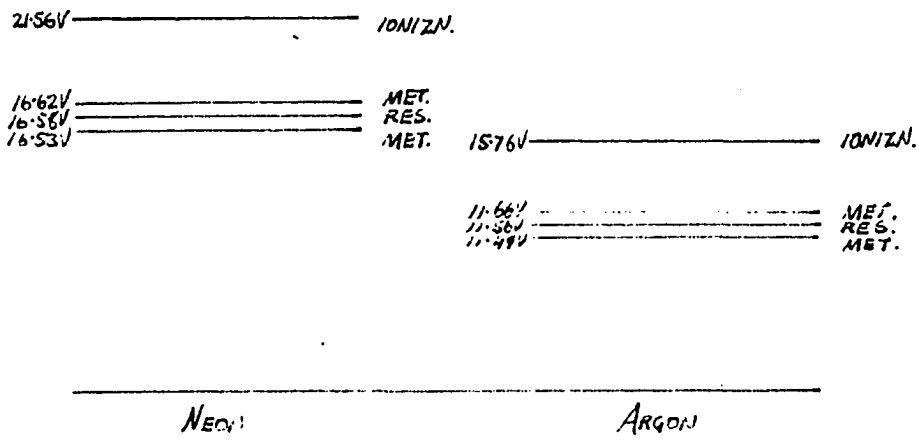

Figure 16. Energy level diagrams for neon and argon

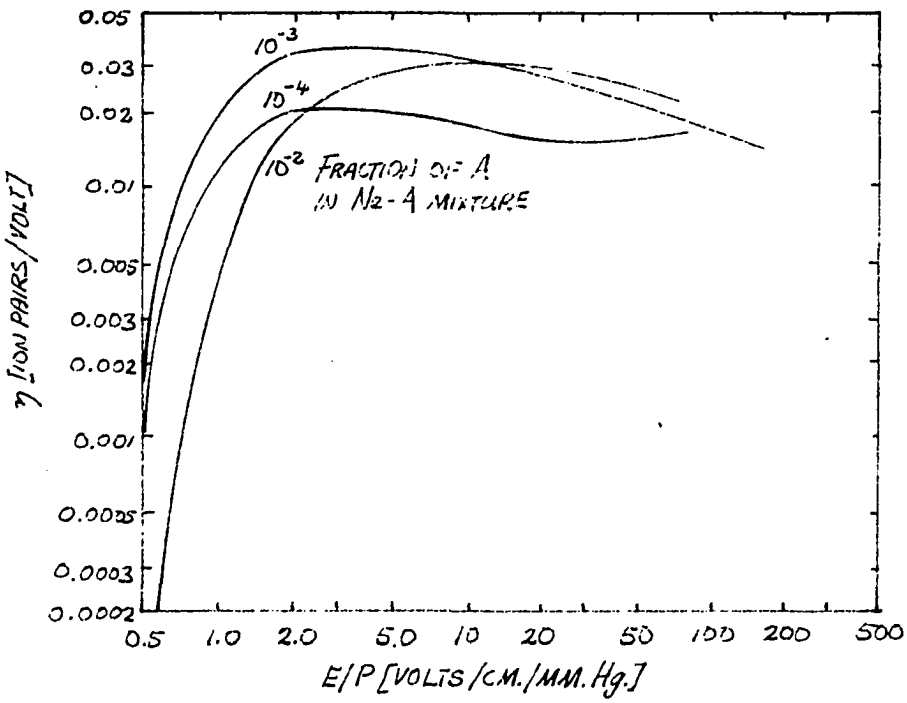

Figure 17. Variation of the ionization coefficient for various neon-argon mixtures

the literature. In the following section a new and very different means of formulation will be described and the many system parameters involved will be presented in the form of a single critical equation which must be satisfied for equilibrium operation. An analysis of the transient behavior of the converter will be undertaken also. In both cases the final equations will be of such a form that the parameters which they contain may all be evaluated from recognized experimental techniques, such as those developed by Langmuir for plasma probe analysis. Account will also be taken of the very recent and important discovery of slow ion reflection.

Initially, an analysis was attempted using the accepted techniques similar to those presented by Talaat (42) for the relatively simple case of the cesium filled diode. His approach, and that used in general for other diode analysis, is based on balance equations at the two electrode plasma sheaths, as well as on an overall voltage equation. The balance equations are those for current, charge and energy at both the emitter and collector plasma sheaths. If an attempt to write such equations for the auxiliary discharge converter is made, complications arise due to the presence of a dark and a luminous plasma, each dependent on conditions in their respective locations, as well as being interdependent on each other. The plasma conditions at the collector itself are extremely complicated. On the emitter side a dark plasma exists, while at the auxiliary anode side there is a luminous plasma. Since the collector is perforated there is a transition region within the perforations, whose characteristics are governed not only by both of the plasmas, but also by the geometic configuration of the collector. Even if the problems of analysis at the collector

could be overcome and balance equations written for both regions the resultant expressions would be both numerous and complex, so that their solution would in itself prove cumbersome. Also no means is provided for determining the important slow ion effective reflection coefficient, R.

In order to avoid these problems several approaches were attempted. Finally, when working on a nuclear criticality problem, it was realized that an analogy could be drawn between the neutron cycle in a controlled nuclear fission cycle and the electron-ion cycle in the Gabor type auxiliary discharge converter.

In fact a theory may be developed in a manner similar to the "Two-Group Theory" presented by S. Glasstone and M. Edlund (18). The initial approach is to assume electrodes of infinite area in which there is no electron or ion loss due to mutual recombination. Furthermore, due to the infinite extent of the electrodes, the ambipolar diffusion loss is zero. The operating cycle is depicted in Figure 18. The ionization by impact of electron and gas atoms corresponds to fission produced by thermal neutrons and the resulting ions produced correspond to the fast neutrons emitted along with the fission fragments. Therefore p_i, the ionization probability, corresponds to η, the number of fast neutrons produced per thermal neutron absorbed. A fraction, $(1 - k_m)$, of the ions are lost to the collector before returning to the main discharge region. This corresponds to resonant capture of the fast neutrons and so k_m corresponds to p, the resonant escape probability. Electrons emitted from the emitter correspond to thermal neutrons and the fractions, α, of these which enter the auxiliary discharge region correspond to the thermal neutrons which escape capture, while thermalized, and cause a nuclear fission.

Assuming that the converter is operating under space charge limited conditions, it is required that $\sqrt{\frac{m}{M}}$ ions pass through the emitter sheath for each electron emitted. Thus, for an electron emission rate of $\frac{J_o}{e}$ an ion arrival rate of $\frac{J_o}{e}\sqrt{\frac{m}{M}}$ is required if ion reflection is considered negligible. In the simple cycle considered $p_i\ k_m \alpha \frac{J_o}{e}$ ions arrive when $\frac{J_o}{e}$ electrons are emitted. For equilibrium conditions

$$\frac{J_o}{e} = \alpha\ p_i\ k_m \sqrt{\frac{M}{m}}\ \frac{J_o}{e}$$

$$1 = \alpha\ p_i\ k_m \sqrt{\frac{M}{m}} \qquad (2)$$

Equation 2 is analogous to the "Four-factor Formula" of nuclear reactor theory. It is interesting to make very rough estimates of the order of p_i, k_m, and $\sqrt{\frac{M}{m}}$ in order to find the order of magnitude of α, the fraction of electrons which escape capture by the collector and are permitted to enter the auxiliary region. p_i can be expected to be of the order of 0.25, k_m will be shown to be proportional to the fractional apperture of the collector and so can be assumed at 0.5, while for a gas such as argon or neon $\sqrt{\frac{M}{m}}$ is about 200. Therefore

$$\alpha = \frac{1}{p_i\ k_m \sqrt{\frac{M}{m}}} = \frac{1}{0.25 \times 0.5 \times 200} = \frac{1}{25}\ .$$

Thus, under the above idealistic conditions one out of each 25 electrons emitted is required by the auxiliary discharge for the productions of ions. This initial very approximate analysis serves to show the feasibility of the system in that the drain on the main supply of electrons for

ion production does not amount to a large fraction of the whole. A more detailed analysis is justified.

Cyclic analysis considering losses

In the previous analysis electrodes of infinite area were considered and it was hence assumed that loss of ions and electrons by ambipolar diffusion was zero. Also, mutual recombination of ions and electrons within the interelectrode space was considered negligible, as was the recollection of electrons at the emitter. We now consider finite circular electrodes of radius r and area A separated by an axial distance d between emitter and collector and by a distance H between collector and auxiliary anode, as shown in Figure 19. It is assumed that recombination occurs and that a certain fraction of the emitted electrons are recollected, and that a certain fraction of the ions are absorbed by the collector. The important phenomenon of slow ion reflection will also be taken into account.

In the formulation of the following theory it is assumed that the potential profile already discussed and shown in Figure 12 is present. In Figure 20 electrons are accelerated into the plasma by the potential V_{Ef} at a rate of $\frac{J_o}{e}$ electrons/sec cm^2. Most of these do not return from the plasma to the emitter due to the retarding potential profile. However, assuming that they have a Maxwellian velocity distribution within the plasma, a fraction, $(1 - p_E)$, have sufficient energy to overcome the potential V_{Ef} and return to the emitter. Therefore, the net rate of electron injection from emitter to plasma is $\frac{J_o}{e}\ p_E$ electrons/sec cm^2. Within the plasma, the electrons are subjected to two types of electrostatic

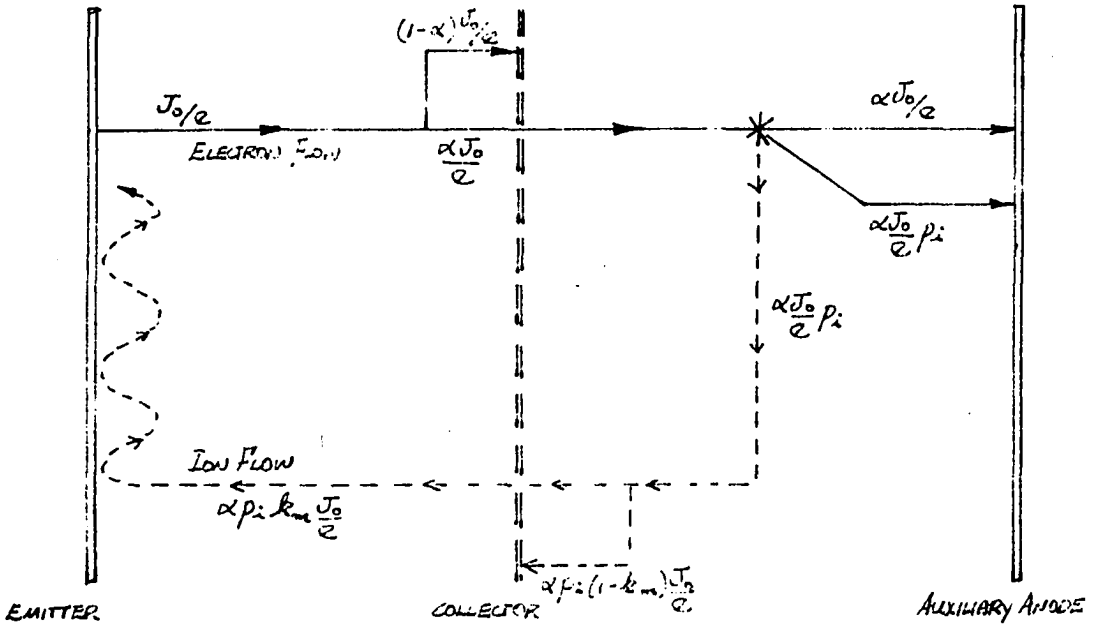

Figure 18. Operation cycle for a Gabor mode auxiliary discharge system with electrodes of infinite area

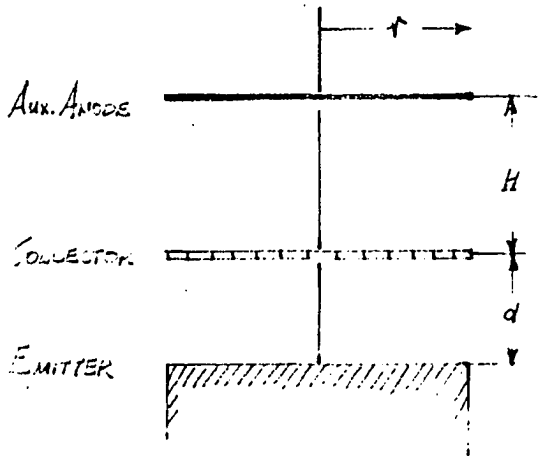

Figure 19. Schematic of electrode system

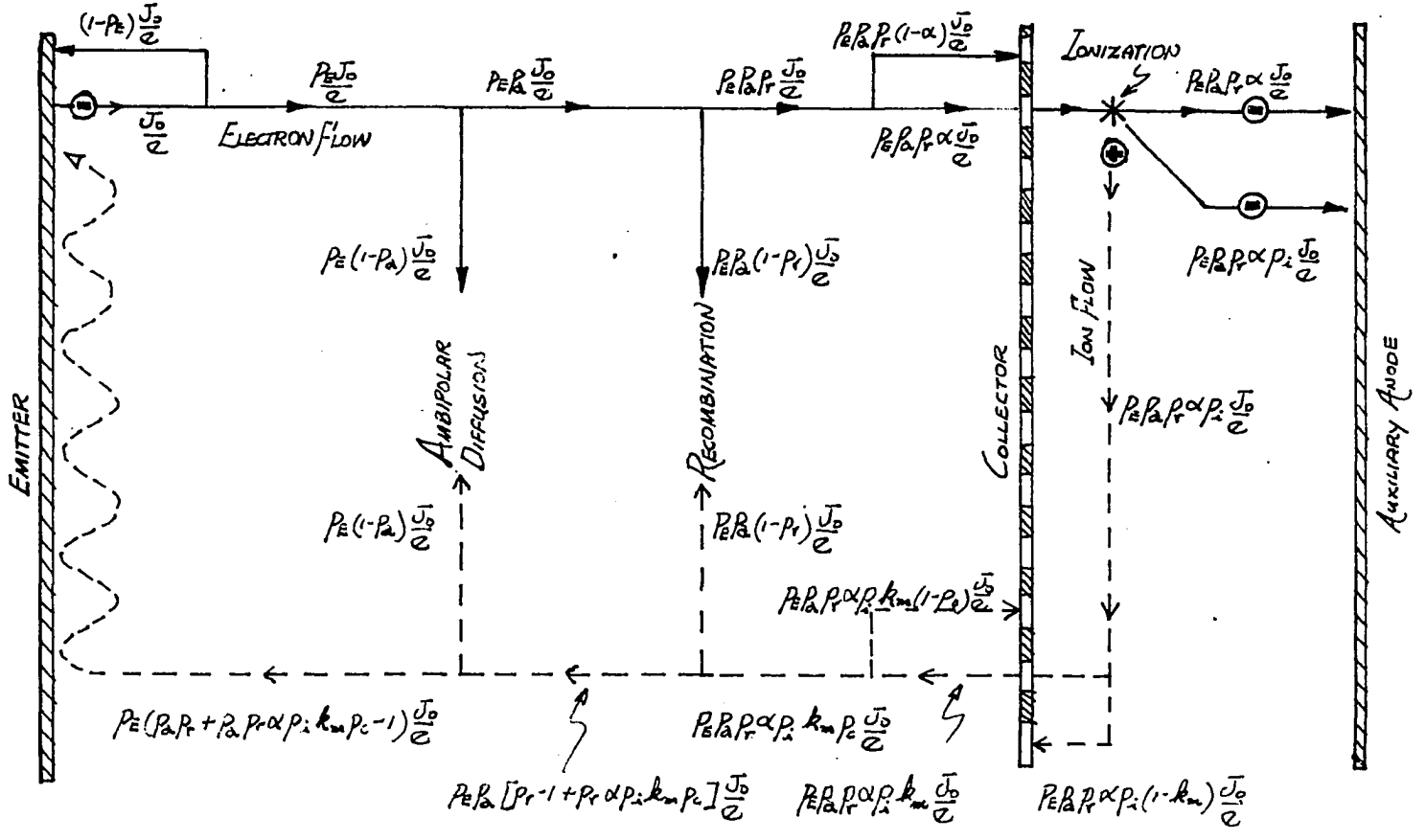

Figure 20. Operating cycle for a Gabor mode auxiliary discharge system

forces. The main force caused by the potential V_p results in a drift to the collector. However, in a finite system there is also radial ambipolar diffusion. This is of consequence when the electron and ion densities in the plasma are high. Although high densities are not used in practice, ambipolar diffusion will be considered here for completeness. When there is no interaction between the electrons and ions in a plasma, the density of both, at any given point, must be the same to maintain charge equilibrium. However, when the density is high, the electrons and ions interact. Consider the case of an arbitrary density distribution in space at time t = 0 as represented in Figure 21a. The electrons, whose mass is much less than that of the ions, diffuse faster and so the distribution in Figure 21b would be expected. However, when this occurs, an electric field results which accelerates the ions towards the low density regions yet retards the electrons, so that under equilibrium conditions the flow rates of ions and electrons from the high density region are equal. The electrons and ions which diffuse ambipolarily recombine in general when they reach the walls of the containment vessel. It is now assumed that a fraction, $(1 - p_a)$, of the electrons which do not return to the emitter are lost from the plasma by ambipolar diffusion. Therefore, the rate of electron loss from the plasma is $p_E(1 - p_a) \frac{J_o}{e}$ electrons/sec cm^2. The rate of ion loss must then also be the same.

Recombination of ions and electrons to form a neutral gas atom or molecule constitutes another cause of electron loss from the plasma. It is assumed that $(1 - p_r)$ is the probability that an electron which has not returned from the plasma to the emitter or suffered an ambipolar diffusion will recombine with a positive ion to form a neutral atom or molecule.

Therefore, the loss rate of electrons from the plasma due to recombination is $p_E p_a (1 - p_r) \frac{J_o}{e}$ electrons/sec cm^2. A similar rate of ion loss is therefore assumed. Ambipolar diffusion and recombination constitute the principle means of electron loss from the plasma; therefore, the rate of arrival of electrons at the collector, under equilibrium conditions, is $p_E p_a p_r \frac{J_o}{e}$ electrons/sec cm^2. Of these, a fraction α are assumed to penetrate through into the auxiliary discharge region so that the rate of absorption of electrons by the collector is $p_E p_a p_r \alpha \frac{J_o}{e}$ electrons/sec cm^2 and the rate of arrival of electrons in the auxiliary discharge region is $p_E p_a p_r (1 - \alpha) \frac{J_o}{e}$ electrons/sec cm^2. In the auxiliary region, the predominant force is that due to the accelerating potential E_a and so ambipolar diffusion & recombination are neglected. If the probability of impact ionization between an electron and a gas atom or molecule during the time an electron is being accelerated from the collector to the auxiliary anode is p_i, the rate of ion production is $p_E p_a p_r \alpha p_i \frac{J_o}{e}$ ions/sec cm^2. As in the infinite case, it is assumed that a fraction k_m of these ions penetrate the collector and enter the main discharge region. Thus, the rate of arrival of ions in the main discharge region is $p_E p_a p_r \alpha p_i k_m \frac{J_o}{e}$ ions/sec cm^2.

Due to the potential profile at the collector, slow ions are attracted to it from the main plasma. However, due to the phenomena of slow ion reflection, the number of these ions actually absorbed is relatively small. Let $(1 - p_c)$ be the probability that a slow ion is absorbed by the collector from the main discharge region. Then, the net rate of arrival of slow ions into the main discharge region is $p_E p_a p_r \alpha p_i k_m p_c \frac{J_o}{e}$ ions/sec cm^2. These ions are subject to ambipolar diffusion and recombination,

but the rate of loss is the same as for electrons and has already been calculated. Therefore, the rate of ion arrival at the emitter is

$$p_E p_a p_r \alpha p_i k_m p_c \frac{J_o}{e} - p_E(1 - p_a) \frac{J_o}{e} - p_E p_a(1 - p_r) \frac{J_o}{e} \text{ ions/sec cm}^2,$$

or

$$p_E(p_a p_r \alpha p_i k_m p_c + p_a p_r - 1) \frac{J_o}{e} \text{ ions/sec cm}^2. \qquad (3)$$

These ions which reach the emitter are not immediately absorbed but according to Gabor (17) are reflected with a probability R. As a result, each ion makes an average of $\frac{1 + R}{1 - R}$ passages through the emitter sheath and so as far as space charge neutralization is concerned each ion, which is eventually absorbed by the emitter, does the work of $\frac{1 + R}{1 - R}$ ions. Now, from Langmuir's classical probe theory an unrejected ion of mass M can neutralize the space charge due to the single passage of $\sqrt{\frac{M}{m}}$ electrons through the emitter sheath. Therefore, when reflection is considered, one ion can neutralize $\left[\frac{1 + R}{1 - R}\right] \sqrt{\frac{M}{m}}$ electrons on the average. Therefore, $p_E(p_a p_r \alpha p_i k_m p_c + p_a p_r - 1) \frac{J_o}{e}$ ions neutralize

$$p_E(p_a p_r \alpha p_i k_m p_c + p_a p_r - 1) \frac{J_o}{e} \left[\frac{1 + R}{1 - R}\right] \sqrt{\frac{M}{m}} \text{ electrons.}$$

But the rate of electron emission is initially $\frac{J_o}{e}$ electrons/sec cm^2 and the rate of electron return through the emitter sheath is $(1 - p_E) \frac{J_o}{e}$ electrons/sec cm^2; therefore, the total electron space charge neutralized by the ions is associated with an electron flow rate through the sheath of

$$\frac{J_o}{e} + (1 - p_e) \frac{J_o}{e} = (2 - p_E) \frac{J_o}{e} \text{ electrons/sec cm}^2 \qquad (4)$$

Therefore,

$$(2 - p_E)\ \frac{J_o}{e} = p_E(p_a p_r\ \alpha\ p_i\ k_m\ p_c + p_a p_r - 1)\ \frac{J_o}{e}\ \frac{(1 + R)}{(1 - R)}\ \sqrt{\frac{M}{m}},$$

which becomes

$$(p_a p_r\ \alpha\ p_i\ k_m\ p_c + p_a p_r - 1)\ \frac{p_E}{2 - p_E}\ \sqrt{\frac{M}{m}}\ \left[\frac{1 + R}{1 - R}\right] = 1 \qquad (5)$$

Equation 5 is the critical auxiliary discharge equation and must be satisfied for equilibrium conditions when the system is operating under space charge limited conditions.

Determination of Terms in the Critical Equation

The basis of the approach to the theoretical model of the auxiliary discharge thermionic converter having been presented, it is now necessary to find a means of determining each of the parameters of the critical equation. Therefore, it is necessary to express each in terms of plasma or electrode properties which may be experimentally observed by means of recognized methods. Thus, temperature, pressure and linear dimensions as well as electron temperature and density are acceptable.

Probability of reabsorption of emitted electron

It is assumed that $\frac{J_o}{e}$ primary electrons per second enter the plasma from the emitter and that the probability of such an electron being reabsorbed by the emitter is $(1 - p_E)$. Therefore we can write

$$1 - p_E = \frac{\text{Rate of electron return to emitter}}{\text{Rate of electron emission from the emitter}}$$

In order to calculate the rate of electron return to the emitter, it is necessary to know the random electron current in the plasma at the emitter. This may be expressed, in terms of the average electron concentration n_{eE} in the plasma at the emitter and the average electron velocity v_{eE}, as $\frac{n_{eE}\, e\, v_{eE}}{4}$. The average electron velocity may be related to the electron temperature by

$$v_{eE} = \sqrt{\frac{8k\, T_{eE}}{m\pi}},$$

where T_{eE} is the electron temperature in the plasma at the emitter and k is the Boltzmann constant. Due to the presence of a retarding potential V_{Ef} at the emitter, the current which penetrates the barrier is less than the random current but is exponentially related to it by

$$\exp\left[-\frac{e\, V_{Ef}}{k\, T_{eE}}\right].$$

The electron current from the plasma to the emitter is then

$$n_{eE}\, e \sqrt{\frac{k\, T_{eE}}{2\pi\, m}} \quad \exp\left[-\frac{e\, V_{Ef}}{k\, T_{eE}}\right]$$

and the rate of electron return to the emitter is

$$n_{eE} \sqrt{\frac{k\, T_{eE}}{2\, \pi\, m}} \quad \exp\left[-\frac{e\, V_{Ef}}{k\, T_{eE}}\right].$$

The probability of an emitted electron being reabsorbed by the emitter is then

$$1 - p_E = \frac{n_{eE}\, e}{J_o} \sqrt{\frac{k\, T_{eE}}{2\pi\, m}} \exp\left[- \frac{e\, V_{Ef}}{k\, T_{eE}} \right] \qquad (6)$$

The electron temperature T_{eE} is the sum of the electron temperature as it leaves the emitter and $\frac{e}{k}\ V_{Ef}$, which corresponds to the increase in electron temperature on entering the plasma through the net potential difference of V_{Ef} volts at the emitter sheath.

Probability of ambipolar diffusion of electrons

The probability of ambipolar diffusion of electrons from the main discharge region is

$$1 - p_a = \frac{\text{Rate of ambipolar electron diffusion}}{\text{Rate of electron production}}$$

As was discussed previously, under equilibrium conditions, an electrostatic field develops which causes equalization of the rate of electron and ion diffusion to the walls of the containment vessel. In other words $\vec{\Gamma}_+ = \vec{\Gamma}_e$, where $\vec{\Gamma}_+$ and $\vec{\Gamma}_e$ are the ambipolar flow rates of the ions and electrons respectively. It is therefore possible to write flow equations for the ions and electrons, where it is assumed that the electron and ion distribution is symmetrical about the axis of the cylindrical containment vessel of radius r and height d as in Figure 22.

Considering the positive ions, the flow equation may be written as

$$\vec{\Gamma}_+ = n_+ \vec{v}_+ = -D_+ \nabla n_+ + \mu_+ n_+ \vec{E}_s \qquad (7)$$

where n_+ and $\vec{v}_+$ are the positive ion density and velocity respectively at a point (a,ϕ,z) within the vessel and D_+ and μ_+ are the average diffusion

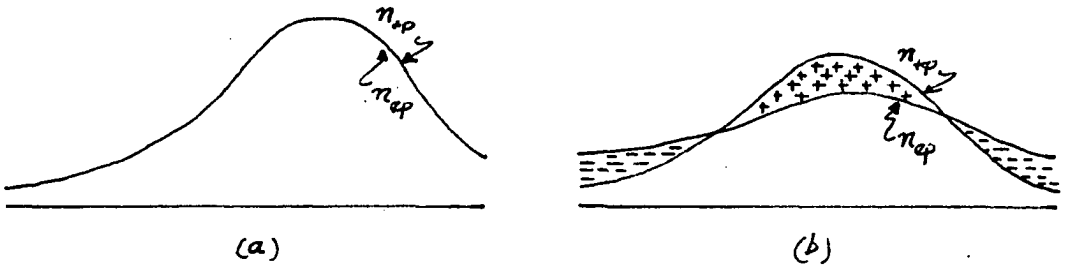

Figure 21. Electron and ion density distribution (a) before and (b) during ambipolar diffusion

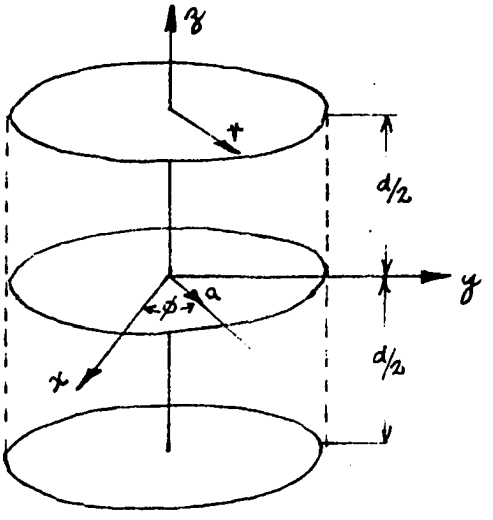

Figure 22. Plasma containment vessel showing dimensions used in ambipolar diffusion calculations

coefficient and average mobility (8) respectively. $\vec{E}_s$ represents the field produced by the space charge. Expressed in terms of velocity Equation 7 becomes

$$\vec{v}_+ = \frac{-D_+ \nabla n_+}{n_+} + \mu_+ \vec{E}_s$$

A similar equation may be written for electrons

$$\vec{v}_e = \frac{-D_e \nabla n_e}{n_e} - \mu_e \vec{E}_s .$$

$\vec{E}_s$ may now be eliminated from both equations and on setting $n_+ \approx n_e = n$,

$\nabla n_+ \approx \nabla n_e = \nabla n$ and $\vec{v}_+ \approx \vec{v}_e = \vec{v}$, the result

$$\vec{v} = - \frac{\nabla n}{n} \left[\frac{D_+ \mu_e + D_e \mu_+}{\mu_+ + \mu_e} \right] \qquad (8)$$

is obtained. The quantity in parentheses is a diffusion coefficient for the positive ions and electrons interacting on each other so that they both diffuse together. This quantity is called the ambipolar diffusion coefficient and is defined as

$$D_a = \frac{D_+ \mu_e + D_e \mu_+}{\mu_+ + \mu_e} \qquad (9)$$

which gives

$$\vec{\Gamma} = \vec{v} n = -D_a \nabla n \qquad (10)$$

In order to obtain the ambipolar diffusion equation, consider the transient situation for which the continuity equation for the time variation in concentration in any element of space may be written as

$$\frac{\partial n}{\partial t} + \Gamma \cdot \nabla \quad = 0,$$

which on substituting for Γ from Equation 10 gives the ambipolar diffusion equation

$$\frac{\partial n}{\partial t} = D_a \nabla^2 n \tag{11}$$

Diffusion is exponential in nature under transient conditions, so that the particle density at any particular time may be given as

$$n(a,z,\phi,t) = N(a,z,\phi) \quad \exp(-t/\tau),$$

where τ is the ambipolar diffusion decay constant. Under these conditions the diffusion equation becomes

$$D_a \nabla^2 n = -n/\tau \tag{12}$$

or,

$$\nabla^2 n + \frac{1}{D_a \tau} \quad n \quad = \quad 0 \tag{13}$$

This equation is a standard characteristic value problem whose solution depends on the geometry of the container in which the diffusion takes place. For cylindrical geometry with radial and axial dependence Equation 13 gives the separated equations.

$$\frac{d^2n}{dz^2} + n\alpha^2 = 0 \tag{14}$$

$$a^2 \frac{d^2n}{da^2} + a \frac{dn}{da} + \beta^2 a^2 n = 0, \tag{15}$$

where

$$\frac{1}{D_a \tau} = \alpha^2 + \beta^2 ,$$

and α and β are constants. The solution to Equation 14 is of the form $n = n_o \cos dz$, which satisfies the boundary conditions of zero particle concentration at the walls of the container if $\alpha = \frac{\pi}{d}$.

The solution to Equation 15 is of the form $n = n_o J_o(\beta a)$, which satisfies the boundary conditions if $J_o(\beta r) = 0$, or $\beta = \frac{2.405}{r}$.

Therefore, the complete solution is of the form

$$n = n_o \cos \frac{\pi z}{d} J_o \left(\frac{2.405\ a}{r} \right) \tag{16}$$

If $\Lambda^2 = D_a \tau$ is defined as the diffusion length squared, then

$$\frac{1}{\Lambda^2} = \alpha^2 + \beta^2 = \left(\frac{\pi}{d}\right)^2 + \left(\frac{2.405}{r}\right)^2 \tag{17}$$

The rate of ambipolar electron diffusion may now be calculated from Equation 11, which becomes from Equation 12

$$\frac{dn}{dt} = \frac{-n}{\tau} = \frac{-nD_a}{\Lambda^2} .$$

Thus the rate of electron ambipolar diffusion out of an elemental volume dV is given by

$$\frac{n_e D_a}{\Lambda^2} \; dV \quad \text{electrons/sec}$$

and the total diffusion rate from the volume V is

$$\frac{D_a}{\Lambda^2} \int_V n_e dV = \frac{D_a \, n_{ep} V}{\Lambda^2} \quad \text{electrons/sec} \tag{18}$$

where n_{ep} is the average electron concentration in the plasma and V is the volume of the container.

The probability therefore of an electron undergoing an ambipolar diffusion is

$$1 - p_a = \frac{D_a n_{ep} V \left(\frac{1}{\Lambda^2} \right)}{\frac{J_o}{e} \pi r^2} \tag{19}$$

An expression which permits the approximation of the ambipolar diffusion coefficient may be obtained by the use of the relationship between mobility and diffusion coefficients, $D = \frac{k}{e} \mu T$, in Equation 9, giving,

$$D_a = \frac{k}{e} \; \mu_+ \mu_e \; \frac{T_+ + T_e}{\mu_+ + \mu_e}$$

Due to the greater mobility of the electrons, this expression is approximated closely by $D_a = \frac{k}{e} \mu_{+p} \left(\overline{T_e + T_g} \right)$ for the complete volume, where $\overline{T_e + T_g}$ is the average of the sum of the electron and gas temperatures, and the ion temperature approximates that of the gas. The use of this expression

in Equation 19 gives

$$1 - p_a = n_{ep}^{d}\, \mu_{+p}^{k}\, \frac{(\overline{T_e + T_g})}{J_o} \left[\left(\frac{\pi}{d} \right)^2 + \left(\frac{2.405}{r} \right)^2 \right] \qquad (20)$$

The average positive ion mobility μ_{+p} is a term which is not directly available from recognized plasma observations; however, its relationship to resistivity may be used for its evaluation, giving

$$\mu_{+p} = \frac{1}{n_{+p} e \, (\rho_{+n} + \rho_{++})} \qquad (21)$$

Here ρ_{+n} is the average contribution to plasma resistivity that is due to ion-neutral atom collision and ρ_{++} is that due to ion-ion collision.

The resistivity ρ_{+n} is given by

$$\rho_{+n} = \frac{1}{n_{+p} e \, \mu_{+n}} \qquad (22)$$

where μ_{+n} is the mobility of the ions in the neutral gas, which in the case of an argon-neon Penning mixture is the mobility of argon ions in the neon gas. Brown (6) gives the value of μ_{+n} at 291° K and 760 mm Hg as 7.6 cm^2/volt sec, which at the gas temperature $T_g{}^{\circ}$K and gas pressure P mm Hg is $7.6 \left(\frac{760}{P} \right)\left(\frac{T_g}{291} \right)$. Therefore, Equation 22 becomes

$$\rho_{+n} = \frac{3.15 \times 10^{17} P}{n_{+p} \, T_g} \quad \text{ohm cm} \qquad (23)$$

The resistivity ρ_{++} is given by

$$\rho_{++} = \frac{1}{n_{+p} e \, \mu_{++}} , \qquad (24)$$

where μ_{++} is the mobility of positive ions under the influence of other positive ions. It is assumed that collision between two positive ions takes place when the distance between them is less than or equal to r_{++}, the collision radius, which is given by

$$\frac{e^2}{4\pi \epsilon_o r_{++}} = k T_g, \tag{25}$$

as is consistant with assumptions made in kinetic collision theory. Some simplifying assumptions are made in estimating μ_{++}. If it is assumed that the ions start with zero gas velocity in the direction of the field after each collision, the distance an ion travels in time t, with constant acceleration a, is

$$s = \frac{1}{2} a t^2 \tag{26}$$

The assumption of an initial velocity of zero in the direction of the field is an acceptable first approximation, since for each ion with a positive initial velocity there will be, on the average, another with an equal negative velocity. The acceleration may be found by assuming the ions have a charge e of a single electron, so for an ion mass M the acceleration due to a field E is Ee/M. Then, from Equation 26,

$$s = \frac{1}{2} \frac{Ee}{M} (x/c_{+p})^2,$$

where t is the ratio between the path length of a particular ion and c_{+p} is its average thermal velocity.

Integrating to obtain the average distance traveled by N ions,

$$\bar{s} = \int_0^N \tfrac{1}{2} \frac{Ee}{M} \left(\frac{x}{c_{+p}} \right)^2 \frac{dN}{N} ,$$

where dN/N is the proportion of the particles having free paths between x and x + dx. Assuming that the number of ions having collisions in the interval between x and x + dx is proportional to the number entering this interval and the length of the interval, it is found that

$$\frac{dN}{N} = \frac{1}{L_{++}} \exp\left(-x/L_{++}\right), \, dx$$

where L_{++} is the mean free path. Then,

$$\bar{s} = \frac{Ee}{2Mc_{+p}^2 L_{++}} \int_0^\infty x^2 \exp(-x/L_{++}) \, dx$$

$$\bar{s} = \frac{Ee \, L_{++}^2}{Mc_{+p}^2} \tag{27}$$

The average time T between collisions is $T = \frac{L_{++}}{c_{+p}}$ and the average drift velocity is

$$v_d = \frac{\bar{s}}{T} = \frac{Ee \, L_{++}}{Mc_{+p}} .$$

Then the mobility is

$$\mu_{++} = \frac{v_d}{E} = \frac{eL_{++}}{Mc_{+p}}$$

In terms of r_{++},

$$L_{++} = \frac{1}{\sqrt{2}\ \pi\ n_{+p} r_{++}^{2}}$$

so the resistivity is

$$\rho_{++} = \frac{\sqrt{2}\ \pi\ r_{++}^{2} M c_{+p}}{e^{2}} \qquad (28)$$

The mean plasma thermal velocity is related to the gas temperature T_g by

$$\tfrac{1}{2} M c_{+p}^{2} = \tfrac{3}{2}\ k\ T_g$$

Therefore,

$$c_{+p} = \sqrt{\frac{3k\ T_g}{M}}$$

and since

$$\frac{e^{2}}{4\pi\ \epsilon_o\ r_{++}} = k\ T_g\ ,$$

$$r_{++} = \frac{e^{2}}{4\pi\ \epsilon_o\ k\ T_g}$$

Therefore,

$$\rho_{++} = \frac{\pi\ e^{2}\ \sqrt{6M}}{(4\pi\ \epsilon_o)^{2}\ (k\ T_g)^{3/2}} \qquad (29)$$

The probability of ambipolar diffusion may now be determined by substituting for ρ_{+n} and ρ_{++} in Equation 21 using this result in Equation 20, giving

$$1 - p_a = \frac{dk\,(\overline{T_e + T_g})}{e\,J_o(\rho_{+n} + \rho_{++})} \left[\left(\frac{\pi}{d} \right)^2 + \left(\frac{2.405}{r} \right)^2 \right] \qquad (30)$$

Probability of electron-ion recombination

When the sources of ionization are removed from an ionized gas, it quickly returns to a neutral state. This is due to the ambipolar diffusion of ions and electrons to the walls, as well as recombination of electrons and ions in the volume of the gas. In general, the recombination process may be divided into two main types; ion-ion recombination and direct electron-ion recombination (3). In either case, the loss of ions is proportional to the ion concentration, so that

$$\frac{dn_{+p}}{dt} = \frac{dn_{ep}}{dt} = - \alpha\, n_{+p}\, n_{ep},$$

where α is the recombination coefficient for the particular situation. Since the positive and negative particle concentrations are equal, $n_{+p} = n_{ep} = n$. Then,

$$\frac{dn}{dt} = - \alpha\, n^2,$$

which specifies the rate of loss of charged particles from the plasma that is due to recombination.

In the case of ion-ion recombination, an electron first attaches itself to a neutral atom and then this negative ion collides with a positive ion and the recombination process is completed. The relative importance of this process depends on the probability of electron attachment, which varies considerably with different gases and also is very dependent on impurities present in the system. However, for the noble gases, the probability of attachment is found to be negligible (9), and so ion-ion recombination may be neglected for a noble gas Penning mixture.

The recombination of electrons and ions takes place by the mechanisms of radiative and dissociative recombination. In radiative recombination an electron coming close to a positive ion drops into a low-lying electronic orbit and radiates its excess energy. The probability for such a recombination has been calculated, using quantum mechanics, and a recombination coefficient of 10^{-12} cm^3/sec has been predicted but this does not agree in order of magnitude with experimental determinations. Although relatively few determinations have been made, most place the radiative recombination coefficient, α_e, in the range of 10^{-11} to 3.4×10^{-10} cm^3/sec. Using a probe technique, Kenty (27) measured the radiative recombination in argon at an electron temperature of 3100° K and found $\alpha_e = 2 \times 10^{-10}$ cm^3/sec.

The mechanism of dissociative recombination consists of the combination of a positive molecular ion and an electron, resulting in the dissociation of the molecule into two neutral parts by the process

$$XY^+ + e \longrightarrow X + Y$$

In this case, agreement is found between theory and experiment. For pure argon, a particularly high dissociative recombination coefficient of 3×10^{-7} cm^3/sec is obtained. Using a microwave technique, Biondi (3) showed that this high value is due to the presence of argon molecules. The following process takes place,

$$A^+ + 2A \longrightarrow A_2^+ + A.$$

However, atomic argon atoms result if argon ions are formed by collision with metastable atoms only. In the specific case of a neon-argon Penning mixture, where argon atoms collide with metastable neon atoms, the process is

$$Ne^m + A \longrightarrow A^+ + Ne + e$$

In this case, no dissociative recombination is possible; therefore, since radiative and dissociate recombination are both eliminated, plasma decay must be by diffusion alone. This is verified by Biondi (3) for a mixture of helium-0.1% argon. Therefore, in subsequent calculations involving noble gas Penning mixtures, p_r may be taken as equal to unity.

If recombination must be taken into account, e.g. using a single gas, then the probability of an electron recombining in passing through the main plasma is calculated as follows:

$$1 - p_r = \frac{\text{Rate of electron recombination}}{\text{Rate of electron emission from emitter}}$$

$$= \frac{\alpha_r n_{ep}^2 d \pi r^2}{J_o/e \pi r^2}$$

$$= \frac{\alpha_r \, e \, n_{ep}^{2} \, d}{J_o} \qquad (31)$$

Probability of electron entering the auxiliary region

The probability α of an electron entering the auxiliary region from the main discharge region is dependent mainly on the dimensions of the collector aperture and the geometric configuration of the collector. While it may be possible to set up a mathematical model to represent the complex transition from the main discharge plasma to the auxiliary discharge plasma for very simple geometry, it is unlikely that this could be expressed in terms of parameters readily available from standard plasma measurements. In practice, as will be discussed, the collector may be fabricated from such geometrically complex components as woven wire mesh, or perforated sheet. In order to develop a realistic mathematical model, consideration would have to be taken of the variation of the potential profile within the perforations as well as in front of the complete collector. It seems highly improbable that direct measurements, which would permit determination of the internal potential profile, could be made.

Consideration has also been given to the possibility of adapting the work which has been done on the analysis of potential conditions within the grids of both vacuum tubes and such gas filled tubes as thyratrons. In practice various geometries have been considered and empirical characteristics have been developed for vacuum tubes. However, since the relationships are empirical, it is impossible to introduce them into the complete converter model as general expressions. In addition, complexities would certainly arise due to the presence of two different plasmas,

consisting of neutral atoms, molecules, positive ions and electrons, rather than a simple vacuum.

With the foregoing in mind, a completely different approach was made to the problem and an expression for α was obtained in terms of other more readily determinable parameters. Consider the basic circuit in Figure 11. I_L is the load current and is therefore the sum of the rate of electron departure from the emitter and the rate of positive ion arrival at the emitter. The electron departure rate is $p_E J_o/e$ electrons/sec cm^2 for electrodes of unit area.

From the analysis leading to the formulation of the critical equation, the rate of ion return for a net electron departure rate of $p_E J_o/e$ is, by Equation 3,

$$p_E(p_a p_r \alpha p_i k_m p_c + p_a p_r - 1) \quad J_o/e \quad \text{ions/sec cm}^2.$$

Using Equation 4, this becomes

$$(2 - p_E) \quad \left[\frac{1 - R}{1 + R}\right] \quad \sqrt{m/M} \quad (J_o/e) \quad \text{ions/sec cm}^2$$

Therefore, the net rate of negative charge departure from the emitter, the load current, is

$$I_L = p_E J_o + (2 - p_E) \left[\frac{1 - R}{1 + R}\right] \sqrt{m/M} \quad J_o \quad \text{amps/cm}^2. \tag{32}$$

From circuit analysis, the current to the collector is $I_L - I_a$, if I_a is the auxiliary current. I_a is the net arrival rate of negative charge at the auxiliary anode and, from Figure 20, it is seen to be

$$I_a = p_E p_a p_r \alpha J_o + p_E p_a p_r \alpha p_i J_o$$

$$= p_E p_a p_r \alpha (1 + p_i) J_o \quad \text{amps/cm}^2. \tag{33}$$

The ratio of auxiliary current to load current may now be expressed as

$$\frac{I_a}{I_L} = \frac{p_E p_a p_r \alpha (1 + p_i)}{p_E + (2 - p_E)\left(\frac{1-R}{1+R}\right)\sqrt{m/M}} \tag{34}$$

This is an important relationship in an auxiliary discharge system, where the relative magnitude of the auxiliary current has a significant influence on the overall efficiency of the converter.

This relationship is now used in conjunction with the critical equation to find an expression for α. It has been shown already that p_r may be taken as unity and it will be shown that p_c is very close to unity so that the critical equation, Equation 5 may be approximated by

$$\frac{p_E}{2 - p_E}\sqrt{\frac{M}{m}}\left[\frac{1 + R}{1 - R}\right](p_a \alpha p_i k_m + p_a - 1) = 1 \tag{35}$$

Since,

$$\frac{p_E}{2 - p_E}\sqrt{\frac{M}{m}}\left[\frac{1 + R}{1 - R}\right] \text{ is of the order of } 10^3,$$

Equation 35 becomes

$$p_a \alpha p_i k_m + p_a \approx 1 ;$$

therefore

$$p_a \approx (1 + \alpha p_i k_m)^{-1}. \tag{36}$$

Using the same approximations, Equation 34 becomes

$$\alpha = \frac{I_a}{I_L} \quad \frac{1}{p_a(1 + p_i)} .$$

Upon substituting for p_a from Equation 36, this becomes

$$\alpha = \frac{I_a}{I_L} \left[\frac{1 + \alpha p_i k_m}{1 + p_i} \right] .$$

Solving for α,

$$\alpha = \frac{I_a}{I_L} (1 + p_i - p_i k_m I_a/I_L)^{-1} . \tag{37}$$

Further, for a probability of ionization of about unity and auxiliary to load current ratios of about 1:30, α may be approximated by

$$\alpha = (I_a/I_L)(1 + p_i)^{-1} \tag{38}$$

The reciprocal of α is plotted against the probability of ionization for various current ratios in Figure 23. As expected, as the probability of ionization increases at fixed current ratios, the fraction of electrons required by the auxiliary discharge decreases ($1/\alpha$ increases).

Probability of ionization

It is assumed that the converter is filled with a neon-argon Penning mixture and that the auxiliary system is adjusted to operate under optimum

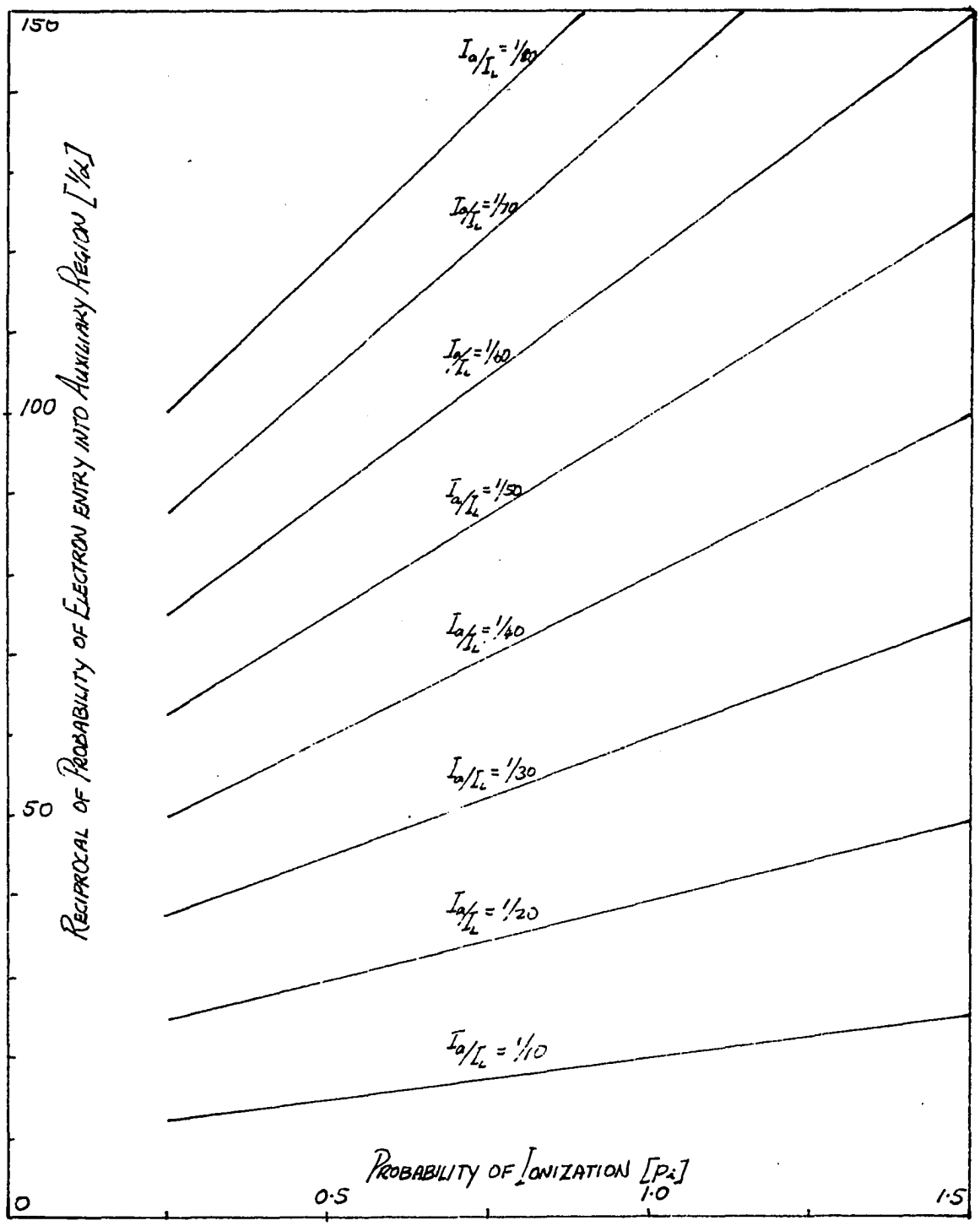

Figure 23. Variation of $1/\alpha$ with the probability of ionization for various current ratios

conditions. As shown in Figure 17, optimum ionization conditions are achieved with a mixture of 1000 parts of neon to one part argon if the potential gradient per unit pressure E/P is adjusted to 3.8 volts/cm mm Hg. The ionization coefficient, η, thus achieved is 3.9×10^{-2} ion pairs/volt. Since the potential profile in the auxiliary discharge regions is not linear in general, the optimum value of E/P may not be achieved throughout the discharge region. From Figure 17, it is apparent that operation should be with an E/P greater, rather than less than, the optimum since the ionization coefficient rapidly decreases as E/P is reduced from 3.8 volts/cm mm Hg. In this way, most of the discharge region operates at, or above, 3.8 volts/cm mm Hg and is an effective ion source.

The probability of an electron which enters the auxiliary region producing an ion is (43)

$$p_i = \eta E_a \quad \text{ion pairs/electron} \tag{39}$$

Operation is at E/P = 3.8 volts/cm mm Hg; therefore

$$E = 3.8 P \text{ volts/cm} \tag{40}$$

and

$$E_a = E h \text{ volts}, \tag{41}$$

where h is the length of the region within which effective ionization takes place.

The substitution of Equation 40 and Equation 41 into Equation 39 results in

$$p_i = 3.8\ \eta\ h\ P$$

$$= 3.8 \times 3.9 \times 10^{-2}\ h\ P$$

$$= 0.148\ h\ P \qquad \text{ion pairs/electron} \tag{42}$$

It has been assumed that all ions are formed in the auxiliary region. However, as pointed out be Gabor (17), some metastable atoms may be swept into the main discharge region, where they then become ions. However, since the concept of an ion wind is rather transcendental, the effect is not taken into account.

Probability of an ion entering the emitter-collector region

The ions in the plasma of the auxiliary discharge are subjected to the ionizing potential and are accelerated towards the collector. It is reasonable to assume that the majority of ions which reach the collector are fast; therefore, the phenomenon of slow ion reflection discovered by Gabor does not arise in this case. It is also reasonable to assume that those ions accelerated towards the perforations in the collector pass through without being neutralized, while those which collide with the walls of the collector are neutralized and so lost from the process. On the average, the fraction of fast ions which are not absorbed and neutralized by the collector is given directly by the ratio of open to total collector area. Therefore,

$$k_m = \frac{\text{Open area of collector}}{\text{Total area of collector}} \quad . \tag{43}$$

Thus, even for complicated collector geometry, it is a simple matter to determine k_m.

Consider the case of a woven wire mesh with M wires per unit length in one direction and N wires per unit length in the other. If the diameter of the wire is d units, k_m may be calculated by considering Figure 24a.

$$k_m = \frac{(1/M - d)(1/N - d)}{1/MN} = MNd^2 - d(M + N) + 1 \qquad (44)$$

Another form of collector is a perforated sheet as shown in Figure 24b. In this case

$$k_m = \frac{\frac{1}{4}\pi d^2}{1/MN} = \frac{\pi}{4} MN d^2, \qquad (45)$$

where d is the diameter of the holes and M and N are the number of holes per unit length in each direction respectively.

Probability of slow ion capture by collector

It is assumed that the fast ions injected into the main discharge region become randomized before any are captured by the collector. Or, in other words, all the ions reaching the collector from the main discharge are slow. Therefore, conditions at the collector are similar to those at the emitter as far as slow ion reflection and potential profile are concerned. However, since ions are being considered, the sheath profile has no retarding influence and it may be assumed that the random ion current flows from the plasma to the collector. However, since these are slow ions, there is a probability R of each being reflected. As a result, the ion current actually absorbed by the collector is (1 - R) times the ion

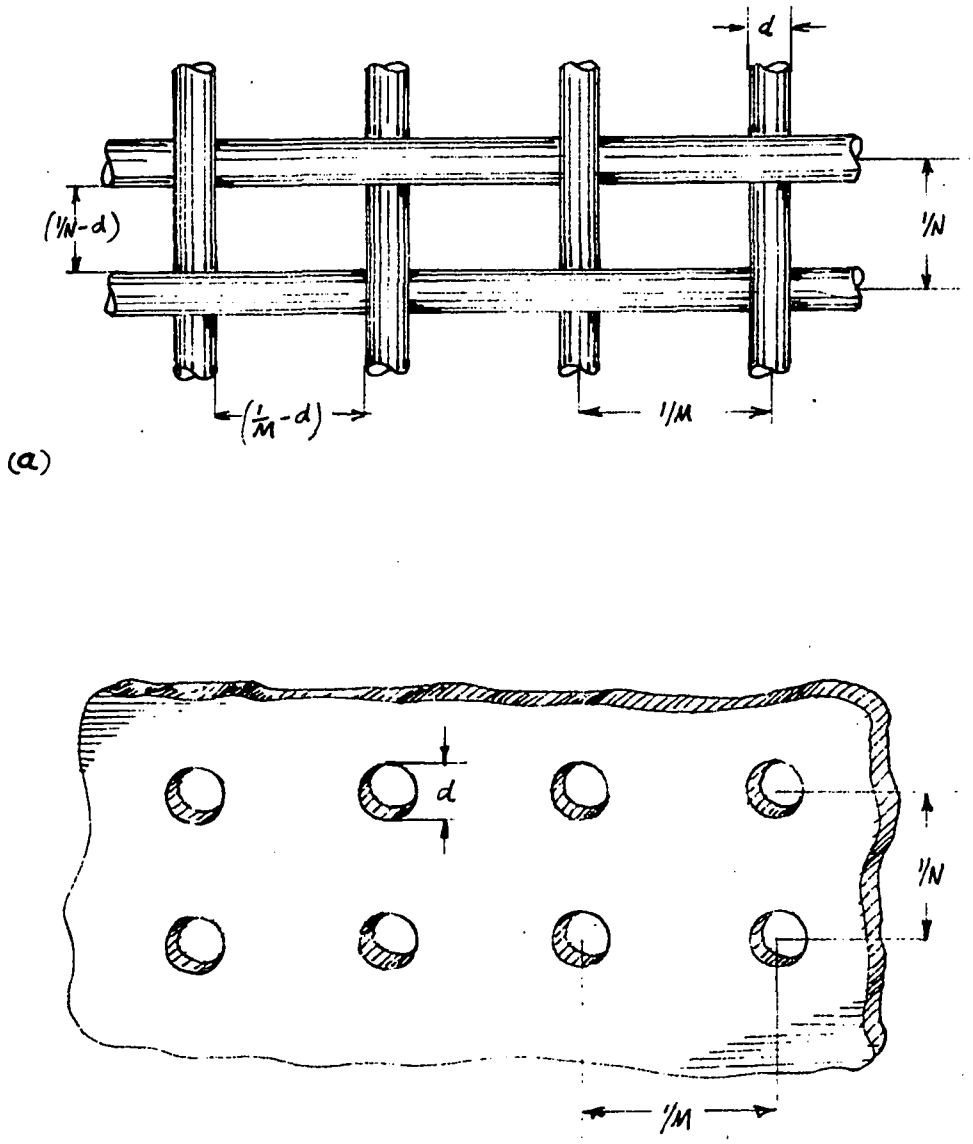

Figure 24. Collector configuration for (a) woven mesh and (b) punched sheet

random current in the plasma. The probability of an ion which enters the main discharge region being absorbed as a slow ion by the collector is then defined as

$$1 - p_c = \frac{\text{Slow ion random current absorbed by collector from dark plasma}}{\text{Fast ion current entering dark plasma from auxiliary region}}$$

The random ion current density in the plasma at the collector is given by

$$\frac{n_{+c}\ e\ v_{+c}}{4},$$

where n_{+c} and v_{+c} are the average ion density and the average ion velocity, respectively, in the plasma at the collector. Then, the slow ion current to the collector is

$$\frac{n_{+c} e\ v_{+c}}{4}\ (1 - R)(1 - k_m)$$

Since the average ion velocity

$$v_{+c} = \sqrt{\frac{8k\ T_{+c}}{\pi\ M}}$$

and $n_{+c} = n_{ec}$ the slow ion current is then

$$n_{ec} e(1 - R)(1 - k_m) \sqrt{\frac{k\ T_{+c}}{2\pi\ M}} \qquad (47)$$

The factor $(1 - k_m)$ accounts for the collector configuration. It is

assumed that slow ions which diffuse towards the auxiliary discharge region through the collector are returned to the main discharge region without being collected at the collector. The fast ion current entering the dark plasma from the auxiliary discharge region has been found to be $p_E p_a p_r \propto p_i k_m J_o/e$ ions/sec. By using Equation 33, this may be put in the form

$$\frac{p_i}{1 + p_i} \; k_m \; I_a/e \quad \text{ions/sec}$$

The probability of slow ion absorption by the collector is then

$$1 - p_c = \frac{n_{ec} e}{I_a} \; (1 - R)\left(\frac{1}{k_m} - 1\right)\left(\frac{1}{p_i} + 1\right) \; \sqrt{\frac{k \; T_{+c}}{2\pi \; M}} \qquad (48)$$

Upon substituting Equation 42 for p_i this becomes

$$1 - p_c = \frac{n_{ec} e}{I_a} (1 - R)\left(\frac{1}{k_m} - 1\right)\left(\frac{6.75}{h \; P} + 1\right) \; \sqrt{\frac{k \; T_{+c}}{2\pi \; M}} \qquad (49)$$

Determination of Resistive Potential Drop within the Main Plasma

As previously discussed, it is assumed that a linear potential gradient is due to the plasma resistivity, ρ_{ep}, which is composed of the sum of ρ_{en}, due to electron neutral atom collision, and ρ_{e+}, due to electron positive ion collision.

The electron neutral atom resistivity may be evaluated, according to Spitzer (41), in terms of the average electron plasma temperature T_{ep}, the elastic collision cross section for an electron gas atom collision q, and

the fraction f of ionized gas in the plasma. Thus,

$$\rho_{en} = 2.2 \times 10^{9} \quad \frac{T_{ep}^{\frac{1}{2}} q}{f} \text{ ohm cm} \tag{50}$$

In order to determine q, a rough estimate must be made for T_{ep}. A reasonable value is 3500° K, which has been used by Schultz (39). The corresponding electron energy within the plasma is then 3500 k/e = 0.302 volts. The collision cross-section q has been evaluated theoretically and experimentally and Brown (6) reports and compares results. There is considerable discrepancy but, since experimental values for p_1, the electron-atom collision probability, are given for neon, these will be used. However, accurate values are not available for the low energy electrons under consideration but, of the three sets of available data, $p_1 = 3$ appears to be a suitable choice. The collision cross-section q is related in cm^2 units to p_c by

$$q = 0.283 \times 10^{-16} p_1 \quad cm^2, \tag{51}$$

which gives the collision cross section for neon under operating conditions as

$$q = 0.283 \times 10^{-16} \times 3 = 0.85 \times 10^{-16} \text{ cm}^2.$$

In light of the uncertainty of the data for p_1, it is appreciated that an error of 1000-2000° K in T_{ep} would not have altered significantly the value of p_c arrived at.

The fractional ionization in the main discharge is

$$f = \frac{\text{Density of ions (or electrons) in the plasma}}{\text{Density of all particles in the plasma}}$$

$$= \frac{n_{ep}}{n_g + n_{ep}}$$

Due to the fact that the dark plasma is weakly ionized, $n_{ep} \ll n_g$ (typically, $n_g = 10^5\ n_{ep}$) so that

$$f = \frac{n_{ep}}{n_g} .$$

n_g may be expressed in terms of temperature and pressure using Gay-Lussac's Laws (9).

$$n_g = \frac{9.68 \times 10^{18}\ P}{T_g} ,$$

where P is the pressure in mms of mercury. Thus,

$$f = \frac{n_{ep}\ T_g}{9.68 \times 10^{18}\ P} \qquad (53)$$

Substituting for q and f in Equation 50 gives

$$\rho_{en} = 2.2 \times 10^9 \sqrt{T_{ep}}\ \ 0.85 \times 10^{-16} \times \frac{9.68 \times 10^{18}\ P}{n_{ep}\ T_g}$$

$$\rho_{en} = 1.8 \times 10^{12} \quad \frac{P\sqrt{T_{ep}}}{n_{ep} T_g} \quad \text{ohm cms} \tag{54}$$

Spitzer (41) gives a relationship for the electron ion collision resistivity as

$$\rho_{e+} = 6.53 \times 10^{3} \quad \frac{\ell n\, \lambda}{T_{ep}^{3/2}} \quad \text{ohm cm} , \tag{55}$$

where

$$\lambda = \frac{3}{2e^3} \left[\frac{k^3 T_{ep}^{\ 3}}{\pi m_{ep}} \right]^{\frac{1}{2}} .$$

The combined resistivity of the discharge is then $\rho_{ep} = \rho_{en} + \rho_{e+}$.

Although an electron current J_o flows from the emitter into the plasma, only a fraction, $p_E J_o$, commences its passage through and a fraction, $p_E p_a J_o$, reaches the collector. Therefore, the mean current through the plasma is $\frac{1}{2}(p_E J_o + p_E p_a J_o)$ or $\frac{J_o p_E}{2}(1 + p_a)$. Therefore, the resistive potential drop within the main discharge is

$$V_p = J_o\, d\, \frac{p_E}{2} (1 + p_a)\, \rho_{ep}$$

$$V_p = J_o d \frac{p_E}{2} (1+p_a) \left\{ 1.81 \times 10^{12} \quad \frac{P\sqrt{T_{ep}}}{n_{ep} T_g} + \frac{6.53 \times 10^{3}}{T_{ep}^{3/2}} \ell n \left[\frac{3}{2e^3} \left(\frac{k^3 T_{ep}^{\ 3}}{\pi n_{ep}} \right)^{\frac{1}{2}} \right] \right\}$$

volts (56)

Transient Analysis

One of the important advantages of the auxiliary discharge system is its ability to modulate the power output. This is achieved simply by applying the modulating signal to the auxiliary electrode. Since the ion supply for space charge neutralization is completely dependent on the existance of a discharge in the auxiliary region, the power output may be virtually reduced to zero by dropping the auxiliary electrode potential below the ionizing potential of the filling gas. Above the operating potential, the rate of ion production varies with the magnitude of the applied auxiliary voltage. While this variation is not exactly linear for certain Penning mixtures, a close approximation may be obtained. From the characteristics of the neon-argon Penning mixture, as in Figure 17, it is seen that an almost constant value of 0.015 for the ion pair production per volt is obtained for E_a/p in the range above 2.0 volts/cm mm Hg if a neon -0.002 percent argon mixture is used. Although this is not the most efficient ionizing mixture, it would provide a close approximation to a linear relationship between ion production and applied auxiliary potential.

If the converter is to be modulated, it is important to analyze its transient response, determine the transfer function of the system and analyze the frequency limitations under specific conditions. In order to do this, a generalized expression will be found relating the charge density as a function of time and position in the plasma with the characteristics of the plasma. It is assumed that the plasma is contained in a cylindrical vessel of radius r and height d. The filling gas is a Penning mixture in which recombination is assumed negligible. It is assumed

that the net rate of ion production within the main discharge region is $q(a,t)$ per unit volume.

The ambipolar diffusion equation for ions or electrons is

Rate of change in concentration = Rate of production - Rate of diffusion

$$\frac{d}{dt} n(a,t) = q(a,t) - [-D_a \nabla^2 n(a,t)], \tag{57}$$

where $n(a,t)$ and $q(a,t)$ are the charged particle concentration and the rate of ion production, respectively, in the plasma as a function of time t, and radius a. D_a is the ambipolar diffusion coefficient as defined in Equation 9.

In cylindrical coordinates, when the concentration is only radially dependent,

$$\nabla^2 n(a,t) = \frac{1}{a} \frac{d}{da}\left(a \frac{dn}{da} \right)$$

$$= \frac{1}{a} \frac{dn}{da} + \frac{d^2 n}{da^2} \tag{58}$$

The diffusion equation then becomes

$$\frac{dn}{dt} = D_a\left(\frac{d^2 n}{da^2} + \frac{1}{a} \frac{dn}{da} \right) + q(a,t) \tag{59}$$

This differential equation is solved using Bessel functions (40). Multiply both sides of the equation by a $J_o(\xi_i a)$, where $J_o(\xi_i a)$ is the zero order Bessell function and ξ_i is such that $J_o(\xi_i r) = 0$. Upon integrating

between zero and r with respect to a, the equation becomes

$$\int_o^r \frac{dn}{dt}\, a\, J_o(\xi_i a)da = D_a\int_o^r a\left(\frac{d^2n}{da^2} + \frac{1}{a}\frac{dn}{da}\right) J_o(\xi_i a)da + \int_o^r a\, q(a,t)J_o(\xi_i a)da \tag{60}$$

Using the finite Hankle transform,

$$\bar{n}_J = \int_o^r a\, n(a,t)\, J_o(\xi_i a)\, da,$$

$$\frac{d\bar{n}_J}{dt} = D_a\int_o^r a\left(\frac{d^2n}{da^2} + \frac{1}{a}\frac{dn}{da}\right) J_o(\xi_i a)\, da + \bar{q}_J(\xi_i,t)$$

Let

$$I_\mu = \int_o^r a\left(\frac{d^2n}{da^2} + \frac{1}{a}\frac{dn}{da}\right) J_\mu(\xi_i a)\, da\ .$$

Integrating by parts,

$$I_\mu = a\frac{dn}{da} J_\mu(\xi_i a)\Big|_o^r - \int_o^r \frac{dn}{da}\left[a\,\xi_i J_\mu'(\xi_i a) + J_\mu(\xi_i a)\right]da$$

$$= -\xi_i\int_o^r a\frac{dn}{da} J_\mu'(\xi_i a)\, da$$

$$= -\xi_i r\, n(r)\, J'_\mu(r\xi_i) + \xi_i \int_o^r n(a)\, [a\xi_i J''_\mu(\xi_i a) + J'_\mu(\xi_i a)]da$$

Therefore,

$$I_o = \xi_i \int_o^r n(a)\, [a\, \xi_i\, J''_o(\xi_i a) + J'_o(a\xi_i)]da$$

$$= \xi_i \left[-\xi_i \int_o^r a\, n(a)\, J_o(\xi_i a)\, da\, \right] = -\xi_i^2 \bar{n}_J \,. \tag{62}$$

The transformed equation is then

$$\frac{d\bar{n}_J}{dt} + D_a\, \xi_i^2\, \bar{n}_J = \bar{q}_J(\xi_i, t), \tag{63}$$

which has the solution

$$\bar{n}_J(\xi_i, t) = \int_0^t \bar{q}_J(\xi_i \tau)\, \exp\, [-D_a\, \xi_i^2 (t - \tau)]\, d\tau, \tag{64}$$

for the initial condition $\bar{n}_J(\xi_i, 0) = 0$. The inverse is obtained by applying the inverse Hankle transformation , so that

$$n(a,t) = \frac{2}{r^2} \sum_i \frac{J_o(a\xi_i)}{[J_1(r\xi_i)]^2} \int_o^t \bar{q}_J(\xi_i,\tau) \exp[-D_a\xi_i^2(t - \tau)]\, d\tau \qquad (65)$$

This is a general equation and may be modified for specific circumstances. For example, when the net rate of ion production is a constant q_o

$$\bar{q}_J(\xi_i) = \int_o^r a\, q_o J_o(\xi_i a)\, da = q_o \frac{r}{\xi_1} J_1(r\xi_i) \qquad (66)$$

and

$$n(a,t) = \frac{2q_o}{r} \sum_i \frac{J_o(a\xi_i)}{[J_1(r\xi_1)]^2} \int_o^t \exp[-D_a\xi_i^2(t - \tau)]\, d\tau$$

$$= \frac{q_o}{4D_a}(r^2 - a^2) - \frac{2q_o}{D_a r} \sum_i \frac{J_o(a\xi_i)}{\xi_i^3 J_1(r\xi_i)} \exp(-D_a\xi_i^2 t) \qquad (67)$$

As t approaches infinity this becomes

$$n(a,t) = \frac{q_o}{4D_a}(r^2 - a^2), \qquad (68)$$

which is the steady condition.

If the net rate of ion production within the main plasma varies exponentially, $q(t) = q_o \exp(-t/\tau_a)$, where τ_a is the time constant associated with the net ion production rate. Then

$$n(r,t) = \frac{2}{r^2} \Sigma_i \frac{J_o(a\xi_i)}{[J_1(r\xi_i)]^2} \frac{r}{\xi_i} J_1(r\xi_i) \int_o^t q_o \exp[-D_a \xi_i^2 (t-\tau) - \tau/\tau_a] \, d\tau$$

$$= \frac{2q_o}{r} \Sigma_i \frac{J_o(a\xi_i)}{\xi_i J_1(r\xi_i)} [\exp(-t/\tau_a) - \exp(-D_a \xi_i^2 t)] (D_a \xi_i^2 - 1/\tau_a)^{-1}$$

This may be simplified by noting that

$$\frac{2}{r} \sum_i \frac{J_o(a\xi_i)}{\xi_i J_1(r\xi_i)} (D_a \xi_i^2 \tau_a - 1)^{-1} = \frac{J_o(a/\sqrt{\tau_a D_a})}{J_o(r/\sqrt{\tau_a D_a})} - 1$$

Therefore,

$$n(a,t) = q_o \tau_a \left[\frac{J_o(a/\sqrt{\tau_a D_a})}{J_o(r/\sqrt{\tau_a D_a})} - 1 \right] \exp(-t/\tau_a)$$

$$- \frac{2q_o}{r} \sum_i \frac{\exp(-D_a \xi_i^2 t) \, J_o(a\xi_i)}{\xi_i (D_a \xi_i^2 - 1/\tau_a) \, J_i(r\xi_i)} , \qquad (69)$$

where the sum is taken over all the positive roots of $J_o(\xi_i r) = 0$.

In a stable system there is a direct connection between the transient and frequency response. The gain and phase functions of a system may be found from its impulse response Y(t) by first finding its Laplace transform Y(s) and then evaluating $|Y(j\omega)| \exp[j\psi(\omega)]$, where $Y(j\omega)$ is the amplitude function for positive frequency ω, and $\psi(\omega)$ is the phase function. In the present case, we assume an impulse input of ions to the

system independent of a, i.e., $q(a,t) = q_o\delta(t)$, where $\delta(t)$ is the Dirac-delta function. Then

$$y(t) = \frac{2}{r^2}\sum_i \frac{J_o(a\xi_i)}{[J_1(r\xi_i)]^2}\frac{r}{\xi_i}J_1(a\xi_i)\int_o^t q_o\delta(\tau)\exp[-D_a\xi_i(t-\tau)]\,d\tau$$

$$= \frac{2q_o}{r}\sum_i \frac{J_o(a\xi_i)}{\xi_i J_1(r\xi_i)}\exp(-D_a\xi_i t)$$

$$Y(s) = \mathcal{L}[y(t)] = \frac{2q_o}{r}\sum_i \frac{J_o(a\xi_i)}{\xi_i J_1(r\xi_i)}\int_o^\infty \exp(-D_a\xi_i\, t - st)\,dt$$

$$= \frac{2q_o}{r}\sum_i \frac{J_o(a\xi_i)}{\xi_i J_1(r\xi_i)}(s + D_a\xi_i)^{-1}$$

$$Y(j\omega) = \frac{2q_o}{r}\sum_i \frac{J_o(a\xi_i)}{\xi_i J_1(r\xi_i)}\frac{1}{\sqrt{\omega^2 + D_a{}^2\xi_i{}^2}}\exp(-j\omega/D_a\xi_i) \qquad (70)$$

The magnitude of the amplitude function is

$$|Y(j\omega)| = \frac{2q_o}{r}\sum_i \frac{J_o(a\xi_i)}{\xi_i J_1(r\xi_i)}\frac{1}{\sqrt{\omega^2 + D_a{}^2\xi_i{}^2}}$$

Figure 25 shows a plot of this amplitude function with frequency for different values of the ambipolar diffusion coefficient D_a. The plot is for points at a radius a = 0.55 cms., with r = 1.1 cms. corresponding to typical experimental values. For operation at a frequency of 60 c.p.s.,

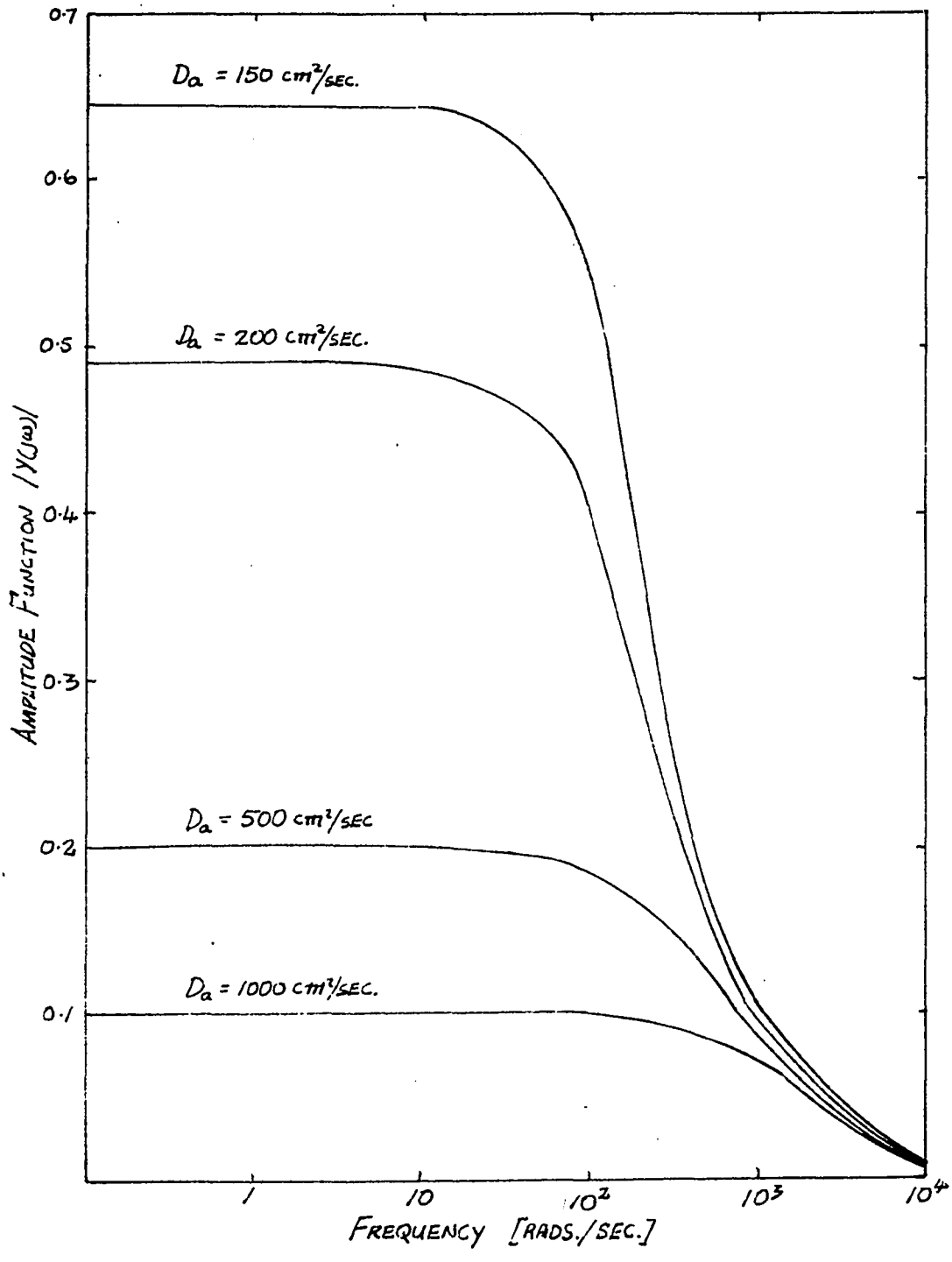

Figure 25. Variation of converter response with the frequency of the ion supply

or 377 r.p.s., an ambipolar diffusion coefficient greater than 500 cm^2/sec would be required for acceptable magnitude and phase response. The above analysis is conservative in that the initial conditions assume no plasma present within the diode space. Under operating conditions, such a plasma would exist with an axial potential gradient associated with the plasma resistive drop. This gradient would assist polar diffusion and so reduce the plasma time constant. As a result, ambipolar diffusion coefficients smaller than those obtained from the above analysis would be acceptable.

EXPERIMENTAL INVESTIGATION

Since no experimental work on the Gabor type converter system has been reported from within the United States and the only source is the Imperical College of London, England, any initial experimental work calls for an analysis which would serve to supplement the rather scanty information available. Also, the report of such a low auxiliary to main discharge current ratio requires verification, since it leads to the contravention of Langmuir's long established probe theory.

The following are the main objectives:

1. To design, construct and operate a system employing the auxiliary discharge converter mode.

2. To verify Gabor's findings (16) of a low auxiliary to main current ratio.

3. To develop an emitter material with suitable mechanical and electrical properties.

4. To analyze the problems confronting the development of such a converter from both the experimental and commercial development viewpoint.

It should be noted that the objective of this work is not to produce a device which converts heat to electricity, but to produce a device whose internal plasma characteristics and mode of operation are the same as those in an actual energy converter operating in the Gabor mode. The new discovery of slow ion reflection and production of a dark plasma in the emitter collector region by means of a combination of electrons from the emitter and positive ions from a separate region are the main sources of interest and are those whose satisfactory investigation will be given priority in all cases.

Converter Design

Configuration

Most experimental systems are based on either cylindrical or planer geometry. In this case, planer electrodes were decided upon because variation of electrode spacing may be accomplished simply during testing and the theoretical analysis is relatively simple for a planer system.

Basic dimensions are governed by the emitter heater capacity of about 150 watts. It was decided to use an emitter of about 1 cm radius. For auxiliary discharge systems the emitter-collector spacing is generally between 3 and 5 mms. Figure 26 shows the design initially proposed for the experimental system. The emitter rests on a cylindrical heat shield, within which a heating element is supported by a ceramic frame. The collector consists of a fine wire mesh with concentric cylinders attached. This is supported at its center by a thin rod which screws into a fixed socket. Thus, by rotating the rod, the emitter-collector spacing may be adjusted.

The addition of the concentric cylinders to the collector is prompted by the results of a theoretical investigation made by H. A. Fatmi (13). The same conclusion may be reached by an intuitive argument.

Assuming an equipotential plasma, the electrons tend to diffuse unpreferentially to both the emitter and collector and so, in terms of electrode areas, the collector receives a fraction $\frac{A_c}{A_c + A_E}$ of the total electron current to the electrodes. Thus, the larger the effective collector area the greater is the electron current drawn from the plasma. While the assumption of an equipotential plasma and the neglection of ambipolar diffusion are by no means accurate, the intuitive result indicates that it is

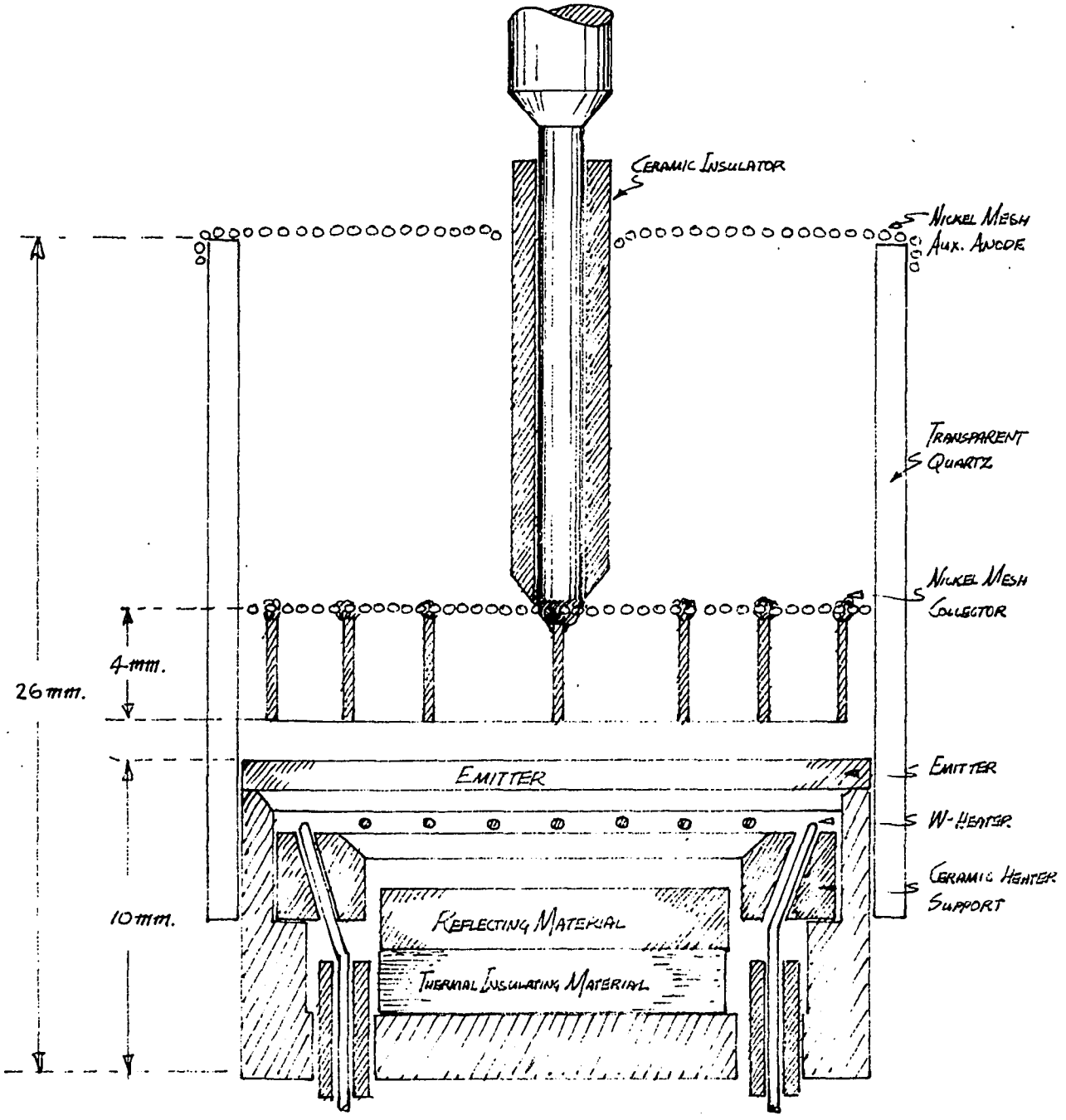

Figure 26. Cross-section of the auxiliary discharge system initially proposed

beneficial as far as electrons are concerned, to use a collector of area larger than the emitter. No mention is made by Fatmi of the effect a large emitter area has on the ion flow from the auxiliary region to the emitter. Certainly the loss of ions to the collector is increased but, since ion reflection is still assumed to exist, this loss remains relatively small. Also, the variation of the ambipolar diffusion with the geometric configuration of the collector has been neglected. This diffusion loss varies directly with the interelectrode space and inversely with the square of the effective emitter area. If a collector is used which in effect subdivides the dark plasma into separate cells, ambipolar loss may be expected to increase.

Since the plasma characteristics of the Gabor mode are of primary interest, a simple planer configuration is of great advantage from the analytical viewpoint. It was therefore decided to modify the initial design by removing the concentric cylinders so that the main discharge region has simple planer geometry.

In order to contain both the dark and luminous plasmas, both regions are surrounded by a 2.2 cm internal diameter quartz tube. This tube, as well as being capable of withstanding high temperatures, is transparent and so facilitates the observation of the electrodes and the interelectrode regions. This is important since an optical pyrometer is used for temperature measurements and a luminous discharge must be present in the auxiliary discharge region when operating in the correct mode. The auxiliary anode is also formed by wire mesh in order to permit easy observation of the auxiliary region. The initial heater design was found to be rather complicated and a simpler design was adopted consisting of a

spiral "pan-cake" tungsten coil supported by its own leads as shown in Figure 27 and spot welded to the tungsten-nickel feed-through leads. The heat shield was also redesigned to take the form of two concentric nickel cylinders attached by three small spot-welded strips about its base. A cap on the inner heat shield forms the base plate for the emitter material. This has a 0.7 mm circular depression of 1.61 cms in diameter. The collector is fabricated from a 100 x 100, 0.0045 ins. diameter nickel mesh, spot-welded to a cross of nickel to act as a support. The cross is in turn spot-welded to a stainless steel rod. This rod carries a 3.6 cm bar of soft iron which may be magnetized by induction and used for rotating the rod and so adjusting the interelectrode spacing. The quartz containment tube rests on supports about the outer heat shield and is capped by the auxiliary anode.

The selection of a suitable containment vessel proved quite a problem. Initially it was proposed to use a bell-jar system mounted on a stainless steel base plate. However, since vacuums to 10^{-8} mm Hg are required during processing of the electrodes, it was felt that this requirement exceeded the range of such a system. Complete glass containment was then considered. This has the great disadvantage of not permitting adjustment or repair of the system once it has been enclosed. Also, there are many fabrication problems due to the intricate nature of the assembly. However, a suitable envelope was available with seven tungsten feed-through leads with individual current capacities of 20 amps and this was used.

A platinum/platinum-13-percent rhodium thermocouple spot-welded to the inner heat shield, close to the emitter, and a small hole in the

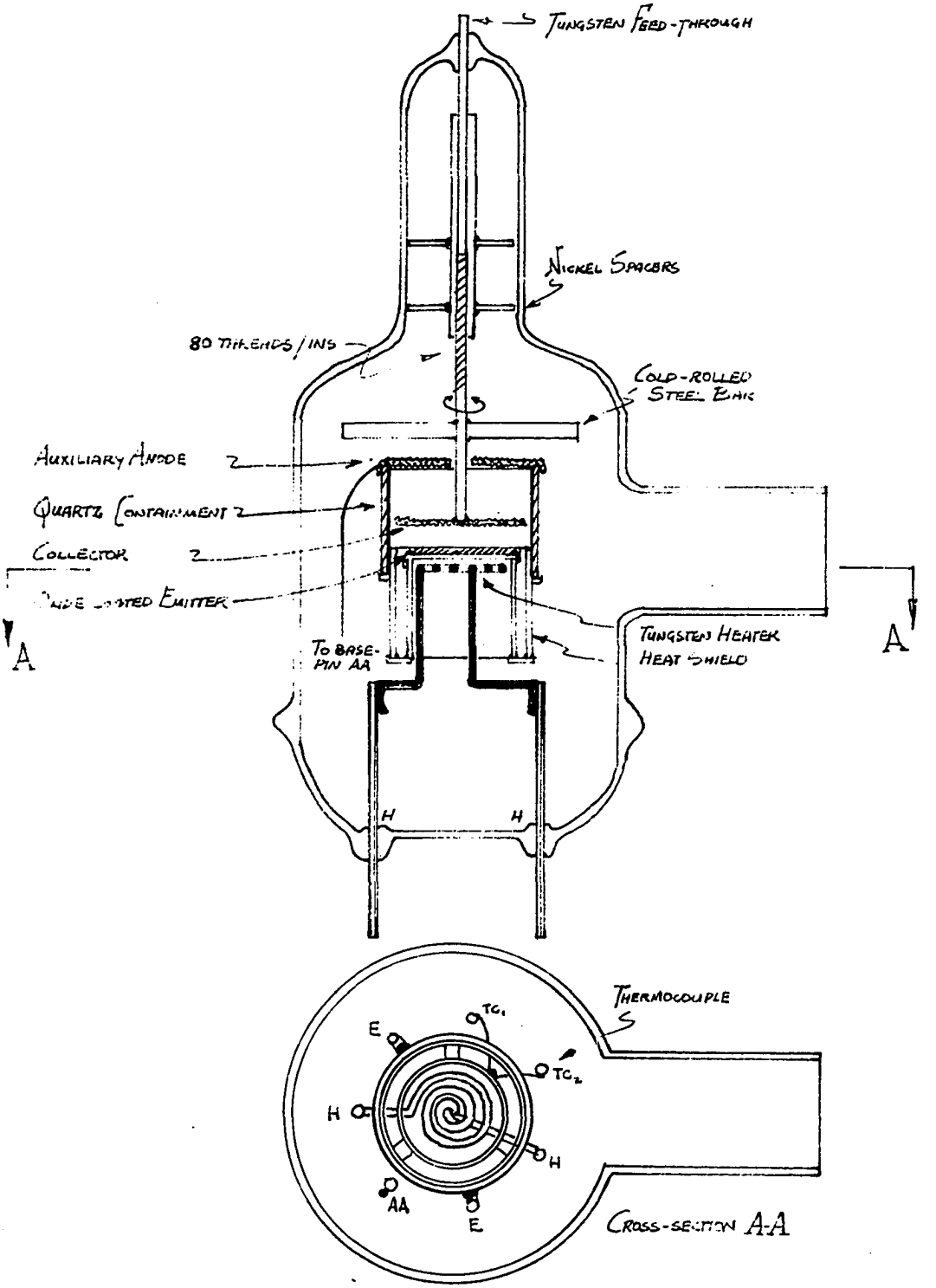

Figure 27. Cross-section of the auxiliary discharge system in the final form

outer heat shield permit both electrical and optical temperature measurement. Nickel, platinum, tungsten and stainless steel were used in the fabrication of the system. The fabrication proved difficult due to the small dimensions and the accuracy required. It was not possible to cut the glass envelope close to the base, and as a result the protruding glass rim prevented radial access to the lower part of the assembly. A means of overcoming this problem was observed at the University of London, England, where all electrode and heater leads are joined to the feed-through leads by means of cylindrical coupling sleeves with radial screws. This simple arrangement permits the free assembly of the electrode system apart from the glass envelope, and at any time permits ready removal of the system from the base for repair or adjustment.

Emitter design

An emitter work function of about 2.3 eV represents a suitable compromise between the output voltage and current density requirements, at an acceptable emitter temperature. Most of the elements have work functions in the range from 3 to 5 eV but a relatively small number have work functions between 2 and 3 eV. Table 1 lists these elements. Accurate determination of a material's work function is very difficult, since it is so dependent on surface phenomena such as attached impurities, crystal structure, smoothness etc. In any case, even if accurate values were available for the perfect material they would not be of great significance since contamination can be expected in a practical converter. Variations in the work function actually achieved may be as much or more than 0.5 eV from that observed under the best measurement conditions.

Table 1. Work function ϕ of pure metals

Material	Work function ϕ (eV)
L_i	2.48
N_a	2.28
K	2.22
C_s	1.93
B_a	2.51
C_e	2.84

From the work function viewpoint, L_i, N_a or K would be acceptable; however, they are immediately rejected in this case due to their low melting points of 459° K, 370.5° K and 335.3° K respectively. The use of a cesium coating introduces the containment problems and most of those of the cesium converter. So this too is rejected. The work function of pure cesium is 2.84 eV and under practical conditions could be expected to increase to about 3.0 eV. Barium then promises to be the most suitable of the pure metals.

Numerous composite emitters have been investigated and most present relatively low work functions. The structure consists of a bare material which is impregnated with an atomic film of some other material. The combination is found to result in a work function less than that of either of the two separate materials. Of those in Table 2 the thoriated tungsten emitter is in most general commercial use, however its work function

is not low enough.

Table 2. Work functions ϕ of atomic film emitters

Emitter	Work functions ϕ (eV)
W-C_s	1.64
W-B_a	1.56
W-T_h	2.86
T_a-T_h	2.52
W-B_a-O	1.9-2.5

The oxide-coated or Wehnelt emitter comprises a base metal, such as nickel, tungsten or one of a large number of alloys, coated with the oxides of barium and strontium. This type of emitter is used very extensively commercially. It has the property, as will be discussed, of permitting its work function to be decreased, by an activation process, from about 3.0 eV to as low as 1.5 eV. For this reason, and the fact that high purity oxides are available from most electron tube manufacturers, it was decided to use an oxide coated emitter. Several means of coating are employed. It may be applied by spraying and using a nitrocellulose binder, or by bench coating. The latter consists of passing the backing metal over revolving wheels in a cup of coating, then through an electric furnace. The coating is built up in several layers.

A more sophisticated process for depositing colloidal carbonates makes use of electrophoresis. The base material is placed in a suspension of the coating and an electric field applied between it and another electrode. The suspended particles become charged at one electrode and migrate to the other where they are deposited if conditions are suitable there. The quantity deposited depends on the concentration, applied voltage, and time.

In order to examine the coating process, a number of tests were made. Nickel electrodes were thoroughly cleaned, placed in the colloidal liquid and a constant potential of 100 V was applied between the electrodes. It was found that the organic liquids used to suspend the 1:1 Barium-Strontium carbonate mixture have considerable influence on the yield. For example, amyl alcohol gives a much greater deposit than ethyl alcohol. The bond between the deposited coating and the core metal is also greatly dependent on the type of liquid. Coatings obtained from methyl alcohol show a very poor bond, while those obtained from acetone adhere well. Impurities in the electrophoretic bath alter the concentration of ions and the conductivity of the bath and so produce considerable differences in the electrophoretic yield which may lead to a change in the direction of deposition.

When examined under a microscope, the coatings were found to be relatively uniform and it was found that coatings formed with large inter-electrode distances were smoother than those formed with short distances. Presumably, only the finer grains of carbonate pass from one electrode to the other when the distance is great.

While the coating process seemed satisfactory, certain speculation arose as to the life time of the coating when operating in a gas filled tube, where, under experimental conditions, it might be subjected to ion bombardment. Since the system was to be enclosed in a sealed glass container where replacement of the coating, should it be required, would be very difficult, it was decided to examine the possibility of using a more robust emitter.

Such emitters are required, for example, in many higher-powered cavity magnetrons, for which the so-called "matrix cathodes" were developed. Such cathodes are made by first attaching a fine nickel mesh to a nickel base. A coating consisting of equal parts of barium and strontium carbonate with the addition of finely divided nickel powder, in amounts up to as much as 30% by weight, is then mixed to a paste with methyl alcohol and pressed into the mesh. The nickel mesh, in addition to providing structural solidity, is helpful in reducing the resistance of the interface, or thin slag film, such as barium silicate, which forms over the base metal. The nickel powder reduces the resistivity of the relatively heavy coating (about 25 mg per sq cm). Also, when the emitter is being processed and heated above 1300° K, the fine nickel powder sinters, so that the coating is attached as a robust layer to the nickel base and mesh (34). This type of emitter appears to be well suited to the converter system under investigation and was used. It is interesting to note that Bloss (4) when working with his converter system, first used a commercial BaO-cathode as emitter and experienced a resistance of 5 ohms. He then decided to use a barium-nickel matrix cathode and found the re-

sistance decreased to 0.85 ohms.

Special high grade barium and strontium carbonates for electron tube use were provided by the Radio Corporation of America. Prior to coating the emitter base plate, sample tests were made to determine what appeared to be the most suitable procedure. The coated emitter was then dried in an air conditioned atmosphere at room temperature for three days before the tube was sealed.

Collector design

It is desirable to make the collector work function for a thermionic conversion system as low as possible. While a lower limit is certainly imposed by the back emission effect, at the present state of the art there is little danger that a material can be used where back emission is a problem. For example, at the relatively high collector temperature of 610° K, the saturation back emission electron current density amounts to only 0.1 amps/cm^2 for a 1.0 eV work function material. The production of a suitable collector material is a major problem hindering the satisfactory development of all thermionic conversion systems. In the auxiliary system any suitable collector material may be used. At present there are many ways of achieving low work function surfaces but numerous problems arise when such surfaces are incorporated in a converter system. For example, many composite low work function surfaces rely on a cesium coating. Such surfaces are not acceptable in an auxiliary system, where one of the main advantages is the production of ions without the use of cesium. However, Bloss (4) in Stuttgart, Germany has fabricated and tested an auxiliary system in which the collector consists of a silver

coating on the glass walls of the tube. The desired low work function of about 1.0 eV is achieved by heating a cesium resevoir and periodically depositing a cesium coating. While a low work function was achieved and the experimental device operated satisfactorily, no long term solution for obtaining a suitable collector with other than a cesium coating was presented.

Numerous approaches were made to industry to supply low work function materials, or to coat the collector base. In particular it was hoped that coatings used for low work function photomultiplier electrodes could be applied. However, it was learned from the tube manufacturers that the coatings used are only suitable for low temperature operation and are also very subject to contamination. Finally, since the investigation and analysis of the system does not require the use of a low work function collector the decision to use a simple nickel mesh collector and externally bias the circuit to compensate for work function deficiencies was made. Apparently, this was also the logical conclusion reached by such other workers in the field as Gabor (13) who uses nickel collectors, and Bernstein and Knechtli (1), who use Phillips Type B dispenser cathodes for both emitter and collector. Therefore, it must be realized that throughout the operating and testing procedure a bias voltage will be applied to the collector to compensate for its large work function. This is an external factor and in no way alters the conditions pertaining to the potential profile and plasma which would be observed if a low work function collector were used. Thus, the results and the parameters evaluated apply directly to a converter operating in the Gabor mode.

Before the emitter coating was applied all converter system components, as well as the glass containment tube, were ultrosonically cleaned in an acid bath, then rinsed and dried. After 3 days the tube was mounted in a glass-blowing lathe and sealed.

Vacuum System Design

Although the auxiliary discharge converter does not operate at very low pressures, pressures to 10^{-8} mm Hg are required during activation of the oxide coated emitter. For this reason, high vacuum equipment and technology must be used. Three separate forms of pumping are provided.

The vacuum system in its final form is represented in Figure 28. A Cenco Megavac rotary pump is used to exhaust the system to the 1 micron range. A cold trap is placed in line with the pump. The liquid nitrogen filling the trap has a boiling point of -195.8° C and so condenses vapors , particularly water vapor, which are detrimental to the operating of the pump. In addition, of course, the gas being exhausted is cooled in passing through the trap and is more easily pumped as a denser fluid. The needle valve C serves to isolate the roughing pump. A thermocouple gauge between valves C and B measures pressures effectively between 1 and 10^{-3} mm Hg. Copper tubing and rubber hose are used between the roughing pump and valve B since pressures less than 10^{-3} mm Hg are not expected there. Valves A and B are Varian stainless steel, Viton A seal valves capable of operating down to 10^{-9} mm Hg. They isolate the untra-high vacuum system. Within this system all fittings are Varian 300 Series stainless steel with Con-Flat flanges and copper gaskets. The cross fitting forms a junction for the roughing line, the gas-filling line, the

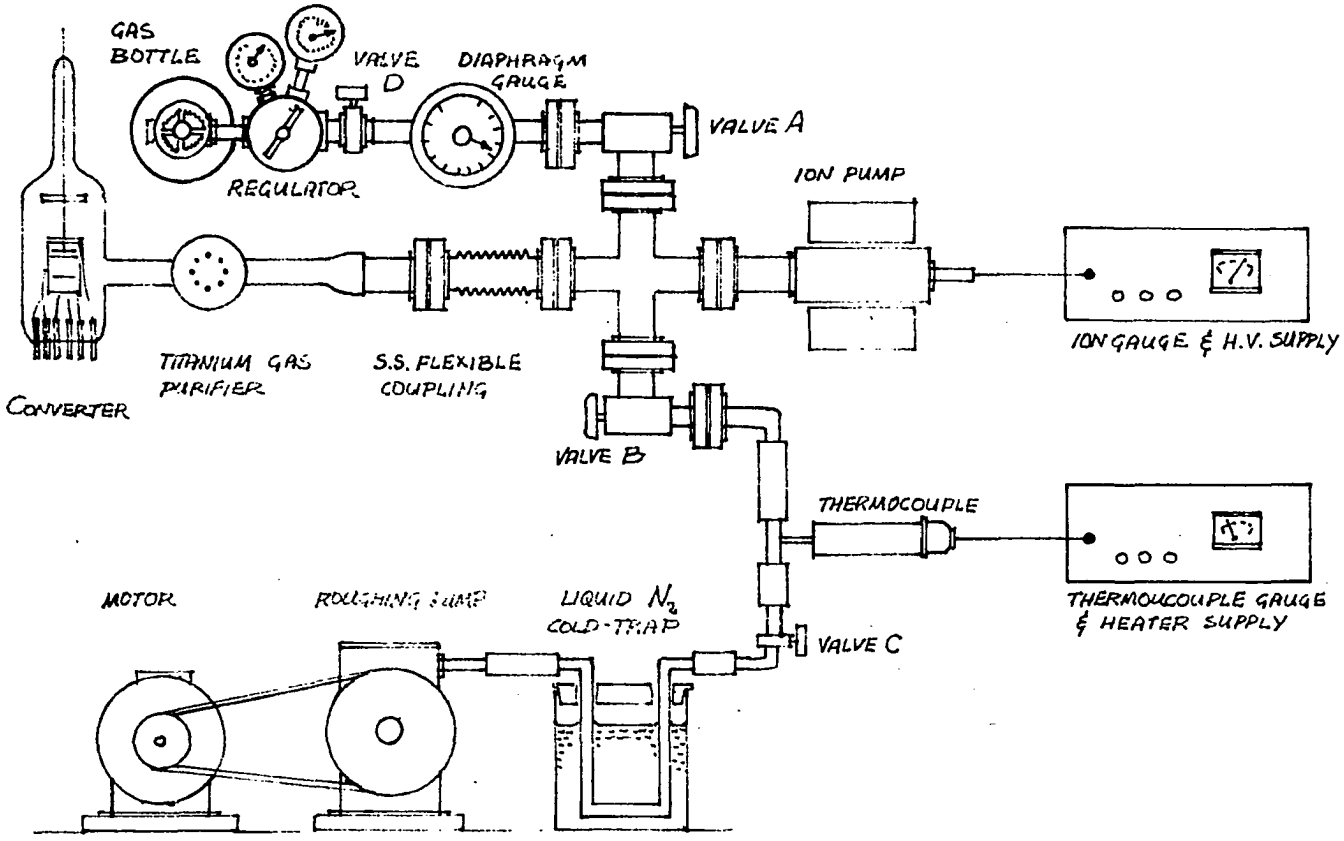

Figure 28. Vacuum system showing pumping and pressure measuring units

converter line, and the ion pump line. The ion pump is a Varian 8 lites/sec Vac Ion pump containing titanium electrodes and supplied by a high voltage source capable of producing 4000 volts. Pumping is achieved by the formation of chemically stable compounds and ion burial. Since the current supplied to the pump bears a linear relation to the density of the gas molecules, this current may therefore be used to indicate the gas pressure directly. It is found that the accuracy of such direct pressure readings is as good as may be obtained with a high quality ionization gauge.

Since the converter must be filled with a Penning mixture, a bottle containing neon-0.1% argon is connected via a regulator valve and a needle valve D to valve A. A diaphragm gauge operating in the 1-760 mm Hg range serves to indicate the gas filling pressure.

A glass tube containing pellets of titanium sponge enclosed in a nickel mesh serves as a means of purifying the filling gas as well as a getter. The arrangement is such that the output coil of an induction furnace may be placed about the gas purifier tube to heat the nickel mesh. The titanium within the mesh is also heated and absorbes all but the inert gases. The converter system and gas purifier tube are connected to the cross fixture by means of a glass-metal junction and a flexible stainless steel coupling. When the system was first assembled and pumped down it was apparent that a leak existed. This was traced, by means of a mass spectrometer leak detector tuned for the helium tracer gas, to a faulty copper gasket at valve B. This gasket was replaced and no further leaks were detected.

Decomposition and Activation of the Emitter

At the time of sealing the tube to the vacuum system, the emitter consists of a mixture of calcium carbonate, strontium carbonate and nickel powder, In order to produce the desired emitter work function, the coating must be processed. This may be broken into two stages, decomposition and activation.

The process of decomposition is chemical in nature. When emitter is heated to about 1150° K, a reaction of the form

$$XCO_3 \rightleftharpoons XO + CO_2$$

takes place. Carbon dioxide is evolved and the barium and strontium compounds are reduced to their respective oxides. The above equilibrium is determined by the dissociation pressure. For a fixed temperature, the dissociation pressure of barium carbonate is always lowest and this pressure is therefore the governing factor. If a temperature of 1150° K is selected for the decomposition process, then it is found that a pressure less than 100 microns should be maintained within the system. Pressure limits are governed by the ability of the pumping system to remove the carbon dioxide as it is evolved. It is found in practice that a short decomposition time is beneficial. During decomposition, the strontium carbonate existing within the mixed carbonates is converted into its corresponding oxide first, while the barium carbonate is converted some time later. When the decomposition is finished, the two oxides exist in separate phases in spite of the fact that mixed crystals of carbonates have existed before. The mixed oxide crystals (BaSr) O are obtained by further heating.

The roughing pump was started and the complete vacuum system baked under infra-red ray lamps for 8 hours. The heat shields and heater were also outgassed by running the heater at 750° K for 30 minutes. When the pressure reached 7.8 microns, the ion pump was turned on and the pumping proceeded as in Figure 29. The irregularity at t = 19 minutes arises from the fact that the valve to the roughing system was temporarily opened. The ion pump is inefficient at pressures above 10^{-3} mm Hg and tends to lock in two high pressure modes. The pump recovered from the first mode without external assistance at t = 26 minutes. However, it locked in the second mode and, since the pump dissipates a large amount of power in this mode, it quickly overheated. So, at t = 29 minutes the power was turned off and the pump cooled for 29 minutes. When turned on at t = 58 minutes, it recovered and proceeded to pump down to 3.7×10^{-7} mm Hg.

The system was then ready for commencement of the decomposition process. The heater was connected to a DC power supply and the process took place as shown in Figure 30. When the heater was switched on, the pressure rose sharply due to the out gassing of the heater and electrodes initially, and then to the evolution of the carbon dioxide during the chemical reaction, which lasted for about 15 minutes. The reaction was initiated at a temperature of about 1130° K and the temperature was gradually increased to 1238° K in order to ensure completion of the process.

After decomposition, the emitter normally gives a reasonable emission current at the operating temperature; however, this current may be increased by a further process, called activation of the emitter. This consists of applying a positive voltage, relative to the emitter, to the

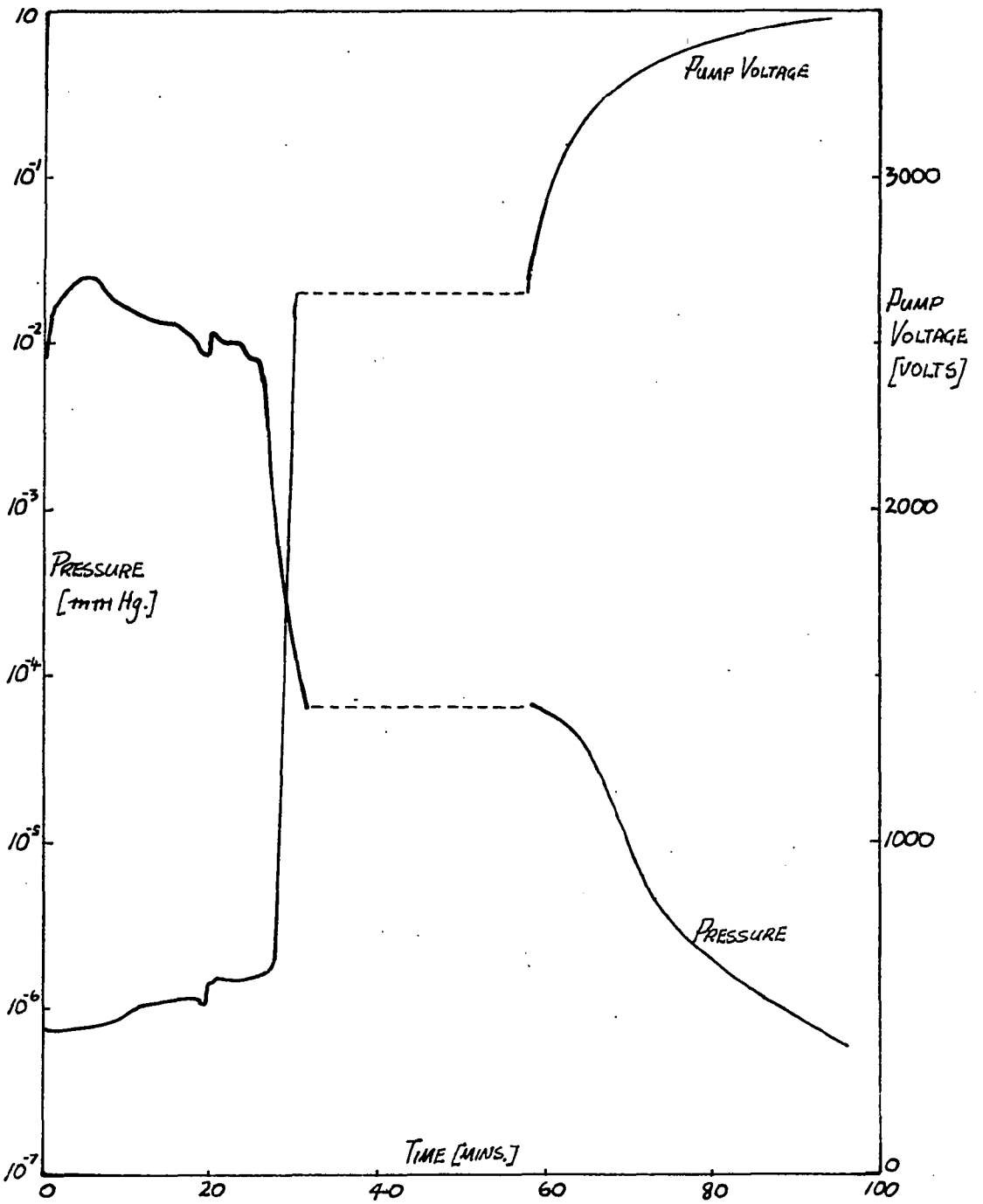

Figure 29. Variation of system pressure with time during the evacuation process

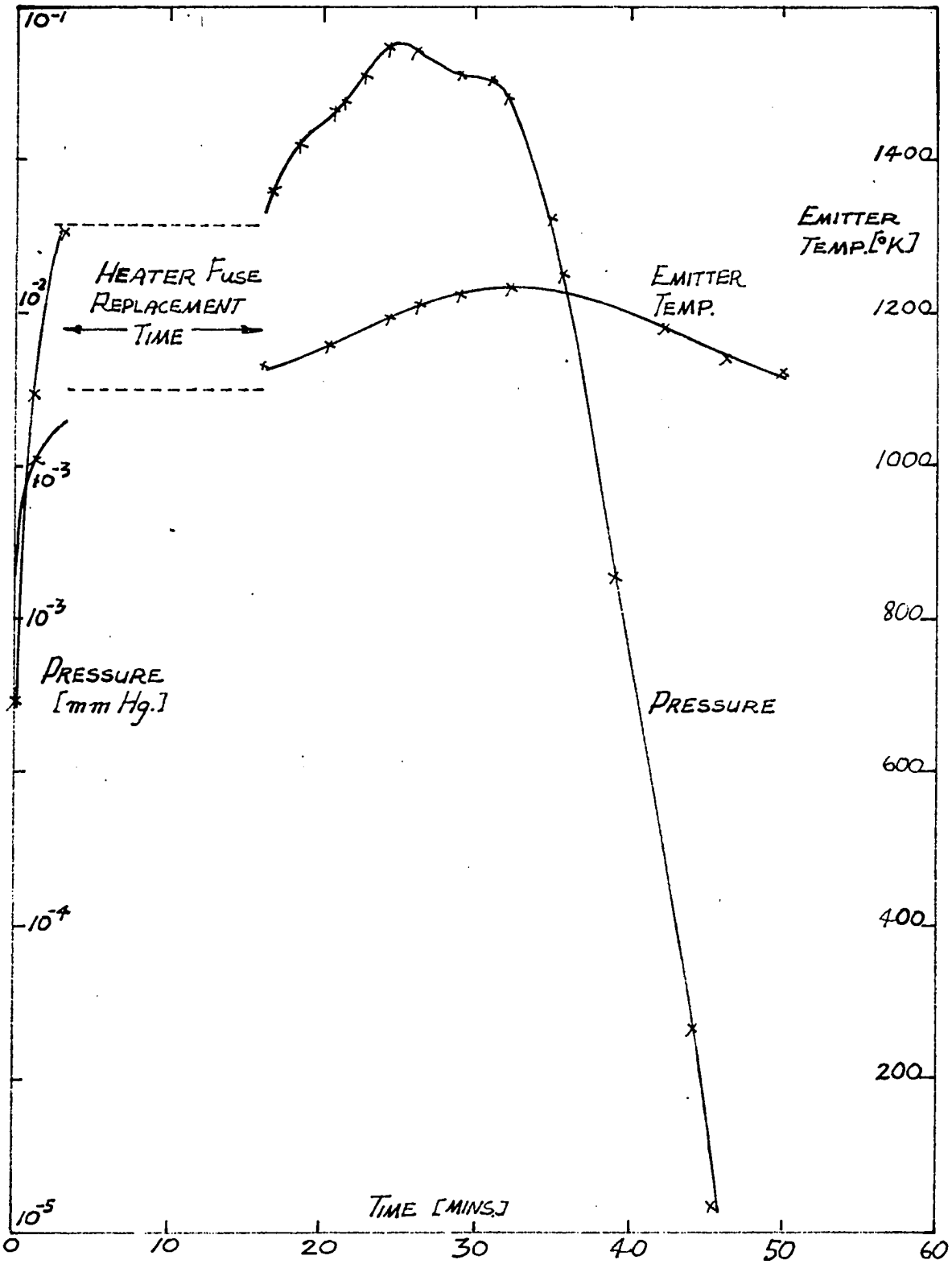

Figure 30. Variation of P and T_E during decomposition

other electrodes and heating the emitter above normal operating temperatures. Results are twofold. In the first case the applied voltage (about 100 V) causes an emission current to flow through the coating which dissociates the oxide electrolytically into barium and oxygen. Oxygen then escapes and barium is produced. Since three processes (reduction of barium oxide to barium, the diffusion of this barium, and its evaporation) determine the formation of the emitter surface, there are optimum activation conditions. The optimum temperature is found to be between 1225° K and 1325° K (22). In addition to the formation of a barium surface layer, the activation process serves to remove residual gases from the other electrodes. Electrons, accelerated by the applied positive potential, are accelerated from the emitter and bombard the collector. Consequently, the heating drives off the residual gases.

Figure 31 shows the variation of collector current, emitter temperature, and pressure during the activation process carried out on the emitter. The emitter temperature was gradually increased in steps from 1100° K to 1240° K and oxygen was evolved during a period of about 50 minutes, each time the emitter temperature was increased. The variation of collector current is interesting in that it rises initially with each temperature increase but then falls off, reaches a minimum and then recovers. This should be expected for at each temperature increase the emitter is poisoned by the gases which are set free. It subsequently recovers due to activation produced by reduction and the arrival of extra barium at the surface.

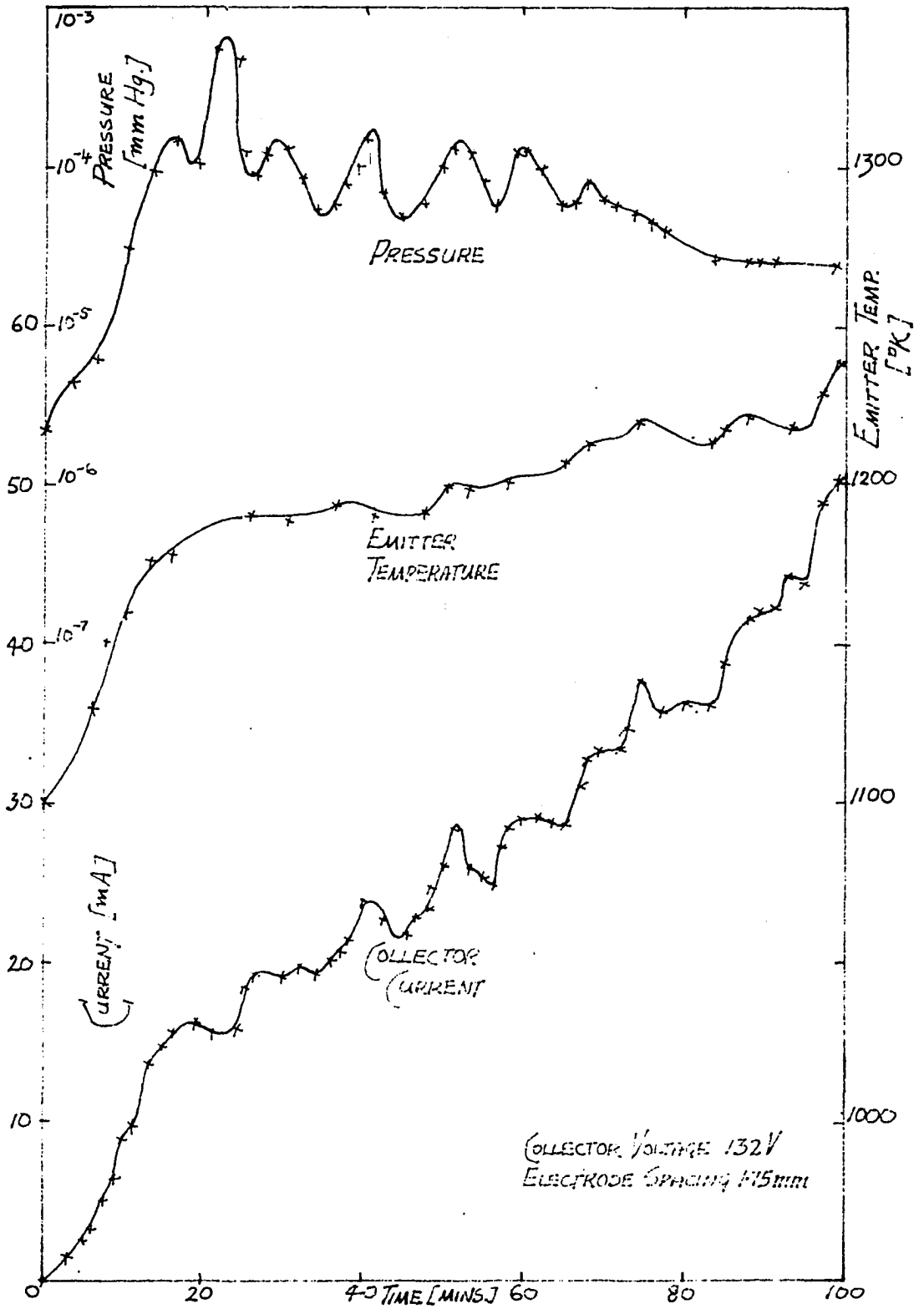

Figure 31. Variation of P, T_E and I_L during activation

At the completion of the activation process, the saturation current of 37.9 mA was emitted at a temperature of 1220° K, corresponding to an effective work function of 2.31 eV. This is very close to the desired value of 2.3 eV.

Heat Loss Analysis

For certain calculations, it is necessary to determine the rate at which heat is being lost by radiation, conduction and convection. While it is possible to calculate the various losses from theoretical and empirical relationships, a much simpler, and in general more accurate, way is by the use of heating or cooling curves (35).

If the heater is turned on, the system heats up exponentially with a time constant T, so that the temperature Θ at any time t is related to the steady state temperature Θ_o by,

$$\Theta = \Theta_o(1 - e^{-t/T}) \tag{72}$$

At any time t the energy contained within a material of mass W and specific heat S is

$$Q = WS\Theta = WS\Theta_o(1 - e^{-t/T})$$

Then, the rate of power exchange at temperature Θ is

$$P_H = \frac{dQ}{dt} = \frac{WS\Theta}{T} \tag{73}$$

From Equation 73, it is apparent that the heat power loss may be evaluated from a knowledge of the mass, specific heat, average temperature and time

constant of the system. All but the time constant are readily available and this may be determined from either a heating or cooling curve test.

A heating test was performed on the converter system and the exponential curve obtained is shown in Figure 32. This has a time constant T of 20 secs. The mass of the emitter, heat shields and collector, which are essentially the parts undergoing substantial temperature change, is 12.5 grs and the specific heat of nickel at 773° K is 0.53 Joules/gr$^{\circ}$ C. In general, the objective of the test would be to calculate the heat loss under certain conditions. In such a case, thermocouples would be positioned so that an estimate of the average temperature could be made. In this case it is of more benefit to evaluate the average temperature, since the heat loss is known to be the heater input power, there being no electrical or other output. This average temperature may then be used as a guide for approximating the collector temperature since there is no direct means for doing so. It is reasonable to assume that the collector is at a temperature close to that of the outer heat shield since both are about the same distance from the emitter and inner heat shield respectively.

The emitter temperature under typical operating conditions is 960° C with a heater power of 140 watts. Since the tungsten heater is close to the emitter, the rest of the inner heat shield will be at a lower temperature. An average of 800° C is reasonable for the combination of the inner shield and emitter. The temperature of the outer shield is unknown, but it has a mass of 6.05 grs. The overall average temperature is

$$\theta = \frac{P_H T}{WS} = \frac{140 \times 24}{12.5 \times 0.53} = 508^{\circ} \text{ C}$$

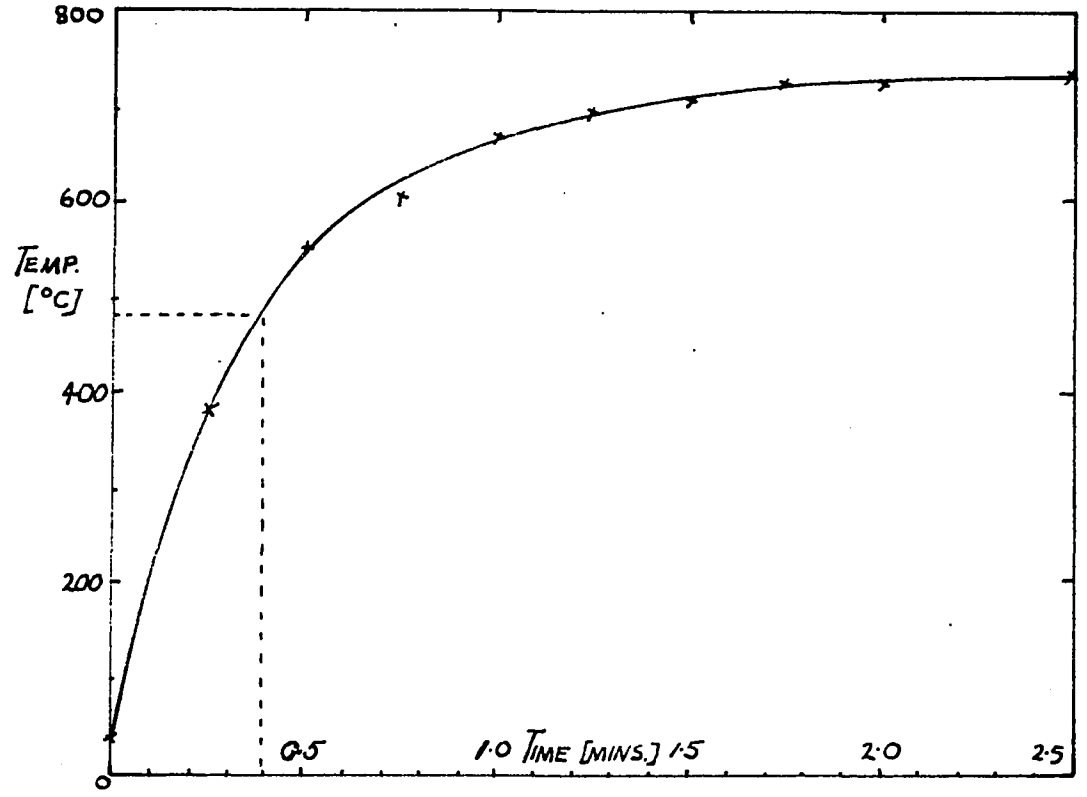

Figure 32. Heating curve for the electrode and heat source system

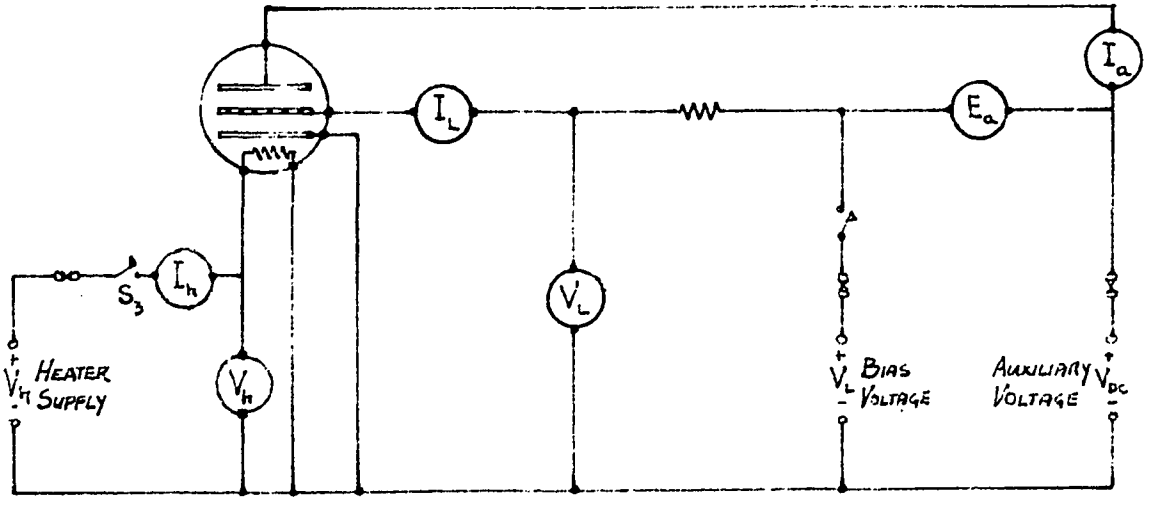

Figure 33. Electrical circuit used for determining the operating characteristic

Therefore, the temperature of the outer heat shield and the approximation to that of the collector are obtained from

$$\theta = 508 = \tfrac{1}{2} \left(\frac{T_c\ 6.05 + 800 \times 5.45}{12.5} \right)$$

as

$$T_c = 166^\circ\ C = 439^\circ\ K$$

Converter Characteristics

Having activated the emitter under high-vacuum conditions, the Penning mixture of neon-0.1% argon was then introduced. The gases were obtained already mixed in the correct proportions. Prior to final evacuation, the region between valve A and the gas bottle was out-gassed and then flushed with a stream of gas before shutting valve A. The branch was then left above atmospheric pressure to ensure that any leakage would be outwards.

With the emitter heater turned off, valve A was opened to permit a small flow of gas. With the roughing pump operating, valve B was opened so that the excess gas was slowly exhausted from the system. Valve A was then fully opened so that the diaphragm gauge indicated the system pressure. When a pressure indication of 4 mm Hg was obtained, valve B was closed.

At this stage the gas purification process was started. The output coil of a Ther-Monic induction furnace was placed about the tube containing the nickel and titanium. A bright pink glow discharge spread down the tubes to both the ion pump and converter. The nickel and the titanium

sponge were heated. After 30 minutes it was assumed that the cleaning process had taken place and the furnace was removed. Final pressure adjustments were then made by opening valve B slightly until the pressure decreased to 1 mm Hg. At this point valves B and A were closed.

The electric circuit of Figure 33 was set up. A DC, rather than an AC, heater supply was used since a certain amount of interference was experienced when an AC supply was initially tested. With the bias voltage set at 2.6 volts, the auxiliary voltage was increased gradually and the auxiliary discharge region was observed for the first traces of any glow which might indicate ionization in that region. With a Penning mixture ionization would be expected at an auxiliary potential of about 5 volts; however, this did not occur. The auxiliary potential was increased further to the limits of the source without ionization. A large voltage source was installed and ionization was finally achieved at a potential of 23 volts and the system operated in the Gabor mode. A bright pink glow covered the auxiliary side of the collector mesh and extended for a distance of about 2.5 mms, the flow extinguished and the collector current dropped to a negligible value. Thus, operation of the converter system was achieved as planned but the need for such a high auxiliary voltage remained unexplained. Since there was an error of a factor of four between the actual and expected values, a further investigation was certainly called for.

At this stage, a glow discharge was observed between the lead to the auxiliary anode and the heat shield. This discharge caused avalanche breakdown of the gas-filling resulting in an effective short circuit on the system. As a result, one of the emitter assembly supports was melted,

the assembly tilted and the heater was short-circuited to ground, as shown in Figure 34.

It was then necessary to replace the affected components, reassemble the converter and process the emitter. In order to ensure that such a gas breakdown would not occur again, the auxiliary anode lead was insulated with two layers of ceramic beads and limiting resistors were placed in series with all power supplies.

Upon operating the system, it was found again that a high auxiliary anode voltage of 23 volts was required to initiate operation in the Gabor mode. Thus, it was decided to proceed with a test to determine the true first ionization potential of the filling gas. This test evolved as follows.

Prior to any ionization, the electron emission from the emitter is space charge limited and the interelectrode profile is as shown in Figure 35a. If an increasing voltage is applied to the collector, with S_2 open, the current collected by the collector should increase as the space charge effect is reduced by the increasing voltage. A certain fraction of the electrons penetrate the collector and reach the auxiliary anode. At the point of ionization, radical changes take place. Due to the presence of ions, the potential profile is depressed and a typical plasma profile exists, as in Figure 35b. The sudden change in profile should have a dramatic effect on the electrons which penetrate the collector to the auxiliary region. After the ionizing process commences, the profile tends to oppose rather than assist electron transit to the auxiliary anode. Therefore, a sharp drop in auxiliary anode current should be noted.

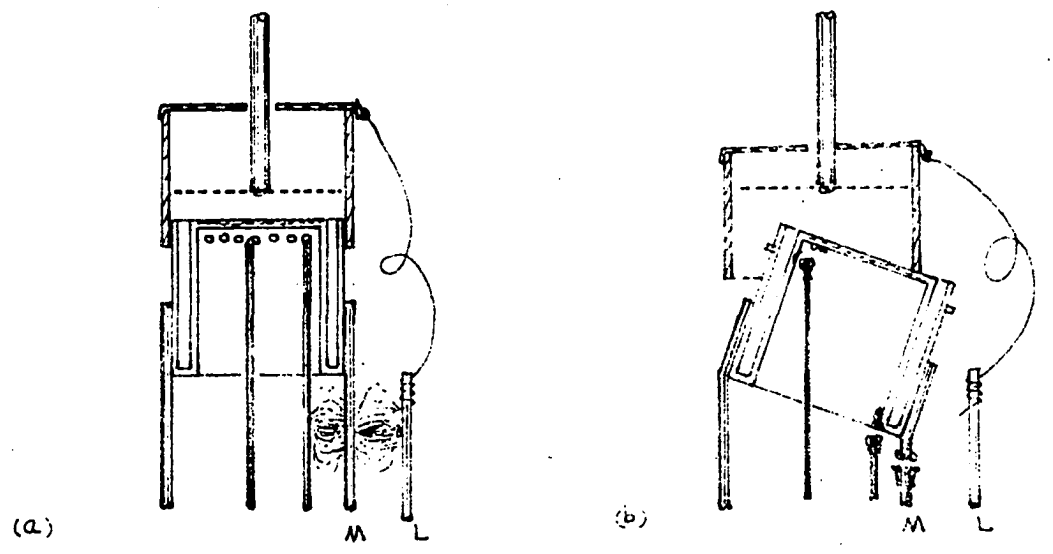

Figure 34. Cross-section of the electrode system (a) during and (b) after the breakdown of the gas-filling

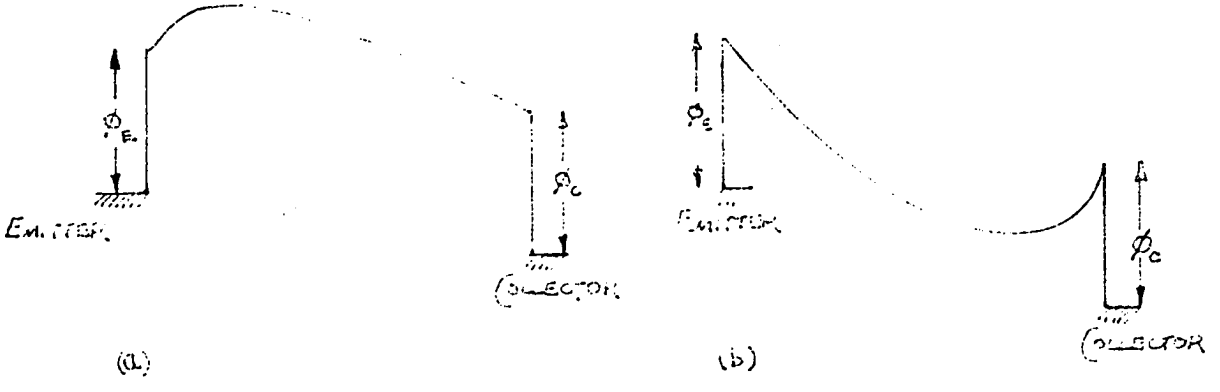

Figure 35. Potential profile in the emitter-collector region (a) before and (b) after the occurance of ionization

The test was carried out and the results are shown in Figure 36. The low value of the auxiliary anode current was a practical problem encountered during the test. An indication of this current was made possible however, by placing a vacuum tube voltmeter between the collector and auxiliary anode. The voltage recorded was that caused by the current leaking through the internal resistance of the instrument. As seen from Figure 36, there is a sharp change, as expected, in the rate of electron arrival at the auxiliary anode. The first ionization potential of the controlling gas is therefore about 20 volts. Argon has a first ionization potential of 15.68 volts and neon a first ionization potential of 21.47 volts. Therefore, it appears almost certain that neon is the only gas contributing significantly to the ion production process. There appears to be a slight change in the slope of the collector current curve at about 12 volts. This could be caused by traces of argon or impurities such as oxygen or nitrogen with first ionization potentials at 13.55 volts and 14.48 volts respectively.

The gas mixture obtained from the Linde Corporation is certified to contain neon with the addition of 0.1% argon. An explanation of the relative absence of argon from the filling gas was offered by a representative of one of the Solid State Affiliate Companies who experienced a similar problem. It is found that when gases of different masses are valved through a small opening there is preferential emission of the lighter gas. Since the gas mixture within the bottle was at 1500 p.s.i. it was necessary to use a very small opening when filling the system and it is assumed that the lighter gas, neon, escaped preferentially. Thus a Penning mixture was not present within the system. This problem must

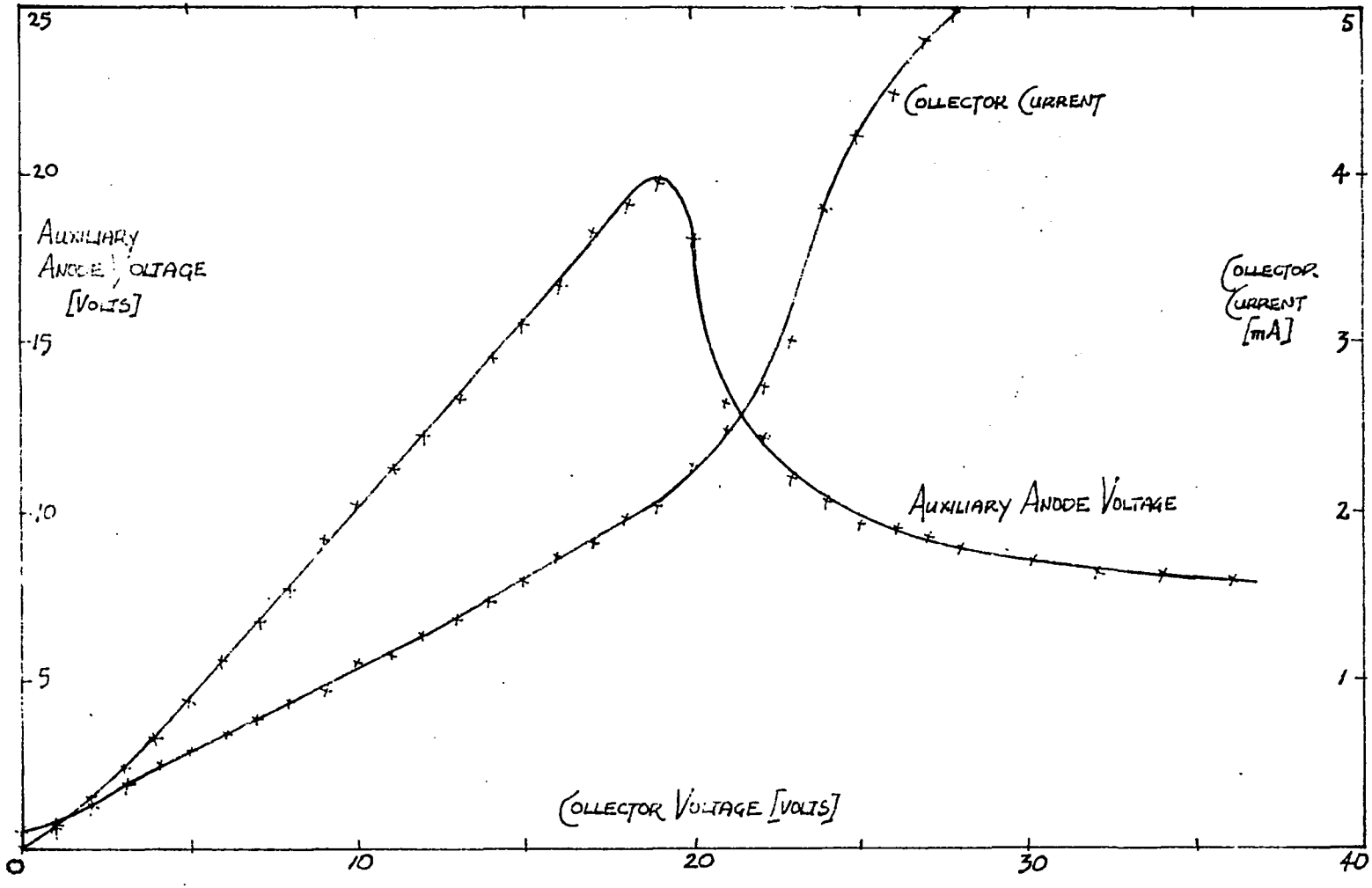

Figure 36. Variation of the auxiliary anode voltage and collector current with the applied collector voltage

have presented itself to other researchers. For example, Gabor uses argon-0.1% mercury. The mercury is evaporated into the system and condensed in a cooled appendage. While such a procedure is not simple, it at least ensures the presence of mercury in the argon.

The fact that a Penning mixture was not present in any way affected the operation of the converter system since the neon produces the ions for space charge neutralization. In this case it is of little consequence that four times as much energy is required to produce a neon ion.

In order to determine the converter system load characteristic, i.e. the variation of output current with voltage, the tube was fired and the data shown in Table 3 obtained.

Table 3. Converter characteristics

V_L volts	I_L mA	I_a μA	I_L/I_a	T_E ° K	I_L mA at T_E=1233° K
0.22	0.07	4.0	17.5	1233	0.07
0.74	0.16	9.0	17.8	1238	0.118
0.925	0.20	10.6	18.9	1239	0.153
1.215	0.27	11.8	22.9	1241	0.201
1.36	0.33	14.3	23.1	1242	0.237
1.48	0.37	15.2	24.4	1243	0.250
1.60	0.43	16.05	26.8	1245	0.295
1.7	0.45	16.5	27.3	1246	0.301
1.91	0.53	17.0	31.1	1248	0.343

Table 3 (Continued)

V_L volts	I_L mA	I_a μA	I_L/I_a	T_E ° K	I_L mA at T_E=1233° K
2.2	0.65	19.1	34.0	1253	0.363
2.35	0.70	20.8	33.6	1255	0.363
2.57	0.75	22.0	34.1	1259	0.365

It was found necessary to increase the emitter temperature above 1183° K in order to achieve a satisfactory current density. This indicates an increase in emitter work function from 2.3 eV after activation under vacuum to 2.88 eV in gas. Such an increase is not surprising because the barium and strontium oxides are themselves very active and readily absorb any impurities present. It is thought that the impurities in this case may have come from sputtering of the emitter during the gas ionization test. Such sputtering would certainly tend to increase the work function. However, this did not hinder the test and the variation of emitter temperature, main and auxiliary current and voltage were noted within the operating range.

A plot of load current against load voltage for an emitter temperature of 1233° K is shown in Figure 37. This is typical and illustrates the steady increase in load current as the collector sheath potential decreases until a point is reached, at the knee of the curve, where the collector surface is at the plasma potential. Subsequently, the current

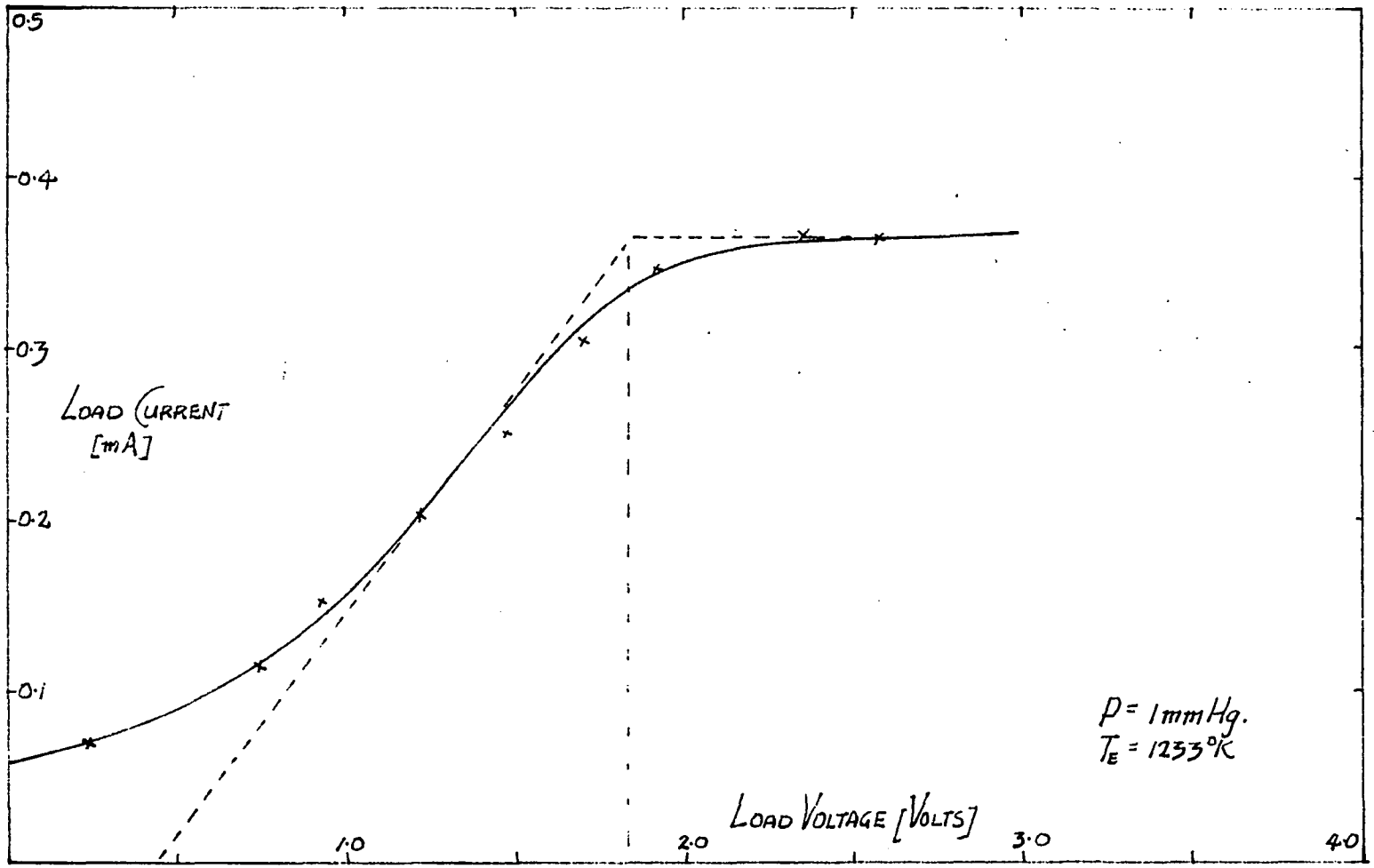

Figure 37. Variation of load current with load voltage at an emitter temperature of 1233° K

drawn is the plasma random current. As seen from Table 3, the load to auxiliary current ratio is 34 when saturation current is being drawn. While this ratio is high, it was expected in light of Gabor's slow ion reflection theory. Higher ratios of up to 170 were obtained briefly at emitter temperatures of about 1275° K and load currents of about 0.015 amps. However, it is not certain that the converter system was operating in the correct mode since it appeared that ionization might be taking place in the main plasma region.

ANALYSIS

The theory developed for the system will now be used to determine the potential profile across the main plasma, the characteristics of the plasma and the parameters of the critical equation. This equation will then be solved for the slow ion reflection coefficient R and thus for characteristics of the complete charge flow system determined for equilibrium conditions.

As previously mentioned, it will be assumed that the system is operating just at the commencement of space charge limitation, and so V_m may be taken as zero.

Potential Profile

From the load characteristic curve in Figure 37, the load voltage V_L (actually the bias voltage corresponding to the point at which the emission becomes space charge limited) is 1.83 volts. This is represented in Figure 38 by a change of 1.83 volts in the emitter Fermi level. The emitter work function ϕ_E was found to be 2.88 eV.

From Gabor's theory (13), the subtangent to the slope of the load characteristic has a magnitude of $4\ k\ T_{ec}/e$. Since the subtangent of the curve in Figure 37 has a magnitude of 1.38 volts, the electron temperature at the collector is 3980° K. The initial temperature of the electrons is that of the emitter (1233° K) and so their temperature has been increased by 2747° K in passing through the main plasma. There is no collector sheath at the knee of the load characteristic so the electron temperature increase must be associated with the accelerating potential V_{Ef} at the emitter sheath as well as the accelerating potential V_p across

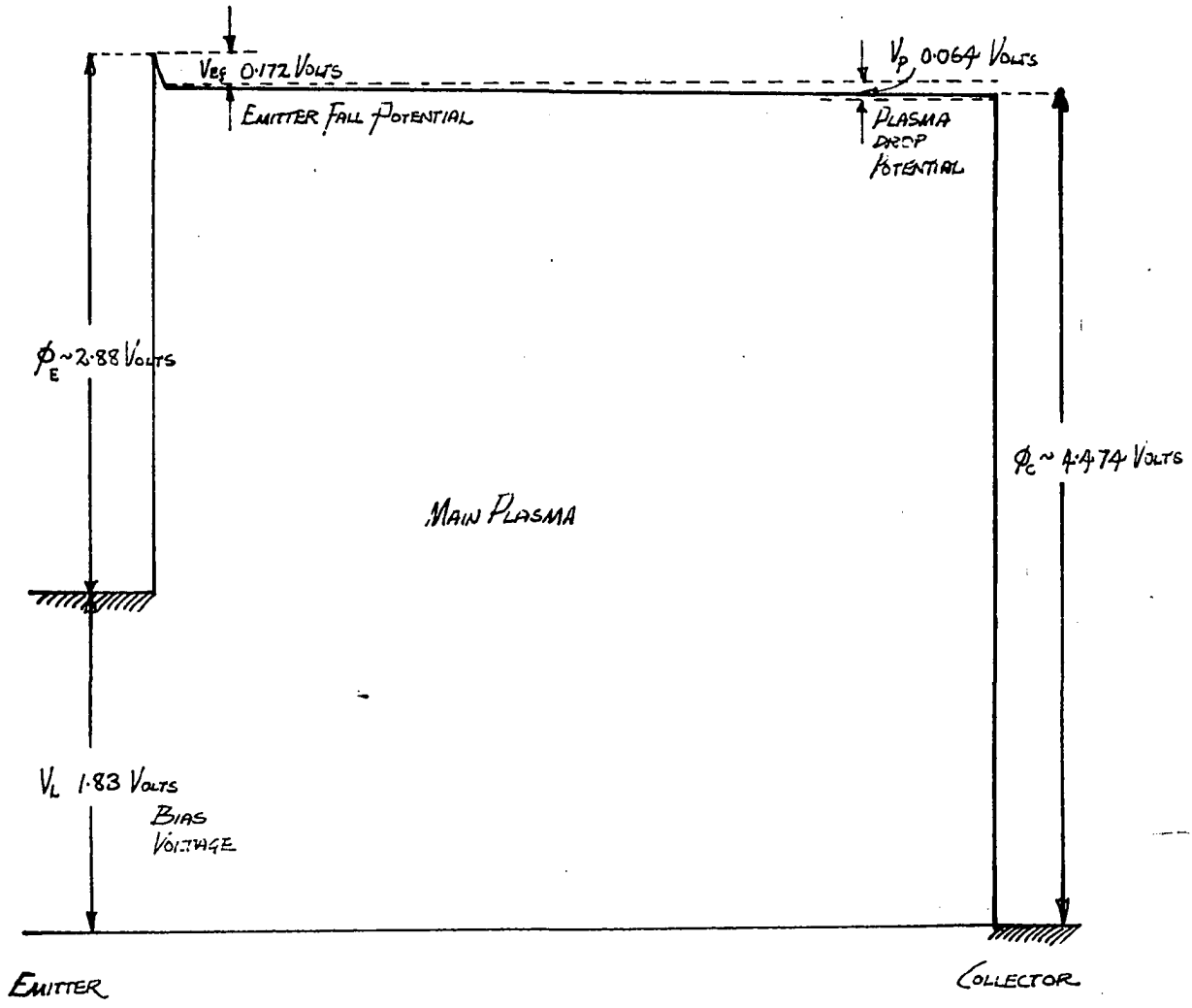

Figure 38. Potential profile in the emitter collector region

the main plasma. Therefore, $V_{Ef} + V_p$ corresponds to the temperature gain of 2747° K. Then, $V_{Ef} + V_p = 2747\ k/e = 0.236$ volts. Thus, the effective work function of the collector is

$$\phi_c = 1.83 + 2.88 - 0.236 = 4.474 \text{ eV}.$$

Since the collector is of nickel, its work function is relatively well known. A value of 4.61 is reported by Wahlin (44). The slight discrepancy is very likely due to a lowering of the collector work function as a result of evaporation of the oxide emitter coating, which would have occurred during activation and particularly during the gas analysis test.

Plasma Characteristics

Electron density at collector

Since there is no collector sheath when operating at the knee of the load characteristic, the collector current is equal to the random plasma current in the plasma at the emitter sheath, which is given by Cobine (9) as $\frac{n_{ec}\ e\ v_{ec}}{4}$. The average velocity ($v_{ec}$) of the plasma electrons at the collector may be expressed in terms of their temperature by

$$v_{ec} = \sqrt{\frac{8k\ T_{ec}}{\pi m}} = 0.62 \times 10^6\ T_{ec}^{\frac{1}{2}} \text{ cm/sec}.$$

Therefore, the electron density at the collector is

$$n_{ec} = \frac{4J_L}{0.62 \times 10^6\ T_{ec}^{\frac{1}{2}}\ e} \text{ electrons/cm}^3$$

Figure 37 shows the current density J_L at the knee of the curve as 0.226 mA/cm^2. Then, n_{ec} is found to be 1.44×10^8 electrons/cm^3.

Potential drop across plasma

The total plasma resistivity is $\rho_{ep} = \rho_{en} + \rho_{e+}$. Equation 55 gives the electron-neutral resistivity as

$$\rho_{en} = 1.81 \times 10^{12} \quad \frac{P\, T_{ep}^{\frac{1}{2}}}{n_{ep}\, T_g} .$$

The average electron concentration in the plasma may be evaluated by an iterative process. An average electron temperature and concentration in the plasma is assumed and ρ_{en} is calculated. It is found that ρ_{e+} is negligible and so the plasma potential fall V_p may be evaluated. Since electron concentrations and temperatures are related in the plasma by the Boltzmann equation,

$$\frac{n_{eE}}{n_{ec}} = \frac{T_{ec}}{T_{eE}} \exp \left[\frac{eV_p}{k\, T_{ep}} \right] , \qquad (74)$$

it is possible to check the accuracy of the assumed values and iterate to a more acceptable solution.

Assume a ratio K_1 between average plasma and collector electron densities of 2.5. (This value is prompted by Gabor's probe analysis (17)). T_g is taken as 836° K, the mean of the emitter and collector temperatures. For an estimate of $T_{ep} = 3500^\circ$ K and $n_{ep} = 3.6 \times 10^8$ electrons/cm^3,

$$\rho_{ep} = \frac{1.81 \times 10^{12}\sqrt{3500}}{3.6 \times 10^{8} \times 836} = 355 \text{ ohm cm}$$

Using the same values, ρ_{e+} may be evaluated.

$$\rho_{e+} = \frac{6.53 \times 10^{3}}{T_{ep}^{3/2}} \ln \left(\frac{3}{2e^{3}} \sqrt{\frac{k^{3} T_{ep}^{3}}{\pi n_{ep}}} \right) \text{ ohm cm}$$

$$= \frac{6.53 \times 10^{3}}{3500^{3/2}} \ln \left(\frac{3}{2 \times 1.6^{3} \times 10^{-57}} \sqrt{\frac{1.38^{3} \times 10^{-69} \times 3500^{3}}{\pi \times 3.6 \times 10^{8}}} \right)$$

This contribution to the plasma resistivity is negligible under present conditions. The potential drop across the plasma is then

$$V_p = J_L \, d \, \rho_{ep} = 0.226 \times 10^{-3} \times 0.4 \times 355$$

$$= 0.032 \text{ volts}$$

Upon substituting the calculated values into the Boltzmann equation, it is found that the ratio K_2 between electron concentration at emitter and collector is 1.32 corresponding to a K_1 ratio of 1.16. A new value of K_1 = 1.28 is selected and the calculation process is repeated. The results of successive iterations are shown in Table 4.

Table 4. Iterative process in determining plasma characteristics

K_1 (trial)	T_{ep} ° K (trial)	$n_{ep} 10^{-8}$ e/cm^3	ρ_{en} ohm cm	V_p volts	T_{ec} $-T_{eE}$ ° K	K_2	K_1	T_{ep} ° K
2.5	3500	3.6	355	0.032	371	1.32	1.16	3795
1.28	3590	1.8	718	0.0645	750	1.52	1.26	3605
1.27	3600	1.83	710	0.0639	742	1.521	1.26	3609
1.265	3607	1.82	711	0.0640	743	1.522	1.261	3608

The final iteration is acceptable so that the average plasma temperature is now taken as 3607° K and the average plasma electron density as 1.82 x 10^8 electrons/cm^3. With these new values, the calculation of ρ_{e+} is repeated and found to be 0.148 ohm cm. This still remains insignificant. Therefore, the overall plasma resistivity is taken as 711.1 ohm cm and it is almost completely due to electron-neutral atom collisions. The potentail profile in Figure 37 may now be completed, the emitter fall potential, V_{Ef}, being 0.172 volts and the plasma fall potential, V_p, being 0.064 volts.

Cyclic Analysis of Charge System

Now that the main plasma has been analyzed and its parameters determined, it is possible to evaluate the probability terms involved in the critical equation. In view of the results from the gas analysis, it is assumed that the filling-gas is neon and so the equations derived for a system filled with a Penning mixture will be modified where necessary.

Recombination of ions and electrons within the main plasma will be considered.

Probability of reabsorption of electron

As derived in Equation 6,

$$1 - p_E = \frac{n_{eE}\, e}{J_o} \sqrt{\frac{kT_{eE}}{2\pi m}} \exp(-eV_{Ef}/kT_{eE}) \qquad (75)$$

The load current density is known to be 0.226 mA/cm^2 and this will be seen to be $p_E J_o$ to a close approximation. Therefore, $J_o = 0.226/p_E$ mA/cm^2. Substituting this and known values into Equation 71 gives

$$1 - p_E = \frac{1.82\times10^{8}\times1.6\times10^{19}}{0.226\times10^{-3}} \sqrt{\frac{1.38\times10^{-23}\times3237\times10^{4}}{2\pi\times9.1\times10^{-31}}} \exp\left(-\frac{11{,}600\times0.172}{3237}\right)p_E$$

and

$$p_E = 0.625$$

Probability of ambipolar diffusion of electron

From Equation 30,

$$1 - p_a = \frac{dk(\overline{T_e + T_g})[(\pi/d)^2 + (2.405/r)^2]}{eJ_o(\rho_{+n} + \rho_{++})},$$

where

$$\rho_{+n} = 1/n_{+p}\, e\, \mu_{+n}$$

Substituting for the positive ion mobility, given by Brown (6) as μ_{+n} = 3550 cm^2/volt sec for operating conditions.

$$\rho_{+n} = (1.82 \times 10^{8} \times 1.6 \times 10^{-19} \times 3.55 \times 10^{3})^{-1} = 9.68 \times 10^{6} \text{ ohm cm}$$

Also,

$$\rho_{++} = \pi e^2 \sqrt{6M}/[(kT_g)^{3/2}(4\pi\epsilon_o)^2]$$

from Equation 29,

$$= \frac{\pi \times 2.57\times10^{-38}\sqrt{6\times3.38\times10^{-26}}\times10^{2}}{(1.38\times10^{-23}\times836)^{3/2}\times1.23\times10^{-20}} = 263 \text{ ohm cm}$$

Then,

$$1 - p_a = \frac{0.4\times1.38\times10^{-23}\times4444[(\pi/0.4)^2 + (2.405/1.1)^2]}{1.6\times10^{-19}\times9.68\times10^{6}\times0.361\times10^{-3}} = 0.00275$$

and

$$p_a = 0.997$$

Probability of electron-ion recombination

From Equation 31,

$$1 - p_r = (\alpha_r e\, n_{ep}^{\ 2}\, d)/J_o$$

Brown (6) gives the recombination coefficient for neon as 2.1 x 10^{-7} cm^3/sec. Therefore,

$$1 - p_r = \frac{2.1 \times 10^{-7} \times 1.6 \times 10^{-19} \times 3.31 \times 10^{-16} \times 0.4}{0.361 \times 10^{-3}} = 1.23 \times 10^{-6}.$$

Probability of ionization

Brown (6) reports the first Townsend ionization coefficients in noble gases for different potential gradients. The plasma glow is observed to extend for a distance of 2.5 mms into the auxiliary region. The mean potential gradient in this region may be assumed to be 27.5/0.25 = 110 volts/cm. The corresponding ionization coefficient is then found to be 3.0 ion pairs/cm mm Hg, and so the probability of ionization is

$$p_i = 3.0 \times 0.25$$

$$= 0.75$$

Probability of ion entering the emitter-collector region

The mesh used was a 0.0045 ins. diameter wire mesh with 100 x 100 wires/ins. Applying Equation 42,

$$k_m = MNd^2 - d(M + N) + 1 = 1.44 \times 10^{-2} \times 20.3 - 4.5 \times 10^{-3} \times 2.4 \times 10^{2} + 1$$

$$= 0.372$$

Probability of electron entering the auxiliary region

From Equation 37 and for the observed auxiliary to current load ratio of 1/33.5

$$\alpha = \frac{I_a}{I_L}(1 + p_i - p_i k_m I_a / I_L)^{-1} = 1/33.5(1 + 0.75 - 0.75 \times 0.372/33.5)^{-1}$$

$$= 0.0171$$

Probability of slow-ion capture by collector

From Equation 48,

$$1 - p_c = \frac{n_{ec} e}{I_a} (1 - R)(1/k_m - 1)(1/p_i + 1)(kT_{+c}/2\pi M)^{\frac{1}{2}}$$

$$= \frac{1.44\times10^{8}\times1.6\times10^{-19}}{6.75\times10^{-6}} (1 - R)(1/0.372 - 1)(1/0.75+1) \sqrt{\frac{1.38\times10^{-23}\times439\times10^{4}}{2\pi\times3.38\times10^{-26}}}$$

$$= 0.225(1 - R)$$

and,

$$p_c = 0.225(3.45 + R). \qquad (76)$$

The probabilities are now substituted into the critical equation

$$(p_a p_r \alpha p_i k_m p_c + p_a p_r - 1)\left(\frac{p_E}{2-p_E}\right) \sqrt{\frac{M}{m}} \left(\frac{1 + R}{1 - R}\right) = 1$$

with the result that

$$[0.997\times0.0171\times0.75\times0.372\times0.225(3.45+R)-0.00275]\left(\frac{0.625}{2-0.625}\right) 192 \left(\frac{1+R}{1-R}\right) = 1$$

This may be put into the form of a quadratic equation

$$R^2 + 12.55R - 9.85 = 0, \quad \text{which yields the positive root}$$

$$R = 0.730.$$

Therefore, under the existing plasma conditions, the ions which reach the emitter are reflected with an effective coefficient of 0.73. This veri-

fies the assumption that slow ions are reflected several times before they are absorbed by the emitter. As expected, the reflection coefficient is less than the 0.98 reported by Gabor (17), since in the present case the emitter fall potential of 0.172 volts produces higher energy ions at the emitter surface than the 0.0276 volts in Gabor's system.

The probability p_c of a slow ion escaping absorption by the collector may now be fully determined by substituting for R in Equation 76, which yields

$$p_c = 0.225(3.45 + 0.73)$$

$$= 0.941$$

The probability terms obtained are summarized as follows:

$p_E = 0.625$	$p_i = 0.750$
$p_a = 0.99725$	$k_m = 0.372$
$p_r = 0.999,998,77$	$p_c = 0.941$
$\alpha = 0.0171$	$R = 0.730$

SUMMARY AND CONCLUSIONS

The principal thermionic energy conversion systems under development have been considered. Due to the possible use of an inert filling gas and low emitter temperatures, it was decided that the auxiliary discharge thermionic converter is worth investigating as a possible alternative to the cesium diode converter. Due to the triode nature of the auxiliary discharge system, the analytical procedure developed in the literature (42) for diode converters could not be adopted satisfactorily. Also, this procedure provides no means for determining the value of the reflection coefficient R for the recently discovered phenomenon of slow ion reflection. As a result, a new cyclic procedure is developed which is similar to that used for the nuclear fission neutron cycle. The result is a single critical equation, involving all the system parameters, including the reflection coefficient R. This equation must be satisfied for operation of the converter under equilibrium conditions.

In order to adapt this equation for experimental analysis, each of the parameters is considered and expressed in terms of plasma or converter characteristics which may be determined by recognized experimental techniques. Using experimental values, the critical equation parameters are calculated in terms of the reflection coefficient R. The critical equation is then solved for R. Thus, the characteristics of the charge system are completely determined. The fact that a reflection coefficient of $R = 0.73$ is obtained serves to verify Gabor's findings.

A transient analysis is also presented in which an expression for the system transfer function is developed. This is of interest if it is desired to generate a time varying power output, or produce ions in the

emitter collector region for space charge neutralization, by applying a repeated high voltage pulse to the emitter.

The design, fabrication and testing of a device to simulate the Gabor-type auxiliary discharge converter mode is described. The fabrication and processing of an emitter to achieve a work function of 2.3 eV is also reported. The system is tested while operating in the Gabor mode and experimental data required for evaluation of the critical equation parameters are obtained.

As a result of the theoretical and experimental analysis, it is apparent that Gabor's finding of a slow ion reflection coefficient is indeed correct, and that it is possible to operate the system as an energy converting device if a suitable low work function material is developed for the collector. No containment problems were experienced as was expected. An increase in emitter work function was noted after an ionizing potential was applied between emitter and collector. It appears that some of the emitter material was deposited on the collector since the work function was found to be below that of pure nickel. Care should be taken to ensure that high voltage leads are well insulated and as far removed from low potential surfaces as possible in order to avoid the consequences of gas breakdown.

RECOMMENDATIONS

Since the critical equation incorporates the system parameters, it should be possible to optimize this equation so that the ratio of output to auxiliary power is a maximum. It is found that this equation is particularly sensitive to variation of the ionization probability p_i, the ambipolar diffusion coefficient p_a and both α and k_m. The two latter terms are associated with the collector geometric configuration. The possibility of designing a collector which would tend to prevent the passage of electrons and aid the passage of ions should be investigated. It seems possible that some configurations may provide a funneling potential profile for ions.

The probability of an emitted electron returning to the emitter was found to be large at 0.375. It should be possible to reduce this value considerably by making the collector larger than the emitter. This was recognized at the design stage, but additions to the collector were not made so that the analytical simplifications associated with planer geometry could be used. Since ions are absorbed by the collector, there is probably an optimum emitter/collector area ratio. It would be beneficial to determine this.

An accurate evaluation of the probability of ionization p_i requires that the potential in the auxiliary discharge region be known. Although estimates may be made from glow-discharge observations, it should be possible to conduct a probe analysis of the plasma. The physical dimension are large enough to permit the introduction of two or three probes.

In order to calculate the plasma characteristics in the emitter-collector region, it was necessary to employ an iterative procedure. This

is a tedious process and could be eliminated by a single probe measurement made in the middle of the main discharge.

A worthwhile project would be the development of a suitable low work function collector. However, this is a major task and is a materials problem rather than one of plasma physics. A collector work function reduction was experienced in the system tested. It might be possible to utilize this fact to achieve a low work function collector coating. Since the emitter is of BaO and SrO and barium is evaporated preferentially, it may be feasible to build up a layer of low work function barium on the collector by sputtering. The emitter work function would be increased in turn, but it may be possible to achieve acceptable values for both emitter and collector work functions. Also, the collector coating could be replenished periodically by applying a high voltage for a short period.

In practice, the requirement that ultra-high vacuum equipment should be required for the processing of the emitter is unsatisfactory when, in fact, the system subsequently operates at a relatively high pressure. The possibility of processing the emitter at atmospheric pressure should be investigated. MacNair (33) reports the achievement of excellent results when decomposition of the $BaCO_3$ takes place in a stream of pure reducing gas, such as hydrogen. In fact the work functions achieved at atmospheric pressure are lower than those under ultra-high vacuum conditions. It is pointed out that the reducing gas should be of high purity for satisfactory results. It would be of considerable benefit if this process could be satisfactorily adapted.

The choice of a suitable filling-gas is most important in an actual converter where the efficient production of ions is essential. As was found, the introduction of a Penning mixture into the system is not a simple matter. By examining specific inert gases, it might be possible to select a suitable single gas. For example, xenon has a relatively low first ionization potential of 12.08 volts. Rather than attempting to use a Penning mixture in future work, it appears that xenon is a good experimental substitute.

Since thermionic energy conversion is a relatively new field, practical applications are not yet receiving a great amount of attention. Due to the relatively high operating temperature of the emitter, few heat sources are readily available. A nuclear fission heat source appears to be one of the most suitable choices. During the development of any thermionic conversion system,this should be kept in mind. For in-pile operation, converters could be incorporated in the fuel element, so that the fissile material acts as the electron emitter. For example, solid solutions of UC-ZrC have been investigated (45) and work functions in the range of 2.8 eV have been reported. Due to the high operating temperatures required, loss of material by vaporization is a problem that has been experienced. Hill and Gifford (23) report on obtaining a low work function of about 2.2 eV by using a BaO-W-UO_2 mixture. Activated compounds such as $BaUO_3$ and Ba_2UO_4 are formed and BaO is evaporated preferentially. It should prove interesting to test the possibility of using a BaO-W-UO_2 emitter and sputtering the collector with the BaO evaporated from the emitter.

Out-of-pile thermionic energy converters could also be used. Such a converter would have the advantage of eliminating the problems and limitations associated with incorporating an electrical system within a fuel element. It appears that an out-of-pile thermionic energy converter could be used as a topping device in a liquid metal cooled nuclear reactor. For example, lithium might be a suitable coolant. It has a boiling point of 1609^{o} K and a work function of 2.48 eV(22). It is envisaged that the converter emitter would consist of a stream of molten lithium emitting 2 amps/cm^2 at a temperature of 1550^{o} K. It might be possible to go even one step further and seed the lithium with a positive ion emitter (32) such as beta-eucryptite (Li_2O, Al_2O_3, $2SiO_2$) and so produce the ions required for space charge neutralization. Reports of such test have not been found in the literature. The further investigation of doped liquid metal emitters should certainly be worthwhile.

APPENDIX

Symbols and Values Used

α	0.0171		Probability of electron passing from main to auxiliary region
α_r	2.1×10^{-7}	cm^3/sec	Radiative recombination coefficient (for neon)
η	0.0271	ions/volt	Ionization coefficient
Λ	0.121	cm	Characteristic diffusion length in main plasma
μ_{+n}	3550	cm^2/volt sec	Characteristic diffusion length of neutral atoms (for neon)
ρ_{++}	263	ohm cm	Resistivity of main plasma due to ion-ion collision
ρ_{+n}	9.68×10^6	ohm cm	Resistivity of main plasma due to ion-neutral collision
ρ_{e+}	0.174	ohm cm	Resistivity of main plasma due to electron-ion collision
ρ_{en}	355.0	ohm cm	Resistivity of main plasma due to electron-neutral collision
ρ_{ep}	355.2	ohm cm	Average resistivity of main plasma
ϕ_a	4.61	eV	Auxiliary anode work function
ϕ_c	4.47	eV	Collector work function
ϕ_E	2.88	eV	Emitter work function
A	3.75	cm^2	Cross-sectional area of containment cylinder
d	0.40	cms	Emitter-collector spacing
d	0.011	cms	Diameter of wires in collector mesh
E_a	27.5	volts	Auxiliary potential
e	1.6×10^{-19}	coulombs	Electron charge
f	1.57×10^{-8}		Fractional ionization in main discharge

h	0.25	cms	Length of effective ionization region
I_a	6.75×10^{-6}	amps/cm^2	Auxiliary current density
I_L	0.362×10^{-3}	amps	External load current
J_{ec}	0.226×10^{-3}	amps/cm^2	Random electron current density at collector
K_1	1.265		Ratio of average main plasma electron density to that at the collector
K_2	1.530		Ratio of average electron density at emitter to that at the collector
k_m	0.327		Probability of an ion passing from auxiliary to main discharge
M	3.38×10^{-26}	kilograms	Mass of ion (for neon)
M	49	wires/cm	Number of wires per unit length in collector mesh
m	9.1×10^{-31}	kilograms	Rest mass of electron
N	49	wires/cm	Number of wires per unit width in collector mesh
n_{+c}	1.44×10^{8}	ions/cm^3	Average ion density in plasma at collector
n_{+p}	1.82×10^{8}	ions/cm^3	Average ion density in plasma
n_{eE}	2.2×10^{8}	electrons/cm^3	Average electron density in plasma at emitter
n_{ec}	1.44×10^{8}	electrons/cm^3	Average electron density in plasma at collector
n_{ep}	1.82×10^{8}	electrons/cm^3	Average electron density in plasma (main)
n_g	1.16×10^{16}	atoms/cm^3	Average neutral atom density in plasma (main)
P	1.0	mm Hg	Gas-filling pressure
P_H	140	watts	Heat dissipation rate from emitter assembly

p_l	3	cm^2	Probability of electron-atom collision
p_a	0.99725		Probability of electron not diffusing ambipolarly
p_c	0.940		Probability of slow ion not being absorbed by collector
p_E	0.625		Probability of electron not being re-absorbed by emitter
p_i	0.75		Probability of an ionizing collision per electron in auxiliary plasma
p_r	$1 - 1.23 \times 10^{-6}$		Probability of electron not recombining in main plasma
q	0.85×10^{-16}	cm^2	Electron-atom collision cross-section in main plasma
R	0.73		Slow ion reflection coefficient
r	1.1	cm	Radius of plasma containment
S	0.53	Joules/gr ^oC	Specific heat of nickel
T	24	secs	Heating time constant of emitter assembly
T_{+c}	439	^oK	Temperature of ions at collector
T_E	1233	^oK	Temperature of emitter
T_{eE}	3236	^oK	Temperature of plasma electrons at emitter
T_{ec}	3980	^oK	Temperature of plasma electrons at collector
T_{ep}	3607	^oK	Temperature of plasma electrons (average)
T_g	836	^oK	Temperature of gas in main plasma (average)
$\overline{T_e + T_g}$	4443	^oK	Average of sum of electron and gas temperature in main plasma
V	1.52	cm^3	Volume of main discharge region
V_{Ef}	0.172	volts	Emitter fall potential

V_{cf}	0.0	volts	Collector fall potential
V_{min}	0	volts	Potential minimum in emitter double sheath
V_p	0.064	volts	Plasma drop potential
W	12.5	grs	Mass of emitter assembly and collector
Γ_+			Ambipolar ion current density
Γ_-			Ambipolar electron current density
θ			Average emitter system temperature at time t
θ_o			Steady-state emitter system temperature
μ_+			Positive ion mobility
μ_{+p}			Average ion mobility in main plasma
μ_{++}			Average ion mobility in ions
τ			Ambipolar decay constant
a			Acceleration of an ion in an electric field E
$\bar{c}_{+p}$			Average thermal velocity of plasma ion
D_+			Average positive ion diffusion coefficient
D_-			Average electron diffusion coefficient
D_a			Ambipolar diffusion coefficient
E			Electric field
E_{ep}			Average electron energy in plasma
$\bar{E}_s$			Space charge field for ambipolar diffusion
H			Collector-auxiliary anode spacing
J_o			Child-Langmuir space charge limited electron current density

J_L	Emitter current density
L_{++}	Mean free path for an ion-ion collision
n_+	Positive ion density at point (a,ϕ,z) in plasma
$\bar{n}_J$	Finite Hankle transform
q	Effective rate of ion production in main plasma
R_L	Load resistance
r_{++}	Collision radius for ion-ion collision
s	Distance traveled by ion
$\bar{s}$	Average distance traveled by ion
V	Potential difference in vacuum converter
V_m	Potential maximum with respect to emitter
V_L	Output load voltage
v_+	Positive ion velocity at point (a,ϕ,z)
$\bar{v}_d$	Average ion drift velocity
v_{eE}	Electron velocity in plasma at emitter
v_{ec}	Electron velocity in plasma at collector
v_{+c}	Ion velocity in plasma at collector

ACKNOWLEDGEMENTS

The author wishes to express sincere appreciation to Dr. Harry Hale, Electrical Engineering Department, for his most helpful guidance and assistance and especially to Dr. Abdel-Aziz A. Fouad, Electrical Engineering Department, whose lectures initiated the interest in thermionic conversion, who was a source of inspiration when it was needed, and whose help in so many ways made this work possible.

Gratitude is also expressed to the members of the Instrument Shop, Physics Department, in particular to Roy Picht who fabricated the electrode system, and also to John T. McConnell and members of the Electrical and Glass Shops.

Finally grateful acknowledgement is made to the members of the Solid State, Industrial Affiliates Research Program, Iowa State University, who financed the research.

LITERATURE CITED

1. Bernstein, W. and Knechtli, R. New approach to thermionic energy conversion. Institute of Radio Engineers, Proc. 49: 1932-1936. 1961.

2. Biondi, M. Mechanism of electron ion recombination. Physical Review 83: 1078-1080. 1951.

3. Biondi, M. and Brown, S. C. Measurement of ambipolar diffusion in helium. Physical Review 75: 1700-1705. 1949.

4. Bloss, W. Investigations on noble gas filled thermionic converters. Advanced Energy Conversion 3: 315-321. 1963.

5. Braddick, H. J. Physics of experimental method. New York, N.Y., Wiley and Sons, Inc. 1954.

6. Brown, S. C. Basic data plasma physics. New York, N.Y., Wiley and Sons, Inc. 1959.

7. Chang, Sheldon S. Energy conversion. Englewood Cliffs, N.J., Prentice-Hall, Inc. 1963.

8. Chanin, L. M. and Biondi, M. A. Mobility of Hg ions in He, Ne, and A. Physical Review 107: 1219-1221. 1957.

9. Cobine, James D. Gaseous conductors. 2nd ed. New York, N.Y., Dover Publications, Inc. 1958.

10. Coltman, J. Thermionic generators: materials are the key to their development. Westinghouse Engineer 20, No. 7: 102-104. 1960.

11. Cook, K. and Fraser, D. Thermionic generator with ion injection. Advanced Energy Conversion 3: 323-331. 1963.

12. Coulliette, J. H. Diffusion of metastable atoms in mercury vapour. Physical Review 32: 636-648. 1928.

13. Fatmi, H. A. New thermionic generator with ion injection. International Conference on Ionization Phenomenon in Gases, Munich, 1961, Official Report 5: 1-6. 1961.

14. Flugge, S. Handbuch der physik. Berlin, Germany, Springer-Verlag, Ohg. 1956.

15. Forman, R. and Ghormley, J. Space charge neutralization in thermionic diodes containing the fission product krypton. Advanced Energy Conversion 3: 385-386. 1963.

16. Gabor, D. New thermionic generator. Nature 189: 868-872. 1961.

17. Gabor, D. Theory of gas discharges with extraneous ion supply. Advanced Energy Conversion 3: 307-314. 1963.

18. Glasstone, S. and Edlund, M. C. Elements of nuclear reactor theory. Princeton, N.J., D. Van Nostrand Co., Inc. 1957.

19. Hass, G. A. and Jensen, J. T. Thermionic properties of UC. Journal of Applied Physics 31: 1231-1233. 1960.

20. Helmes, J. D. and Jepsen, R. L. Electrical characteristics of a Penning discharge. Institute of Radio Engineers, Proc. 49: 1920-1925. 1961.

21. Hernquist, K. and Kanefsky, M. Thermionic energy converters. Radio Corporation of America Review 19: 244-258. 1958.

22. Herrmann, G. and Wagner, S. Oxide-coated cathode. London, England, Chapman and Hall, Ltd. 1951.

23. Hill, F. and Gifford, F. Development of barium-uranium emitter materials. In Thermionic Conversion Specialist Conference, Gatlinburg, Tenn., 1963, Official Report. pp. 279-286. Schenectady, N.Y., General Electric Research Laboratory. 1963.

24. Hodgman, Charles D., ed. Handbook of chemistry and physics. 44th ed. Cleveland, Ohio, Chemical Rubber Publishing Co., Inc. 1963.

25. Jamerson, F. E. and Abrams, R. H. Nuclear generated plasmas in noble gas thermionic converters. Advanced Energy Conversion 3: 363-383. 1963.

26. Johnson, O. E. and Webster, W. M. Plasmatron, a continuously controllable gas discharge development tube. Institute of Radio Engineers, Proc. 40: 645-659. 1952.

27. Kenty, C. Recombination of argon ions and electrons. Physical Review 32: 624-635. 1928.

28. Knowlton, A. E., ed. Standard handbook for electrical engineers. 8th ed. New York, N.Y., McGraw-Hill Book Co., Inc. 1949.

29. Kohl, Walter H. Materials technology for electron tubes. New York, N.Y., Reinhold Publishing Corp. 1951.

30. Langmuir, I. Effect of space charge and initial velocities on the potential distribution and thermionic current between parallel plate electrodes. Physical Review 21: 419-435. 1923.

31. Langmuir, I. Interaction of electron and positive ion space charge in cathode sheaths. Physical Review 33: 954-987. 1929.

32. Laubenstein, R. A. and Kaplan, C. Sources of positive ions for space charge neutralization at low temperature. Advanced Energy Conversion 3: 351-361. 1963.

33. MacNair, D. Hydrogen conversion of thermionic emitters. Physical Electronics Conference, Massachusetts Institute of Technology, 1961, Official Report 21: 1-7. 1961.

34. MacNair, D. Moulded thermionic cathodes. Journal of Applied Physics 24: 1335-1336. 1953.

35. McAdams, W. H. Heat transmission. 2nd ed. New York, N.Y., McGraw-Hill Book Co., Inc. 1942.

36. Martini, W. R. Internal flame-heated thermionic converters. In Thermionic Conversion Specialist Conference, Gatlinburg, Tenn., 1963, Official Report. pp. 356-361. Schenectady, N.Y., General Electric Research Laboratory. 1963.

37. Moss, H. Thermionic diodes as energy converters. Journal of Electronics 2: 305-322. 1957.

38. Rasor, N. S. Cesium vapor thermionic diode. Advanced Energy Conversion 2: 545-568. 1962.

39. Schulta, R. D. Theory of direct conversion of heat to electricity in an auxiliary discharge rare gas plasma diode. Physical Electronics Conference, Massachusetts Institute of Technology, 1961, Official Report 21: 146-166. 1961.

40. Sneddon, Ian N. Fourier transforms. New York, N.Y., McGraw-Hill Book Co., Inc. 1951.

41. Spitzer, L. Physics of fully ionized gases. 2nd ed. New York, N.Y., Interscience Publishers, Inc. 1962.

42. Talaat, M. E. Generalized theory of the plasma energy converter. American Institute of Electrical Engineers, Paper No. 62-291. 1962.

43. Von Engel, A. Ionized gases. Oxford, England, Oxford University Press. 1955.

44. Wahlin, H. B. Thermionic properties of iron group. Physical Review 61: 509-512. 1942.

45. Yang, L. and Hudson, R. G. Some critical material problems of thermionic cathode systems for fission-heat conversion. Advanced Energy Conversion 3: 93-99. 1963.